博士論文

Studies on morphological and gene expression changes during leaf development in rice

（イネの葉の発生過程における形態的及び遺伝子発現変化に関する研究）

プンヤビー　デックロン

Contents

ABSTRACT

Leaves are the most fundamental and crucial organs as the major sites of photosynthesis in higher plants. Leaf primordia are originated from the flanks of shoot apical meristem and undergo many complex developmental events; axis determination, cell proliferation, cell expansion, cell differentiation, and tissue differentiation. Various aspects of leaf development have been studied, and the mechanisms of spatiotemporal control of cell proliferation and cell differentiation are key events. Many genetic analyses for understanding these processes have been made, and most of the knowledge was obtained in a model eudicot, *Arabidopsis*. However, as the patterns of determination of developmental events differ among plant species, it is needed to study these processes in species other than *Arabidopsis*. Grass leaf can be an excellent model system for analyzing leaf development because developmental and physiological events proceed from the tip to the base along the longitudinal axis of the leaf. However, there are few studies to clarify where the developmental events occur and how these events are regulated during leaf development in rice.

In this study, I examined rice leaves during morphogenesis to obtain basic information regarding the developmental transition by morphological, anatomical, and histochemical analyses. In addition, to understand a whole picture of developmental transition of rice leaf, morphological changes caused by various factors and their links to gene expression pattern were analyzed.

1. Morphological and histological changes during rice leaf development

To determine the morphological changes that occur throughout rice leaf development, I separated mature and immature leaves from wild-type seedlings at 15 days after sowing (DAS) to examine the surface and internal structures of leaves. The leaf stage was defined as plastochron number; P1 represents the youngest primordium, P2 the next youngest, etc. Wild-type seedlings at 15 DAS contained eight leaves, P1 – P8. To understand the variation of surface structure of leaves, P1 – P6 leaf primordia were examined by scanning electron microscopy (SEM). SEM images revealed that the surfaces of P1 and P2 leaf primordia, and most parts of P3 were covered with

undifferentiated epidermal cells without any fine structure but trichome initiation was observed on the epidermal cells at the apical part of the P3. P4 leaf primordium showed different epidermal structures along the apical–basal axis. At the apical-most part, fully differentiated cells were found on the surface. In contrast, this epidermal character was absent on the basal part of P4. On the most parts of P5 and P6 epidermis, mature differentiated cells were observed. Next, I examined the internal structure of P1 – P6. The results indicated that P1 and P2 primordia, and most parts of P3 consisted of small cytoplasm-rich cells, and no tissue differentiation was observed. Cross-sections from the top to the base of P4 leaf revealed differentiated internal tissues at the top and middle parts, and epidermal cells and mesophyll cells rich in cytoplasm at the basal part. Transverse sections of P5 and P6 leaves showed fully differentiated tissues along the leaf axis. These observations indicated that P1 to P3 leaf primordia are in the immature phase and P5 and P6 are in the mature phase of leaf development. It was also suggested that a marked developmental transition would occur around the middle to the basal part of P4 leaf, and the cellular differentiation proceeded in a basipetal direction.

To obtain further evidence of the transition, I examined the cellular components of the P4 leaf; chloroplast and starch accumulation, and lignin deposition of the cell wall by histochemical analysis. Chloroplast autofluorescence was obvious in the apical and sub-apical parts of the P4. However, it was undetectable in the basal part of the P4. Numerous starch granules were detected in the basal part of the P4 leaf blade, but fewer starch granules were observed in the apical and sub-apical parts. Lignin accumulation was observed in the apical and sub-apical parts of P4, but it was not obvious in the basal parts of the P4 leaves.

These results indicated that the dynamic transitions of various aspects of developmental and physiological traits occur around the middle to basal part of the P4 leaf blade. The traits included the epidermal structure, internal structure and cellular components.

2. Gene expression changes during rice leaf development

To obtain a further understanding of the developmental transition and gradient along the leaf axis of P4 leaf primordium at the molecular level, I analyzed expression patterns

of six marker genes—*OsCDKB2*, *OsRBCS2*, *OsTCP1*, *OsTCP12*, *OsGRF10* and *pri-miR396c*—in eight segments from the top to the bottom of P4. In addition, I also examined the expression of these genes in three different growth stages; i.e., the early, middle, and late stages of P4. Higher levels of *OsCDKB2* and *OsRBCS2* expression would represent activation of cell division and photosynthesis, respectively. *TCP* and *GRF* genes are known to be involved in leaf development via regulating cell proliferation, and *pri-miR396c* is reported as a negative regulator of *GRFs*. Overall, the expression patterns of *OsCDKB2*, *OsGRF10*, and *OsTCP1* showed similar trends, which showed higher expression levels in the basalmost part of the P4. The *OsTCP12* displayed two peaks of expression at the basal and middle parts of the P4. *Pri-miR396c* was expressed in the basal part of the P4 in the late stage but the highest level of expression was not observed at the basalmost part in the early and middle stages. The expression of *OsRBCS2* was highest at the apical part of P4 in the early stage of development while the peak was not obvious in the middle and late stages.

The experiments showed that the expression peaks of marker genes shifted toward the basal part of the P4 leaf as developmental stage progress, indicating that these genes are influenced by developmental and/or physiological events that proceed in the basipetal direction. Thus, these six marker genes would be suitable to monitor developmental transition along the apical–basal axis of P4 leaves.

3. Effects of altered external and genetic factors on rice leaf development

It is known that plant hormones have roles in various aspects in plant growth and development. Thus, I examined response of leaf development and change of gene expression pattern for four major plant hormones. Generally, auxin, cytokinin (CK) and brassinosteroid (BR) applications showed a negative effect on the leaf growth and the emergence of leaves, although the number of leaf was not affected in auxin-treated leaf. In contrast to these three hormones, gibberellin (GA) treatment induced leaf elongation. Gene expression analysis of the hormone-treated P4 leaves indicates that treatments of these hormones affect expression of at least one marker gene. Auxin treatment affected expression pattern of *OsTCP12*, BR treatment did that of *OsCDKB2*, *OsTCP12* and *pri-miR396c*, CK treatment did that of *OsTCP12*, and GA treatment did that of *OsTCP12* and *pri-miR396c*. Interestingly, expression pattern of *OsCDKB2*, *OsTCP1* and *OsGRF10* did

not change significantly in all conditions except for BR treatment. Although the conserved pattern of the *OsCDKB2* expression would not be consistent with the altered length of auxin-, CK- and GA-treated leaves, if the absolute length of the P4 leaves was considered, the change of the expression range of *OsCDKB2*, *OsTCP1* and *OsGRF10* was correlated with the change of the leaf length of the P4. This indicates that the treatments of these hormones would affect the range of cell proliferation domain in the base of the P4 leaf.

I also analyzed alteration of gene expression patterns in various mutants; *lg, dl, d61, d1, d18h, pla1-4* and *pre.* These mutants show abnormalities in leaf morphology. The expression patterns of five marker genes were unchanged in *lg*, and those of *OsCDKB2*, *OsGRF10* and *OsTCP1* were not obviously altered in all mutants. In contrast, the expression pattern and the level of *OsTCP12* and *pri-miR396c* were affected in most of the mutants. Expression pattern of *OsTCP12* was affected in *d61* and *d1* mutants and the expression level was altered in *dl, pla1-4* and *pre*. Expression pattern of *pri-miR396c* was affected in *d1* and the expression level was altered in the others. In case of *d18h,* expression trends of *OsCDKB2, OsTCP1* and *OsGRF10* would be similar to that of wild-type despite the reduced length of the P4. Consequently, the results indicated that expression patterns and level of the marker genes were affected in *dl*, *d61*, *d1*, *pla1* and *pre* mutants but not in *lg* mutant. The trend of the expression profile in *d18* was globally conserved compared to that of the wild-type controls. The results indicated that the alteration of marker gene expressions differed among the mutants and the sensitivity of *pri-miR396c* and *OsTCP12* expression changes was high while that of *OsCDKB2*, *OsGRF10*, and *OsTCP1* was low.

To confirm whether expression change and level of *OsRBCS2* reflects photosynthetic activity in P4 leaf, *OsRBCS2* expression pattern in dark-grown P4 leaf was observed. I also examined expression pattern of *OsRBCS2* in various leaf morphogenetic mutants. The results indicate that *OsRBCS2* expression level depends on light exposure but does not simply reflect the maturation or differentiation of chloroplasts.

Accordingly, my expression analysis using six marker genes would be useful to characterize developmental features of mutants and to understand the genetic and physiological alterations that could not be determined from the morphological phenotype.

4. Mutant affecting morphology and gene expression pattern of rice leaf

To find new genetic factor controlling leaf development in rice, I analyzed a novel recessive mutant (12T-S-221) showing abnormal leaf morphology. Characteristic phenotypes; a disrupted leaf blade and sheath boundary, a lack of auricles and abnormal ligules, were seen in the vegetative phase of the mutant leaves. In addition, the mutant produced sterile panicles with malformed spikelets at the reproductive stage. Thus, the mutation pleiotropically affects plant development. However, the morphological and histological analyses did not reveal obvious abnormalities in the surface and internal structures of the developing leaves. Expression analysis of five marker genes indicated that expression pattern of *OsTCP12* and *pri-miR396c* was affected in the P4 leaf of the mutant. Therefore, regarding leaf development, a possible function of the gene is to establish normal boundary of leaf blade and sheath via modulating leaf growth.

In conclusion, I characterized the developmental progression of wild-type leaves. The results revealed the dynamic transition of developmental events, in particular, from cell proliferation to cell differentiation in the P4 leaf primordium. I developed several molecular markers showing dynamic expression from tip to base of P4 and applied them to various growth conditions and mutants. The changes in expression patterns of marker genes varied among the conditions and mutants, indicating that my marker genes are useful for detecting effects on the transition process from cell proliferation to cell differentiation during leaf development. The results would provide basic knowledge regarding the developmental transition and effects of various factors on the transition process.

CHAPTER 1

General introduction

Rice is one of the most important commercial crops in the world and is usually consumed by most of people in Asian countries as a staple food. Nowadays, however, population rapidly increases which would result in the insufficient food supply in the future. To find solutions to this problem, agricultural technologies, genetic resources and molecular tools have been continuously accumulated. In particular, biotechnology and molecular genetics have been improved substantially which enable the progression of molecular breeding in rice.

One of the targets of rice breeding is the improvement of photosynthetic efficiency because it is closely related to the productivity of carbohydrates and ultimately to yield. Photosynthetic capacity depends on the appropriate size and proportion of photosynthetic organs, especially leaves. It is considered that the suitable size and shape of leaves will enhance the efficiency of light capture. Thus, one of strategies for enhancing photosynthetic capacity is to manipulate the size and shape of leaves. In fact, mutations and natural variations related to the size and shape of leaves have been identified as genetic resources for breeding of high-yield rice. For example, *GPS* (*GREEN FOR PHOTOSYNTHESIS*) gene has been identified as a QTL locus which regulates photosynthesis rate. *GPS* allele is a natural variation of *NAL1* gene that was originally identified as a regulator of leaf morphogenesis (Takai *et al*., 2013). Enhanced photosynthesis rate in the *GPS* allele was achieved through increasing mesophyll cells between vascular bundles (Takai *et al*., 2013). Several QTLs controlling size and shape of flag leaf have been mapped on rice chromosomes. In particular, the width of flag leaf shows a positive correlation to the yield per plant (Zhang *et al*., 2015). Besides genes identified by QTL analyses, functional analysis of *OsBAK1* gene has proved that the modified expression level of the gene can improve agronomic traits such as plant height, leaf erectness and grain size (Li *et al*., 2009). These examples indicate the genetic resources affecting leaf size and shape would potentially contribute to breeding for high-yield rice. Despite the importance of leaf-related traits for rice breeding, understanding of

molecular and genetic mechanism in leaf development is still insufficient and it is necessary to gain more insights about leaf development for efficient breeding in rice.

Although the leaf is the most fundamental organ among above-ground organs in plants, the leaf development is complex and comprised of several processes such as axis determination, cell division and expansion, tissue differentiation and specification (Doonan, 2000, Blein *et al*., 2010 and Andriankaja *et al*., 2012). Many genetic analyses for understanding these processes have been made and most of the knowledge was obtained in a model eudicot, *Arabidopsis* (Berná *et al*., 1999, Tsukaya *et al*., 1995 and 1997). However, as the patterns of determination of developmental events differ among plant species, it is needed to study these processes in species other than *Arabidopsis*.

Grass leaf can be an excellent model system for analyzing leaf development because developmental and physiological events proceed from the tip to the base along apical-basal axis of the shoot. However, although several studies about some traits of leaves have been attempted, there are few studies to clarify where the developmental events occur and how these events are regulated during leaf development.

In this thesis, to understand the whole picture of developmental processes of rice leaf, morphological change and their links to the gene expression pattern were analyzed. In Chapter 2, I observed morphological and histochemical changes in various stages of leaf primordia for understanding spatiotemporal dynamics of leaf development. In Chapter 3, to monitor the morphological and physiological changes occurring during leaf development, I developed several molecular markers that reflect the transition between mature and immature states of the leaf cells. Moreover, expression patterns of these marker genes were analyzed in fine segments along the apical-basal axis of leaf primordia. In Chapter 4, the effects of various plant hormones and mutations on the leaf development were analyzed using the molecular markers. Finally in Chapter 5, I identified a novel mutants affecting leaf morphology. The characteristics of this mutant were analyzed by morphogenetic and molecular analyses based on the knowledge from the previous Chapters.

CHAPTER 2

Morphological and histochemical changes during rice leaf development

2.1 Introduction

Morphology of rice leaves has been well-studied (Kaufman, 1959, Itoh *et al.*, 2005a and 2006b). Mature rice leaf is comprised of two parts, leaf blade (leaf lamina) and leaf sheath along the longitudinal axis. Leaf blade functions as a central part for photosynthesis. Leaf sheath acts as a protective part of young leaves and culms. In addition, lamina joint is differentiated at the base of leaf blade which has a role for controlling leaf bending along the shoot axis. At the boundary between leaf blade and sheath, two additional tissues; a ligule and auricles are observed. On the other hand, microscopic observations have revealed that many specialized tissues and cells are differentiated in mature leaves in rice.

The leaf morphology, tissues and cell identities are gradually established during the development and the morphological events would start at specific stage of the leaf. Leaf stage is usually defined by plastochron number (Pn). P1 is the youngest leaf primordium that was just protruded from the shoot meristem and P2 is the next one and so on (Itoh *et al.*, 2005). Morphogenetic events occurring at each plastochron in rice were roughly reported, however, the detailed timing of the start, transition and end of the events are not obvious.

Recent publications reported the developmental and physiological transition of some traits in maize and rice leaves, but they focused on global change of gene expression pattern associated with mainly photosynthetic process (Li *et al.*, 2010, Kusumi *et al.*, 2010a, 2010b and Nelson, 2011). The reports suggested that the sink- source boundary of photosynthetic product was established during the young leaf primordium stage. The sink region was located at the basal part and chloroplast differentiation was observed at the apical part of the specific stage of the leaf primordium (Nelson, 2011 and Wang *et al.*, 2014). Thus, transition processes occur at the specific stage and part of young leaf primordium not only in developmental events but also in physiological traits.

In this chapter, to obtain details of morphological changes that occur during leaf development and to grasp the critical stage of the developmental transition among the leaf stages, various stages of primordia were investigated by morphological and histological analysis. In addition, to understand links between developmental and physiological transition, change of some cellular components along the apical-basal axis at the transition stage of leaf primordia were examined by histochemical analysis.

2.2 Materials and Methods

2.2.1 Plant materials

A wild-type rice variety (cv. Nipponbare) was used for morphological analysis. The seeds were sterilized with 1% sodium hypochloride solution for 60 min and washed with the distilled water 3 times and submerged in the distilled water at 28°C for 1 day, then they were sown on the soil. The seedlings at 15 days after sowing were examined.

2.2.2 Scanning electron microscope

Dissected and separated leaves and shoot apex were fixed with PFA solution (4% paraformaldehyde in 0.1M NaP buffer, 1%Triton-X) overnight, and then rinsed with 0.1M NaP buffer 1 h and dehydrated with a graded EtOH series and the final step of ethanol (100%EtOH) was replaced with liquidized *t*-butyl alcohol by incubating in an incubator (model SLI-220, EYELA, Japan) at 37°C overnight. All specimens were transferred into liquidized *t*-butyl alcohol, and then incubated at - 20 °C for 10 min. The frozen specimens were completely dried up by a freeze dryer (model JFD-320, JEOL, Japan). The dried specimens were coated with platinum (Ion sputter E-1030, HITACHI, Japan) and observed by using a scanning electron microscope (model S-4000; Hitachi, Japan) at 10 keV.

2.2.3 Paraffin and plastic sectioning

For plastic sections, leaf blades, leaf sheaths, and a part of leaf blades-sheath boundary of P5 and P6 leaves were fixed with PFA solution overnight, rinsed with 0.1 M Na-phosphate buffer for 1 hour, and dehydrated through a graded EtOH series, followed by infiltration with Technovit 7100 (Heraeus Kulzer) for 4 days and embedded. Samples were cut into 3 μm sections using a rotary microtome (model HM360; MicroEdge, Tokyo, Japan), stained with 0.5% Toluidine Blue O in 0.1% sodium carbonate buffer, and observed by a light microscope (model AX80; Olympus, Tokyo, Japan). For paraffin sections, P4 leaf primordium was separated into four parts, and they were fixed with PFA solution, and finally embedded in Paraplast Plus (Oxford Labware, St. Louis, MO). All

samples were cut into 8 μm sections and they were stained with triple stains (hematoxylin, 1%, Safranin-O and 1% Fast-Green), and then examined by a light microscope.

2.2.4 Histochemical analysis

To observe starch and lignified cell walls, cross-sections of eight segments of P4 leaves were subjected to stain with iodine-potassium-iodide (IKI) solution and by double staining with Safranin-O and Orange-G, respectively. For observation of chloroplasts, autofluorescence of the cross-sections of eight segments was observed by a fluorescence microscope (model BX60; Olympus).

2.3 Results

2.3.1 Phenotype and leaf stages of wild-type seedling

A coleoptile and five true leaves were emerged in the seedling of Nipponbare at 15 days after sowing (DAS) (Figure 2-1A). After the separation of these emerged leaves, three younger leaf primordia were found inside of those leaves. Thus, wild-type seedlings at 15 DAS contained eight leaves, P1 – P8, corresponding to the eighth to first leaves, respectively.

Figure 2-1B showed phenotype of the dissected leaves. The first leaf is corresponding to P8, and lacks leaf blade and lamina joint. The second (P7) to fourth (P5) leaves showed obvious differentiation of the leaf blade and sheath disrupted by a ligule (Figure 2-1B). The boundary of leaf blade and sheath on the fifth (P4) leaf was also recognized at the basalmost part of the P4 leaf primordium (Figure 2-1B). Sixth (P3) leaf is too tiny to recognize the differentiation of leaf blade and leaf sheath. P1, P2 leaf primordia and shoot apical meristem (SAM) would be surrounded by P3 leaf primordium.

2.3.2 Surface structure of leaf primordia

To understand the variation of the epidermal structure of the leaves, surface structure of SAM and P1 to P6 leaf primordia was observed by scanning electron microscope (SEM). SEM images revealed that the surface of SAM, P1 and P2 leaf primordia was covered with the undifferentiated epidermal cells without any fine structures (Figure 2-2A). The surface of P3 leaf was similar to that of P2 leaf primordium, but developing trichomes were observed on the epidermal cells at the distal part (Figure 2-2B), and their initiation was seen in the middle part of P3 (Figure 2-2C). At the basalmost part of the P3 leaf, a hollow of leaf primordium that may be the future boundary of leaf blade and leaf sheath were observed (Figure 2-2D). As the P4 leaf primordium showed quite different epidermal structures along the apical–basal axis, I examined the surface at five different parts of P4. At the distal-most part, fully differentiated trichomes, prickles, epidermal papillae, and stomata cells were found on the surface. These structures were also observed on the middle part of the leaf blade (Figure 2-2E and 2- 2F). In contrast, those features

were absent on the surface at the basal part of leaf blade, leaf sheath and lamina joint of the P4 (Figure 2-2G to 2-2I). The epidermal features of P5 and P6 leaves in most parts were similar to those of the distal part of the P4 leaf; i.e., mature differentiated cells with papillae and two types of trichome (unicellular and bicellular), and stomata cells were observed on the adaxial (Figure 2-2J and 2-2O) and abaxial sides of the leaf blade (Figure 2-2K and 2-2P) and the abaxial side of the sheath (Figure 2-2M and 2-2R). In contrast, the adaxial side of P5 and P6 leaf sheaths had no papillae or trichomes (Figure 2-2N and 2-2S). However, fully developed stomata were present and the epidermal cells were elongated, indicating that the cells of the adaxial epidermis of P5 and P6 leaf sheaths were mature. The epidermis of the boundary of leaf blade and sheath both of P5 and P6 showed rectangle epidermal cells without any differentiated cells (Figure 2-2L and 2-2Q), indicating that the boundary of the leaf blade and sheath has different properties from those of the leaf blade and leaf sheath. Accordingly, examination of surface structures indicated that cellular differentiation of the leaf epidermis starts at the tip of the P3 and proceeded to the middle part of P4, but do not reach the basal part of the P4.

2.3.2 Inner structure of leaf primordia

Next, I examined the internal structure of P1 – P6 leaf primordia on paraffin- and plastic-embedded sections (Figure 2-3). Examination of shoot apex cross-sections indicated that P1 and P2 primordia consisted of small cytoplasm-rich cells and no tissue differentiation was observed (Figure 2-3A). Most of the cells in P3 were similar to those of P1 and P2, but immature vascular bundles were recognized in the basal and apical parts of P3 (Figure 2-3A and 2-3B). Cross-sections from the top (Figure 2-3F) and middle (Figure 2-3E) regions of the P4 leaf blade showed similar internal structure. Mesophyll cells, phloem cells, xylem cells, bundle sheath cells, and sclerenchymatous fiber cells were differentiated in these regions. Bulliform cells were present on the adaxial side of leaf blade at the middle parts (Figure 2-3E), although they were not obvious in the top of the P4 leaf blade (Figure 2-3F). In addition, the cytoplasm of epidermal cells in the top (Figure 2-3F) and middle (Figure 2-3E) regions of the P4 leaf blade were not strongly stained, indicating that the epidermal cells in these regions were vacuolated. The internal structures of the basal part of the leaf sheath (Figure 2-3C) and leaf blade (Figure 2-3D)

were different from those at the top and middle parts of P4. Most of the epidermal cells and mesophyll cells were rich in cytoplasm, although xylem and phloem cells were obvious. In particular, lacunae (air spaces) observed in the mature leaf sheath (Figure 2-3G and 2-3J) could not be seen (Figure 2-3C). Transverse sections of P5 and P6 leaves showed similar anatomical features. Mesophyll cells, all of the components of the vascular bundle, and sclerenchymatous fiber cells were fully differentiated along the leaf axis (Figure 2-3G to 2-3L). Bulliform cells were present on the adaxial side of the leaf blade (Figure 2-3I and 2-3L).

Observation of the surface and internal structures of leaf primordia during development indicated that most of the cells of P1 to P3 leaf primordia were in an undifferentiated state, whereas the cells of P5 and P6 were fully differentiated. These observations indicated that P1 to P3 leaf primordia are in the immature phase and P5 and P6 are in the mature phase of leaf development. However, differentiated and undifferentiated cellular characters were observed in the top part and the basal part of P4 leaf, respectively, indicating that a marked developmental transition would occur around the middle to the basal part of the P4 leaf and cellular differentiation proceeded in a basipetal direction.

2.3.3 Changes in cellular components along the apical–basal axis of the P4 leaf primordium

Morphological analysis indicated that the P4 leaf primordium contains a transition region where transformation of immature cellular characters into the mature state occurs. To obtain further evidence of the transition, I examined the cellular components of the P4 leaf, chloroplast and starch accumulation, and lignin deposition of the cell wall of the P4 leaf by histochemical analysis.

2.3.3.1 Chloroplast differentiation

The color of the dissected P4 leaf at the apical part was green, whereas the basal part was whitish in color (Figure 2-4A), indicating differences in chloroplast differentiation and accumulation of chlorophyll between apical and basal parts of the leaf. To clarify the pattern of chloroplast differentiation along the apical–basal axis of the P4 leaf

primordium, I examined chlorophyll accumulation in eight segments (P4-1 to P4-8) (Figure 2-4A) of P4 leaf primordium along the apical-basal axis by a fluorescence microscopy. Chloroplast autofluorescence was obvious in the mesophyll cells of the apical (P4-1 to P4-3) (Figure 2-4B to 2-4D) and middle parts of the P4 leaf (P4-4 to P4-6) (Figure 2-4E to 2-4G). However, chloroplasts were not discernible in the sub-basal part (P4-7) (Figure 2-4H) and undetectable in the basal part of the P4 leaf (P4-8) (Figure 2-4I).

2.3.3.2 Starch accumulation

Starch is a major product of photosynthesis in higher plants. Although starch mostly accumulates in the endosperm during seed maturation in rice, it shows temporary accumulation in the leaves (Chatterton *et al*., 1980, Cave *et al*., 1981 and Smith 2007). To determine the pattern of starch accumulation in the P4 leaf primordium, eight parts of the P4 leaf primordium were stained with iodine-potassium iodide solution. Numerous starch granules were detected in the mesophyll cells in the sub-basal and basal parts of the P4 leaf blade (Figure 2-4P and 2-4Q), but fewer starch granules were observed in the apical and middle parts (Figure 2-4J to 2-4L and 2-4M to 2-4O). The mature leaf sheath functions as a sink of photosynthetic product, and starch is synthesized from carbohydrates derived from other photosynthetic tissues (Nelson, 2011 and Wang *et al.*, 2014). The results may indicate that the regional distribution of sink and source of photosynthetic product was established in P4 leaf, and the sink part is independent of differentiation of the leaf blade and sheath in P4.

2.3.3.3 Lignified cell walls

Lignin is a phenolic polymer that provides rigidity to cell walls by crosslinking with polysaccharides. Lignin is mainly deposited in supporting and conducting tissues, such as the sclerenchyma and vascular tissues in mature tissue (Boudet, 2000, Evert, 2006, Smith *et al*., and Wang *et al*., 2013). The results of morphological analysis indicated that the apical part of P4 exhibited mature cellular characters, while the basal part showed immature characters. To determine whether cell wall composition is also different

between apical and basal parts, I investigated the pattern of the lignified cell walls. Red staining by Safranin revealed accumulation of lignin in the epidermal cells, sclerenchyma, and xylem tissues in the apical (P4-1 to P4-3) (Figure 2-4R to 2-4T) and middle (P4-4 to P4-6) (Figure 2-4U to 2-4W) parts of P4 leaves. However, staining in the epidermal cells was not obvious in the sub-basal (P4-7) and basal parts (P4-8) of P4 leaves (Figure 2-4X and 2-4Y). These results suggest that not only the accumulation of cellular components but also the deposition of secondary cell wall was differentially regulated in P4 leaves along the apical–basal axis.

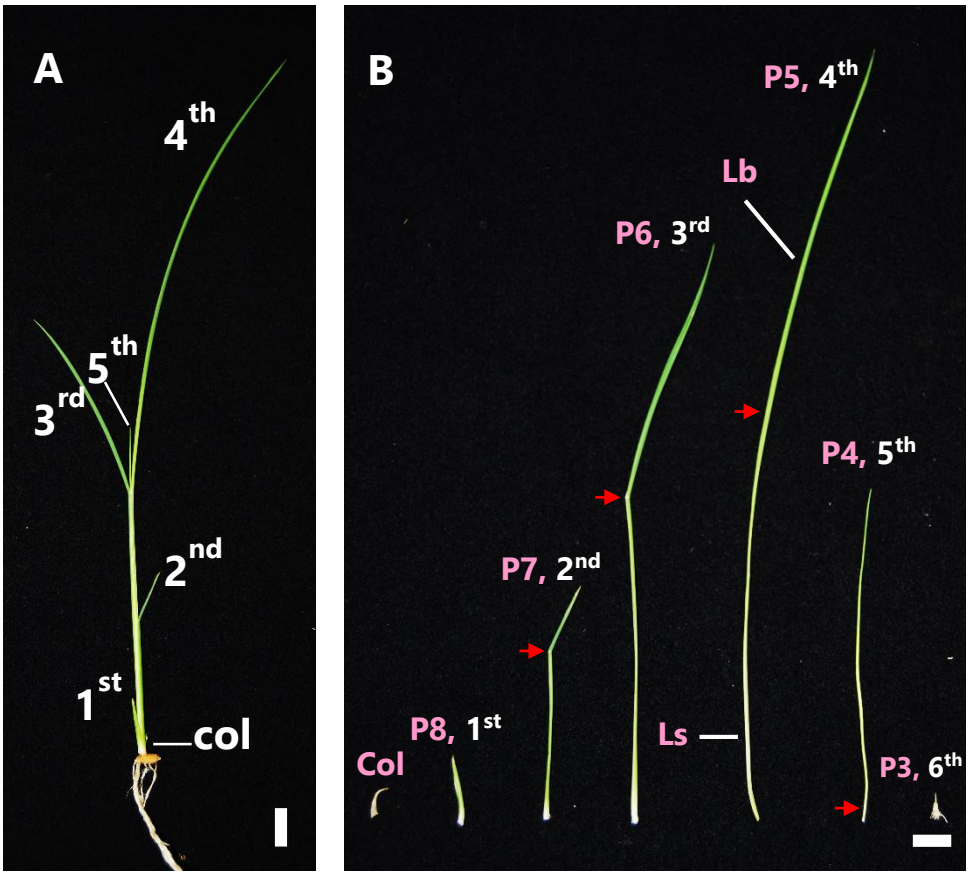

Figure 2-1. Wild-type seedling and stages of the leaves.

A, Wild-type seedling at 15 days after sowing (DAS). **B,** Separated leaves of wild-type seedling. The leaf number (1st to 5th leaves) and plastocrhon number (P3 to P8 leaf primordia) of each leaf are labeled. Red arrows indicate lamina joint. Col; coleoptile, Lb; leaf blade and Ls; leaf sheath. Scale bars = 1 cm.

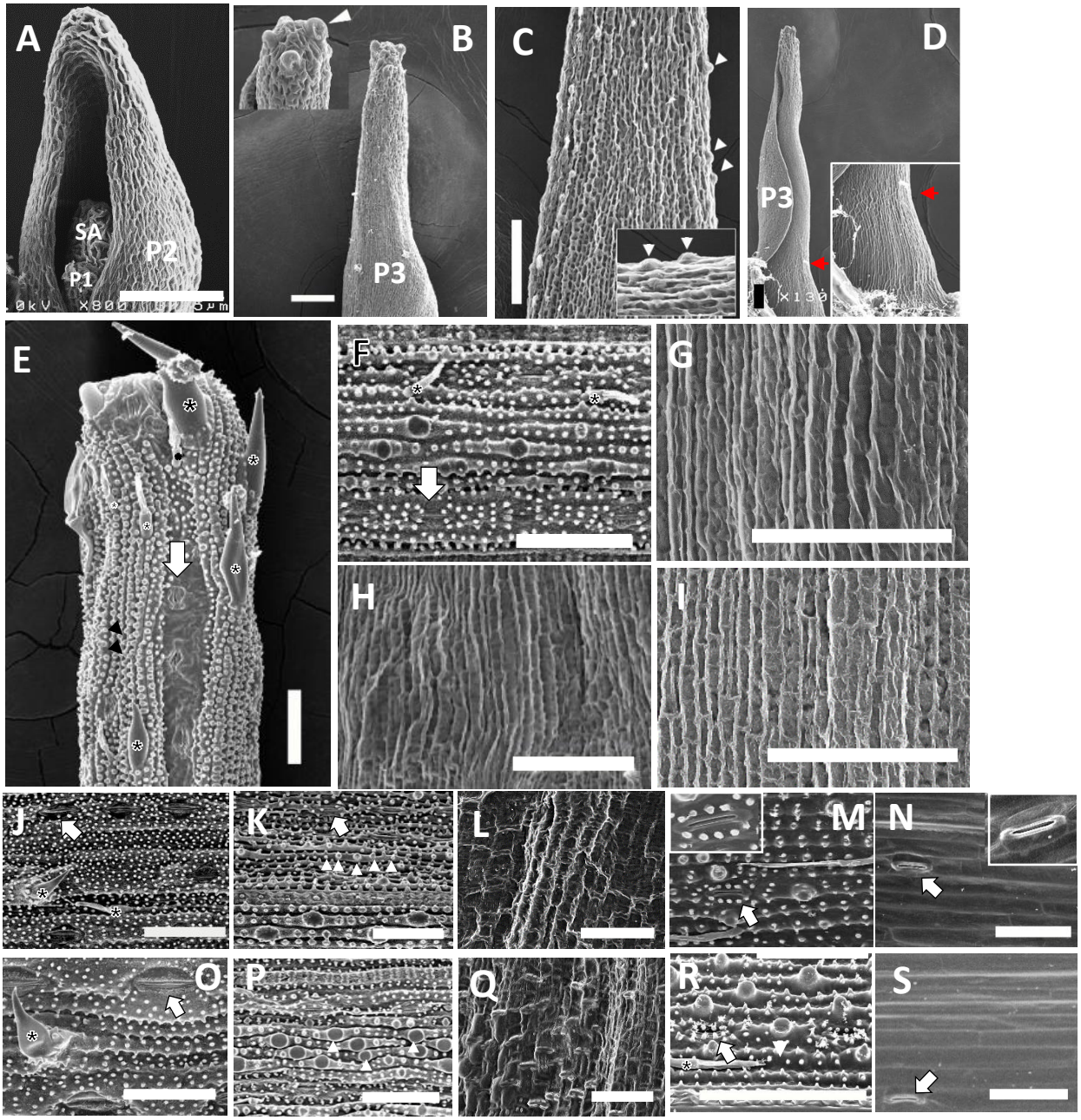

Figure 2-2. Surface structure of wild-type leaves at various stages.
Scanning electron microscopic images of the epidermal structure of P1 to P6 leaves at 15 DAS are shown. **A,** Shoot apex (SA), P1 and P2 leaf primordia. **B,** P3 leaf primordium. Inset: high magnification of P3 tip and arrowhead indicated immature trichome. **C,** The middle part of P3 leaf primordium. Inset: high magnification of the surface. Initiating trichome (arrowhead) was observed. **D,** P3 leaf leaf primordium showing a presumptive boundary of leaf blade and sheath (red arrow). **E,** Apicalmost part of P4 leaf primordium. **F,** Middle part of P4 leaf blade **G,** Basal part of P4 leaf blade. **H,** The blade-sheath boundary of P4 leaf primordium. **I,** P4 leaf sheath. **J,** Adaxial epidermis of P5 leaf blade. **K,** Abaxial epidermis of P5 leaf blade**. L,** Lamina joint of P5 leaf. **M,** Abaxial side of P5 leaf sheath. **N,** Adaxial side of P5 leaf sheath. **O,** Adaxial epidermis of P6 leaf blade. **P,** Abaxial epidermis of P6 leaf blade**. Q,** Lamina joint of P6 leaf. **R,** Abaxial side of P6 leaf sheath. **S.** Adaxial side of P6 leaf sheath. Asterisks, arrowheads and arrows indicated trichomes, papillae and stomata, respectively. Scale bars in **A**= 37.5 µm, **B**, **D**-**S** = 50 µm and **C** = 60 µm.

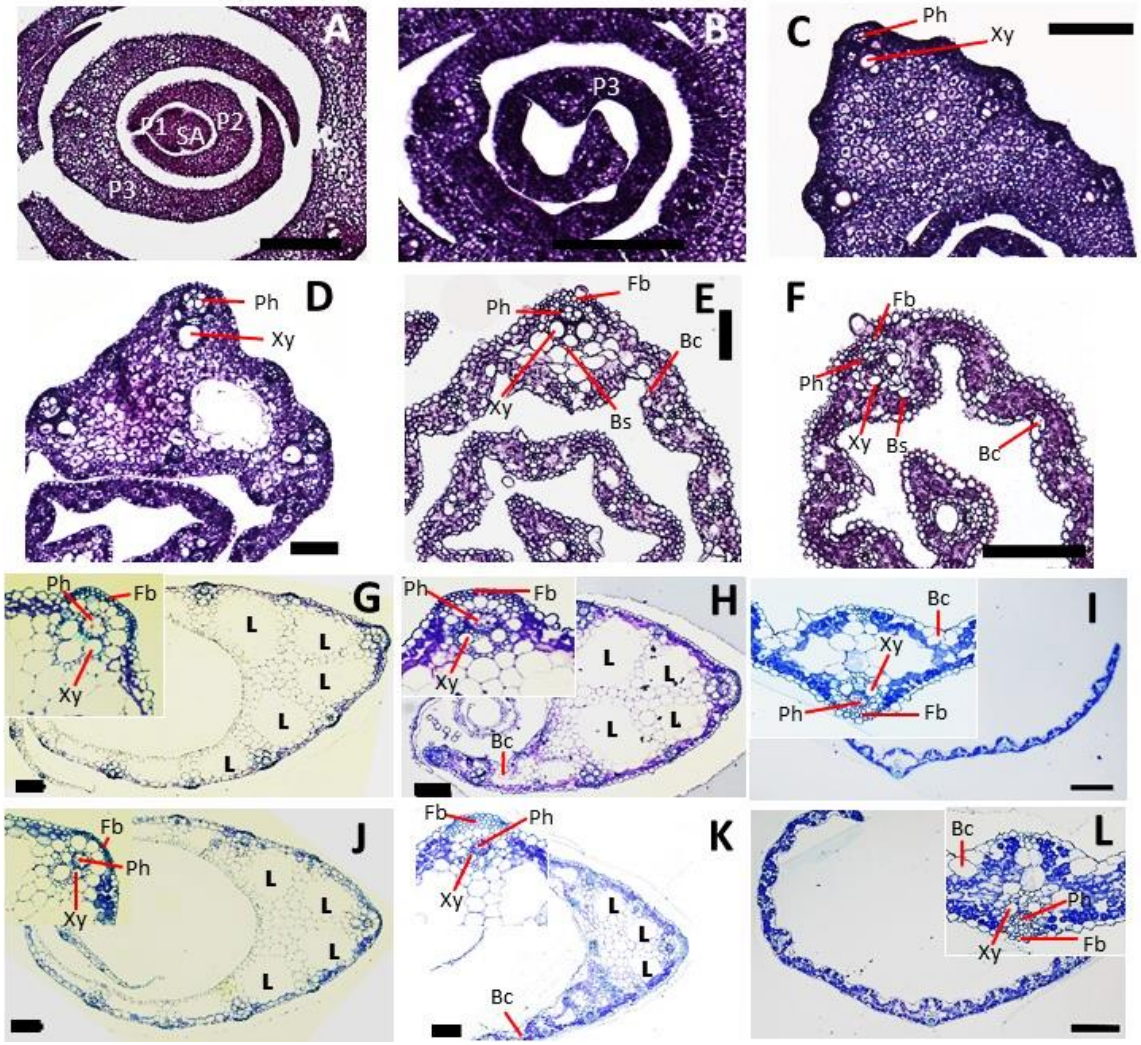

Figure 2-3. Internal structure of wild-type leaves at various stages.

Transverse sections of P1 to P6 leaf primordia at 15 DAS are shown. **A,** P1 to P3 leaf primordia and shoot apex (SA). **B,** P3 leaf blade. **C,** P4 leaf sheath. **D,** Basal part of P4 leaf blade. **E,** Middle part of P4 leaf blade. **F,** Apical leaf blade of P4. **G,** Leaf sheath of P5. **H,** Lamina joint of P5 leaf. **I,** Leaf blade of P5. **J,** Leaf sheath of P6. **K,** Lamina joint of P6 leaf. **L,** Leaf blade of P6. Inset in **G**-**L** showed high magnification views of large vascular tissue. Bc; bulliform cells, Fb; fibre cells, Ph; Phloem, BS; bundle sheath. Scale bars in **A**-**H** and **J**= 100 µm and **I**, **K** and **L**= 250 µm.

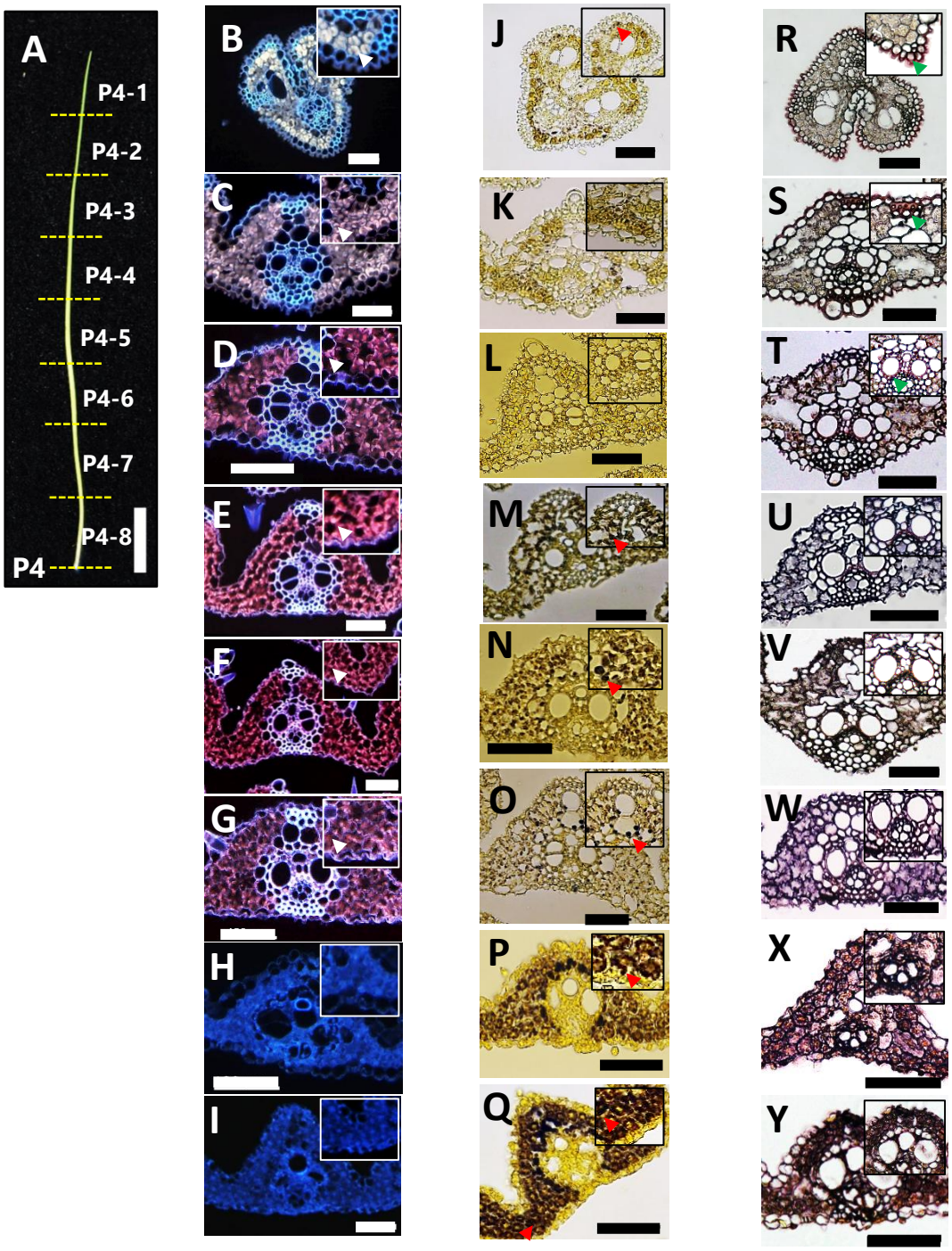

Figure 2-4. Histochemical observation of P4 leaf primordium along the apical-basal axis.

A, Eight segments of dissected P4 leaf primordium along the longitudinal axis (from tip to base; P4-1 to P4-8). **B-I**, Autofluorescence of chloroplasts. White arrowheads indicated chloroplast. **J-Q,** Starch accumulation. Red arrowheads pointed to starch granules. **R-Y,** Lignified cell wall. Green arrowheads indicated lignified tissues. Scale bars in **A** = 1 cm, **B-Y**= 100 μm.

2.4 Discussion

2.4.1 Morphological change during rice leaf development

It is known that leaf differentiation proceeds sequentially in a basipetal manner in grass leaves. However, the timing and relative position of the transition from immature to mature state of leaf characters would be variable among species. Therefore, I examined various characters of the leaves at all stages during development in rice. Morphological analysis revealed that the inner tissues and the surface of P1 to P2 leaf primordia were composed of undifferentiated cells (Figure 2-2A). Most of cellular characters of P3 leaf primordium were undifferentiated state, except for the tip of the leaf primordium showing immature trichomes on the surface (Figure 2-2B) Therefore, the first sign of the cell differentiation were seen at the tip of P3 leaf primordium and the wave of the differentiation signals would proceed from the tip to the base. In contrast, P5 and P6 leaves exhibited mature characters throughout the longitudinal axis of the leaf. The traits included the epidermal structure (trichomes, papilla, stomata), and inner structure (vascular tissues and bulliform cells), and tissue formation (lamina joint). Thus, it indicated that P5 and P6 leaves were mature leaves.

On the other hand, both of surface and inner structures of P4 leaf primordium at the apical and middle parts of the leaf blade showed mature characters (Figure 2-2E, 2-2F and 2-3E, 2-3F), while the basal part of leaf blade and leaf sheath displayed undifferentiated state (Fig. 2-2G, 2-2I and 2-3C, 2-3D). These results indicated that the dynamic transitions of developmental traits occur around the middle to the basal part of the P4 leaf blade. It has been reported that leaf sheath of P4 is located only at the basalmost and shows rapid elongation after the elongation of leaf blade was finished (Itoh *et al.*, 2005). This is consistent with the fact that the basal part of P4 leaf primordium is immature state.

2.4.2 Changes of cellular composition along the apical-basal axis of P4 leaf

The results of morphological and histological analysis indicated the transition zone from immature to mature is present in the middle to the basal part of P4 leaf primordium.

My histochemical analysis also showed that the drastic changes of cellular component occur around the middle and the basal part of P4. Chloroplasts were more differentiated in the apical part than the basal part (Figure 2-4B to 2-4D and 2-4H to 2-4I). Inversely, starch granules were more accumulated in the basal part of P4 leaf blade (Figure 2-4P to 2-4Q). This result is partially consistent with the result of Kusumi *et al.* 2010, showing that younger leaf primordium (length is > 1 cm) accumulated starch grains while older P4 leaves at the middle part (length ≥ 2 cm) did not. Thus, the contrary pattern of chloroplast differentiation to the starch accumulation along the longitudinal axis of P4 leaf would suggest that early boundary of sink-source of rice leaves is established around the middle part of P4 leaf blade. It was reported that mature leaf sheath acts as a temporary sink organ of rice leaves, but also functions as a source before anthesis and about 30% of the grain yield is derived from these parts (Watanabe *et al*., 1997). My results showed that the boundary of the sink-source was at the middle part of the P4 leaf blade, indicating the sink part is independent of differentiation of the leaf blade and sheath in P4. Accordingly, the boundary of sink-source of rice leaves may be variable depending on the leaf and plant stages. The pattern of lignin accumulation is mostly similar to that of cellular character of epidermal structures. Lignin is usually accumulated in the secondary cell walls and its deposition reinforces the cellular and tissue strength. Thus, the lignin deposition should be observed in mature tissues where their growth stopped. This is consistent with my result that lignin accumulation was observed at the distal part of P4 leaf where mature cellular characters were observed.

In summary, my morphological and histochemical analyses indicated that most parts of the P1 to P3 leaf primordia had immature characters, while P5 and P6 leaves were mature. The dynamic transitions of various aspects of developmental and physiological traits occur at the basal part of the P4 leaf blade. In addition, the transition was determined independently of leaf blade and leaf sheath differentiation. Therefore, my analysis suggested that the P4 leaf primordium is the optimal stage of leaf development to uncover the genetic mechanism underlying developmental and physiological transitions during leaf development.

CHAPTER 3

Gene expression change during rice leaf development

3.1 Introduction

Leaves originate from the flank of shoot apical meristem and undergo various developmental events; i.e., axis determination, cell proliferation, cell elongation, cell differentiation, and tissue differentiation. Although various aspects of leaf development have been studied, one of the key events is the mechanism of spatiotemporal control of cell proliferation and cell differentiation. The genetic mechanism underlying the transition from cell proliferation to cell differentiation during leaf development has been the subject of intensive study, because understanding of the mechanism will directly explain how final leaf shape and size are determined in plant.

The duration and activity of cell proliferation during leaf development are regulated under a complex genetic cascade. The genetic factors operating most downstream of the cascade are cell cycle-related genes. Cyclins and their partners, cyclin-dependent kinases (CDKs), are targets of cell division control (Endo *et al.,* 2012 and Lee *et al.,* 2003). In *Arabidopsis*, an altered expression level of the cyclin gene, *CYCD3*, was shown to affect the shape and cell number of leaves by modulating cell proliferation (Gonzalez *et al.,* 2012). Overexpression of the CDK inhibitor gene, *KRP2*, resulted in production of small and serrated leaves, although the temporal patterns of cell division and differentiation were unaffected (Verkest *et al.,* 2005). Several regulators of cell proliferation and cell differentiation processes have been identified. Members of the *TCP* (TEOSINTE BRANCHED1/CYCLOIDEA/PCF) gene family, encoding plant-specific transcription factors, act to regulate multiple developmental pathways, particularly cell proliferation in developing organs. Although the mechanism by which *TCP* genes regulate cell proliferation is largely unknown, some *TCP* genes were shown to directly regulate cell cycle regulators. *TCP20* of *Arabidopsis* binds to the promoter of *CYCB1;1*, which controls cell cycle G2/M progression and positively regulates cell proliferation (Li *et al.,* 2005). *TCP* genes also function as negative regulators or coordinators of cell proliferation during leaf development. In addition to *TCP*, the cooperative action of *GRF* (GROWTH-

REGULATING FACTOR) genes is important for regulating cell proliferation during leaf development. *GRFs* encode putative plant-specific transcription factors and function as positive regulators of cell proliferation, and they are largely expressed in tissues with high degrees of cell proliferation (Kim *et al.,* 2003). Loss-of-function of multiple *GRF* genes showed reduced leaf size and cell number in *Arabidopsis*, suggesting that *GRFs* play redundant roles in modulation of cell proliferation (Gonzalez *et al.,* 2012, Kim *et al.,* 2003 and Liu *et al.,* 2009). *GRF* expression is controlled by the microRNA species, *miR396*, the accumulation level of which is lower in developing leaves and gradually increases during development, with an inverse distribution to that of *GRF* expression (Kim *et al.,* 2003 and Liu *et al.,* 2009). Overexpression of *miR396* affects cell proliferation by reducing cell number, thus resulting in narrow leaves (Liu *et al.,* 2009, Mecchia *et al.,* 2013 and Rodriguez *et al.,* 2010). Although *TCP* and *GRF* transcription factor genes are thought to be important regulators of leaf proliferation, it has been suggested that many genetic factors affect the pattern of leaf proliferation.

The effects of these genetic factors on leaf development have been validated mainly in the model dicotyledonous plant, *Arabidopsis thaliana*. However, the basic pattern of leaf growth is different between monocot and dicot species. In *Arabidopsis*, although the leaf blade and leaf petiole differentiate along the proximal–distal axis during development, cell proliferation activity for leaf blade expansion is observed along both the proximal–distal and mediolateral axes. Recently, proliferative activity was found in the junction of the leaf blade and leaf petiole in early leaf development, suggesting that proliferative cells in this region establish both leaf blade and leaf petiole in a bidirectional manner in *Arabidopsis* (Ichihashi *et al.*, 2011). In contrast, the pattern of leaf growth in grass species, such as maize and rice, is mostly linear, and the proliferating cells are mainly located in the leaf base after establishment of the outline of the leaf (Li *et al.,* 2010 and Nelson, 2011). However, the genetic mechanism regulating the transition from cell proliferation to cell differentiation during rice leaf development is still unclear. For the first step of understanding the mechanism, I analyzed several genetic markers to monitor the developmental and physiological transition of rice leaf primordium.

3.2 Materials and Methods

3.2.1 Plant materials

A rice variety (cv. Taichung 65 (T-65)) was used as wild type. The plants were grown in a greenhouse under natural condition. For expression analysis, P4 leaf primordia of the seedlings about 15 DAS were sampled in three different developmental stages; early, middle and late stages. For observation of shoot apex, the same samples used for the expression analysis were applied to paraffin sections.

3.2.2. RT-PCR and real-time analyses

P4 leaf primordia in three different developmental stages were frozen in liquid nitrogen, and total RNA was extracted using TRIzol reagent (Invitrogen, http://www.invitrogen.com/). First-strand cDNA was synthesized using High-Capacity cDNA Reverse Transcription Kits (Applied Biosystems, USA, http://www.invitrogen.com/) at 25°C for 10 minutes, 37°C for 120 minutes, and 85°C for 5 minutes. Semi-quantitative RT-PCR analysis was performed for appropriate cycles at 95°C for 1 minute, 95°C for 30 seconds, 60°C for 30 seconds, 70°C for 1 minute, and 70°C for 7 minutes.

For real-time PCR, TaqMan assay was performed using TaqMan® Fast Universal PCR Master Mix (2×) (Applied Biosystems) and FAM-labeled TaqMan probes for each gene and a StepOnePlus real-time PCR system (Applied Biosystems). The expression level of each sample was normalized relative to that of an internal control (*OsRAD6*). The averages of three independent assays are shown. The primers and probes for each gene are listed in Table 3-1 and 3-2.

3.3 Results

3.3.1 Screening of marker genes showing dynamic expression pattern in P4 leaf primordium along the apical–basal axis

As described in Chapter 2, P4 is a stage when the dynamic transitions of developmental traits occur. To gain a further understanding of the transition along the longitudinal axis of P4 leaf primordium at the molecular level, I first searched for marker genes reflecting the transition and gradient. For screening, I divided P4 leaves into four parts along the longitudinal axis; i.e., the apical leaf blade, the middle leaf blade, the basal leaf blade, and the leaf sheath (Figure 3-1A). RNA extracted from each part of P4 leaves was subjected to RT-PCR analysis. I first examined the expression patterns of two genes related to physiological events in the leaves. One is *OsCDKB2* encoding a B-type cyclin-dependent kinase with a role in cell cycle progression (Endo *et al*., 2012 and Lee *et al*., 2003). Another is *OsRBCS2* encoding one of the small subunit of RubisCO (ribulose 1,5-biphosphate carboxylase/oxygenase) that accumulates in photosynthetic tissue (Morita *et al*., 2014, Ogawa *et al*., 2012 and Suzuki *et al*., 2007).

RT-PCR results showed that the expression of *OsCDKB2* was higher in the basal leaf blade and leaf sheath but absent in the apical and middle leaf blade of P4 (Figure 3-1B), indicating the cell division activity is high in the basal part of the leaves. *OsRBCS2* was strongly expressed in the apical and middle parts, but was weakly expressed in the basal part of leaf blade and leaf sheath of P4 (Figure 3-1B). This suggests that photosynthetic-related activity is higher in the apical part of P4 than that in the basal part.

Next, I examined the expression patterns of *TCP* and *GRF* genes as potential marker genes for developmental changes in the leaf. It has been reported that *GRF* and *TCP* genes were involved in cell proliferation in leaf development both in rice and *Arabidopsis*. In rice genome, 12 *OsGRFs* (Choi *et al*., 2004) and 26 *OsTCPs* (Sharma *et al*., 2010) have been identified. Among them, I chose *OsTCP1*, *OsTCP3*, *OsTCP12*, *OsGRF9* and *OsGRF10* for RT-PCR analysis. For *OsTCP3* and *OsGRF9*, the difference of expression levels among the four parts of P4 was not observed (Figure 3-1B). *OsTCP1* and *OsGRF10* showed higher expression in the basal leaf blade and leaf sheath of P4, but lower

expression in the apical and middle leaf blade (Figure 3-1B). The expression of *OsTCP12* seems to express in all parts of P4, but it was predominantly observed in the basal part of P4 leaf blade (Figure 3-1B).

In addition to *TCP* and *GRF* genes, one of the *miR396* genes, *pri-miR396c*, was used, because *miR396* has been reported as a negative regulator of *GRF* gene family. *Pri-miR396c* was strongly expressed in the basal and apical leaf blade as well as in the leaf sheath (Figure 3-1B).

The analysis revealed that these six genes (*OsCDKB2, OsRBCS2, OsTCP1, OsTCP12, OsGRF10 and pri-miR396c*) showing differential expression along the apical–basal axis of the P4 leaf. Thus, these genes would be candidates for marker genes monitoring the developmental and physiological change along the apical-basal axis of P4 leaf.

3.3.2 Expression pattern of six marker genes in P4 leaf primordium

To determine the expression dynamics of six marker genes more accurately along the longitudinal axis of P4 leaves, P4 leaf primordium was dissected into eight parts from the top (P4-1) to the bottom (P4-8) (Figure 3-3A) and the expression patterns of marker genes were examined by real-time PCR. In addition, I sampled three different developmental stages of P4, namely early, middle and late stages (Figure 3-2A to 3-2C) and confirmed each growth stage of them by paraffin section. The shoot apex of the early P4 stage showed that P1 leaf primordium had just emerged from the lateral region of the shoot apical meristem (Figure 3-2D). With progression of development, enlarged P1 leaf primordium was observed on the shoot apex (Figure 3-2E and 3-2F). Thus, the three samples of P4 leaf primordia used in this analysis reflect the developmental progression of P1 and possibly other leaf primordia.

Overall, the expression patterns of *OsCDKB2*, *OsGRF10*, and *OsTCP1* showed similar trends. The expression levels of these genes from P4-1 to P4-5 in three developmental stages were low (Figure 3-3B to 3-3D). Particularly, the expression pattern of *OsGRF10* was almost identical to that of *OsCDKB2*, indicating that *OsGRF10* is closely associated with cell division in the regions of the leaf positive for its expression. The expression pattern of *OsTCP1* differed slightly from those of *OsCDKB2* and *OsGFR10*, in that

OsTCP1 was still expressed around the middle part of the P4 leaf (P4-6) (Figure 3-3C), while both *OsCDKB2* and *OsGRF10* were completely downregulated in this region (Figure 3-3B and 3-3D). The expression pattern of *OsTCP12* was unique. Two peaks of expression were observed at the basal and middle parts of the P4 leaf in all developmental stages (Figure 3-3E). One peak was observed around the middle part of P4, and the peak shifted toward the basal parts as development progressed. Another peak was seen at the basalmost part in the three stages. *Pri-miR396c* was expressed in the basal part of the P4 leaf (Figure 3-3F), but its expression pattern was also different from those of *OsCDKB2* and *OsGRF10*. The expression pattern of *pri-miR396c* was characterized by the highest level of expression not in the basalmost region but in P4-7 (Figure 3-3F), although the expression pattern at the late stage was similar to that of *OsTCP1*. The expression pattern of *OsRBCS2* was completely different from those of the other genes examined (Figure 3-3G). The expression level of *OsRBCS2* was highest at the apical part of P4 at the early stage of development, while the peak was not obvious in the middle and late stages (Figure 3-3G). *OsRBCS2* expression was not detected at the basal part of the P4 leaf at any stage of leaf development.

Real-time PCR experiments showed that the expression peaks of all marker genes shifted toward the basal part of the P4 leaf as developmental stage progress, indicating that these genes are influenced by developmental and/or physiological events that proceed in the basipetal direction. As leaf maturation is known to advance in a basipetal manner, these six marker genes would be suitable to monitor developmental transition along the apical–basal axis of P4 leaves.

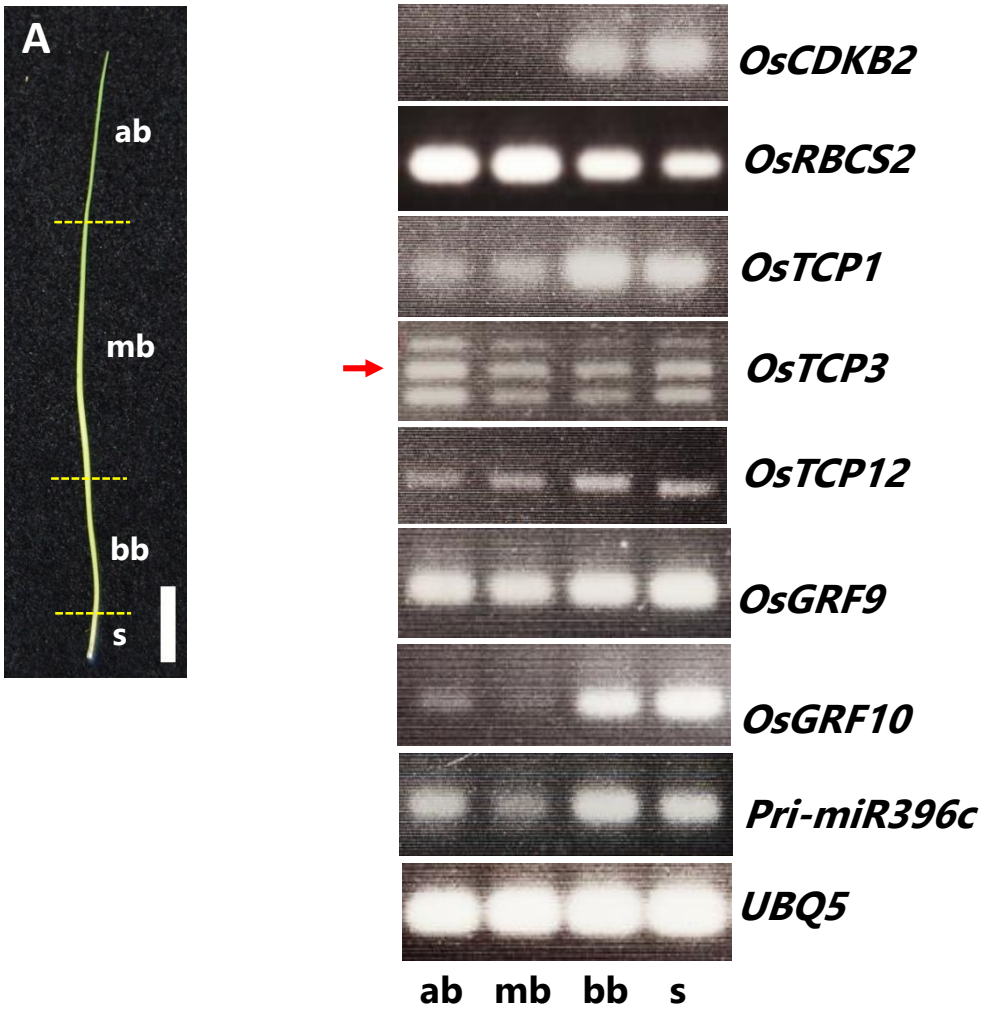

Figure 3-1. Semi-quantitative RT-PCR analysis of eight candidate marker genes in wild-type of P4 leaf primordium.

A, Four segments of P4 leaf. **B,** Expression of eight genes and an internal control, *UBQ5*. ab; apical leaf blade, mb; middle leaf blade, bb; basal leaf blade and s; leaf sheath. Red arrow indicated the correct fragment of *OsTCP3*. Scale bar in **A** = 1 cm.

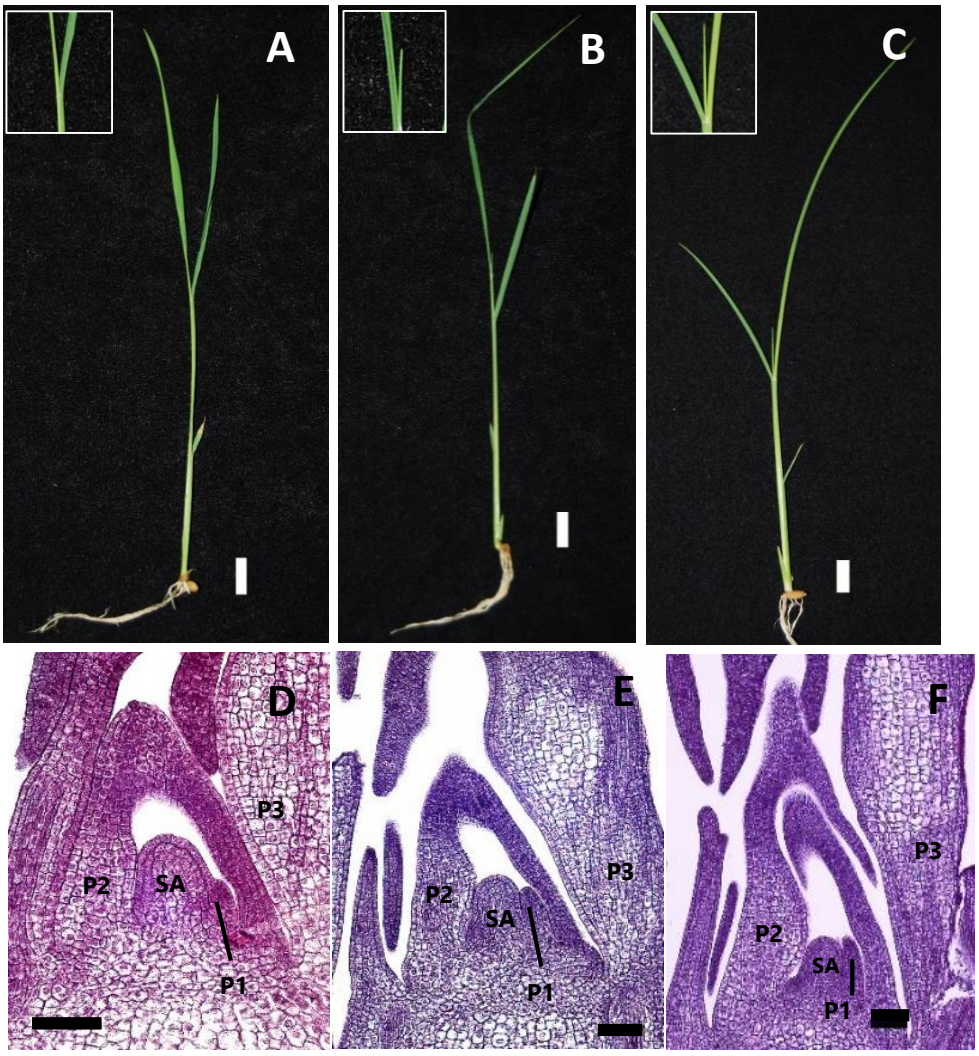

Figure 3-2. P4 leaf and shoot apex at different developmental stages.

A-C, Seedling phenotype when P4 leaf was sampled. **A**, Early stage. Tip of leaf blade of P4 was not observed (inset). **B**, Middle stage. Tip of leaf blade of P4 was just emerged (inset). **C**, Late stage. Tip of leaf blade of P4 was elongating (inset). **D-F**, Longitudinal section of shoot apex (SA) in different developmental stages. **D,** Early stage. **E,** Middle stage. **F,** Late stage. P1 – P3 leaf primordia are labeled. SA; shoot apex. Scale bars in **A-C** = 1 cm, **D-F** = 50 μm.

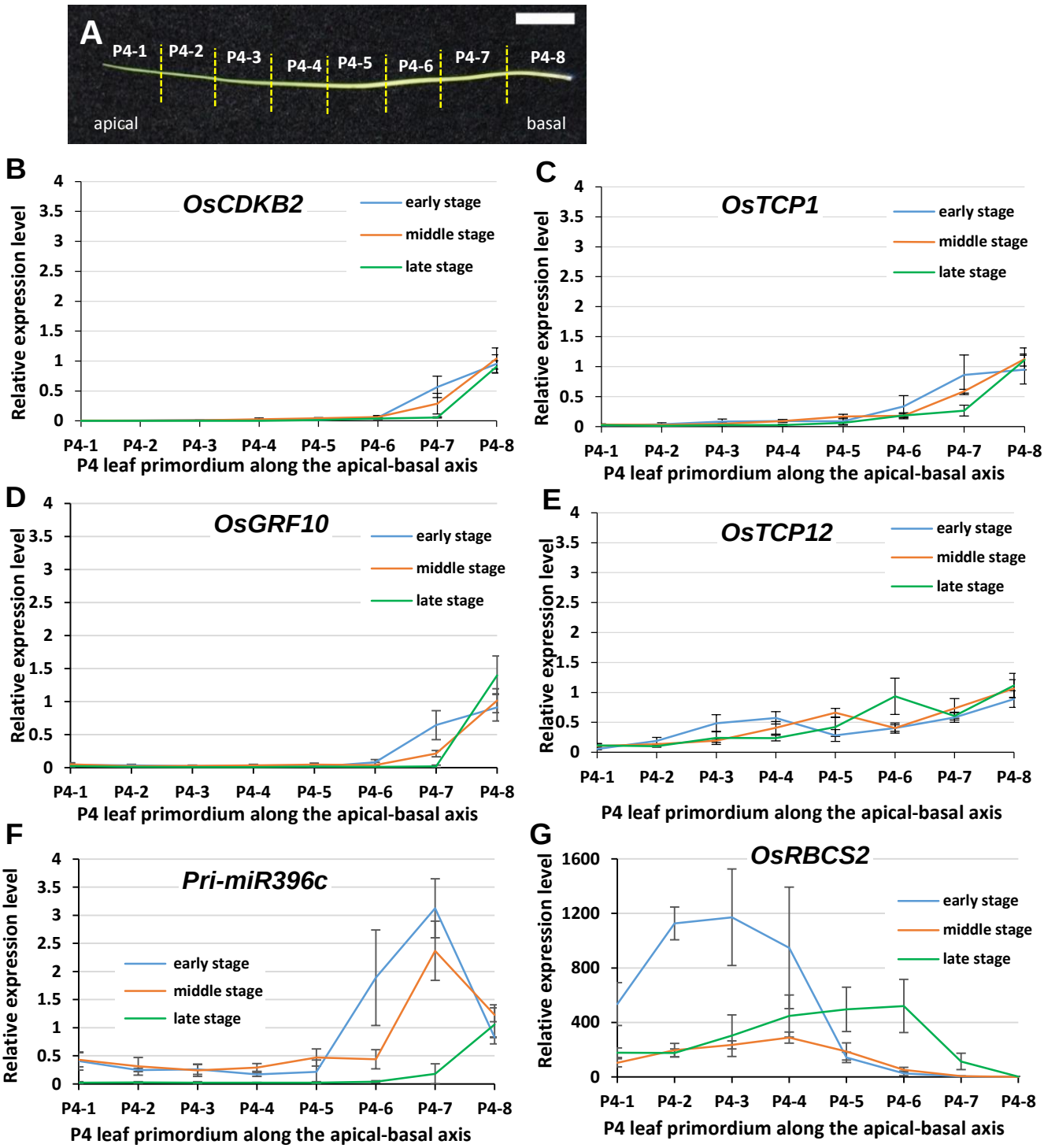

Figure 3-3. Real-time PCR analysis of six marker genes along the longitudinal axis of P4 leaf primordium at different developmental stages.

A, Eight segments of P4 leaf along the apical-basal axis**. B,** *OsCDKB2*. **C,** *OsTCP1*. **D,** *OsGRF10* **E,** *OsTCP12*.. **F,** *Pri-miR396c* **G,** *OsRBCS2*. The numbers along the horizontal axis indicate the position of the P4 leaf along the longitudinal axis as represented in **A**. Expression level was normalized relative to that of an internal control (*OsRAD6*). Scale bar in **A** = 1 cm.

Table 3-1 List of primers for RT-PCR analysis.

Gene	Forward primer	Reverse primer
OsCDKB2	5’-GGAATCCCTCGAAAGTGTCTGA-3’	5’-TCGTACTGCAGCATTTTCTCAAG-3’
OsRBCS2	5’-ATGCAGGTGTGGCCGATT-3’	5’-CAGGGCACCCACTTGGAA-3’
OsTCP1	5’-GGAGGTAGCACAAGTGCACT-3’	5’-CCAATGACATGCGCAGCAGCAG-3’
OsTCP3	5’-CGCGCCACCTGAATTTGT-3’	5’-CTGCATGTCCTTCCTAGAATTCTCT-3’
OsTCP12	5’-GAGCGCCAGCGACTCGTA-3’	5’-TTAAAGAAGAACAGATCAAAACCAGAGA-3’
OsGRF9	5’-GTATTGGCGTTACCCATGCAT-3’	5’-CATAAGAACTGAAAATCGCAATTAGC-3’
OsGRF10	5’-CCCATCTTCTTTCTTCATTCCTCTT-3’	5’-CTTCTCCTCATCCATTCTGACAACT-3’
Pri-miR396c	5’-GCTTGCAGCCATAAAGCTCTTC-3’	5’-TGCCATCTGCCTCTCTCTTGA-3’
UBQ5	5’-ACCACTTCGACCGCCACTACT-3’	5’-ACGCCTAAGCCTGCTGGTT-3’

Table 3-2 List of primers and probes for real-time PCR analysis.

Gene	Forward primer	Probe
OsCDKB2	Forward primer 5'-GGAATCCCTCGAAAGTGTCTGA-3' Reverse primer 5'-TCGTACTGCAGCATTTTCTCAAG-3'	5'-TCCATGGTCTCGACGCTGATGCTC-3'
OsRBCS2	Forward primer 5'-ATGCAGGTGTGGCCGATT-3' Reverse primer 5'-CAGGGCACCCACTTGGAA-3'	5'-CGAGACCCTCTCTTACCTGCCACCG-3'
OsTCP1	Forward primer 5'-GGAGGTAGCACAAGTGCACT-3' Reverse primer 5'-CCAATGACATGCGCAGCAGCAG-3'	5'-CGGTTGGTTGGTTGGTTGGTTTTCCATCG-3'
OsTCP12	Forward primer 5'-GAGCGCCAGCGACTCGTA-3' Reverse primer 5'-TTAAAGAAGAACAGATCAAAACCAGAGA-3'	5'-TCCGGTGTGTGCCCCGCATT-3'
OsGRF10	Forward primer 5'-CCCATCTTCTTTCTTCATTCCTCTT-3' Reverse primer 5'-CTTCTCCTCATCCATTCTGACAACT-3'	5'-CCACCAAGAACCCCAAACCTTACCTCC-3'
Pri-miR396c	Forward primer 5'-GCTTGCAGCCATAAAGCTCTTC-3' Reverse primer 5'-TGCCATCTGCCTCTCTCTTGA-3'	5'-CCTCTCTCTTTCTACGGCTGTGGAGCTGA-3'
OsRAD6	Forward primer 5'-CGCACGACAACAACATCATG-3' Reverse primer 5'-TCCCACGGCGTGTCATC-3'	5'-TCTGGAACGCCGTCATATTCGGACC-3'

3.4 Discussion

3.4.1 Expression patterns of marker genes and their possible functions in leaf development

I selected marker genes based on their expression changes along the apical–basal axis of the P4 leaf. Unfortunately, with the exception of *OsCDKB2* and *OsRBCS2*, the biological functions of most of these marker genes have not been elucidated. *OsCDKB2* encodes a B-type cyclin-dependent kinase that is required for the transition from G_2 to M (mitosis) phases of the cell cycle (Endo *et al*., 2012 and Lee *et al*., 2003). Thus, tissues expressing *OsCDKB2* reflect sites of active cell division. Real-time PCR experiments using wild-type P4 leaves at three stages indicated an expression peak of *OsCDKB2* in the basalmost part of P4. This was consistent with the observation that the cell division zone was located at the base and the cell maturation progress in a basipetal manner in grass species. *OsRBCS2* is a member of the RubisCO small subunit multigene family in rice. It has been reported that *OsRBCS2* to *OsRBCS5* are highly expressed in the rice leaf blade, and there is a positive correlation between the expression level of *RBCS* and maximal Rubisco contents (Morita *et al*., 2014 and Ogawa *et al*., 2012). In addition, *RBCL* and *RBCS* gene have been reported that involve in the final step of chloroplast differentiation (Kusumi *et al.*, 2010a, 2010b). Thus, the sites of *OsRBCS2* expression are considered to be regions of active photosynthesis. Although the expression peak of *OsRBCS2* shifted from the apical to the basal part with progression of leaf development, the peak of expression was observed in the early stage with the lowest level in the middle stage (Figure 3-3G). This was not consistent with the prediction that photosynthetic activity would change sequentially among the three stages. Although I could not determine why the expression level did not change gradually among the stages, it is possible that the *OsRBCS2* expression level is sensitive to environmental cues that I could not predict.

The *TCP* transcription factor genes are known to be involved in multiple developmental pathways, and some have been shown to play key roles in the coordination of cell proliferation and cell differentiation in leaves (Gonzalez *et al*., 2012). *TCP* proteins are generally classified into two main classes based on differences in their conserved domains; i.e., class I and class II. Class I *TCP* proteins have been suggested to promote plant growth

and cell proliferation, while class II proteins act as repressors of cell proliferation. *OcTCP1* (also has known *PCF5*) belongs to class II and is involved in lateral organ development (Martín-Trillo and Cubas, 2010). Although its exact function has not been elucidated, *OsTCP1* may act as a negative regulator of cell proliferation during leaf development. The expression pattern of *OsTCP1* is very similar to that of *OsCDKB2*, but a low level of expression remained in regions where *OsCDKB2* expression was completely down-regulated (e.g., P4-6) (Figure 3-3C and 3-3B, respectively). Thus, it is possible that *OsTCP1* functions in spatial coordination of cell proliferation by suppressing cell division in the basal part of the leaf. *OsTCP12* belongs to the class I *TCP* genes that support the cell proliferation process in plant growth, although context-dependent effects of some class I *TCP* genes were reported in *Arabidopsis*. It has been reported that *OsTCP12* (or *OsTCP19*) is expressed not only in leaves but also in endosperm, roots, and the early panicle (Sharma *et al*., 2010), and my expression analysis suggested that it was expressed in the P4 leaf primordium with two peaks along the leaf axis—the first peak was seen in the middle part of P4 with the other in the basalmost part (Figure 3-3E). Phylogenetic analysis suggested that the closest homologs of *OsTCP12* are *TCP14*/*TCP15* in *Arabidopsis* (Yao *et al*., 2007). Although developing leaves of *tcp14*/*tcp15* double mutants do not show an obvious phenotype, quantitative imaging analysis and SRDX fusion experiments indicated that *TCP14*/*TCP15* modulate leaf shape by repressing cell proliferation. Interestingly, *TCP14* is expressed in young trichomes of developing leaves and plants expressing SRDX-fused *TCP14* showed highly branched trichomes, indicating that *TCP14* also regulates trichome development (Kieffer *et al*., 2011). Although it is unclear whether the function of *OsTCP12* in rice is similar to that of *TCP14* in *Arabidopsis*, and whether the *OsTCP12* is expressed in trichomes, it is possible that the first peak (middle part of P4) of *OsTCP12* was involved in epidermal differentiation of leaves. In support of this suggestion, my morphological analysis indicated that the position of the second peak of *OsTCP12* expression was close to the boundary of tissue with/without epidermal structures, such as trichomes and papillae. However, expression analysis using various mutants suggested another possible function of *OsTCP12*, as discussed in Chapter 4.

GRF genes have been shown to play crucial roles in growth and development of leaves by regulating cell proliferation in a redundant manner in *Arabidopsis* (Gonzalez *et al*., 2012). Twelve *GRF* genes were identified in the rice genome, most of which were

preferentially expressed in young and growing tissues (Choi *et al*., 2004). Although there is no direct evidence that rice *GRFs* promote cell proliferation in leaves, a double mutant of *OsGRF6* and *OsGRF10* showed a semi-dwarf phenotype (Liu *et al*., 2014). Thus, *OsGRF10* may positively regulate leaf growth by controlling cell proliferation. In fact, my expression analysis indicated that the pattern of expression change of *OsGRF10* was almost identical to that of the cell division marker, *OsCDKB2* (Figure 3-3B and 3-3D).

It has been reported that *miR396* regulates the expression of their target genes, *GRFs*, in both *Arabidopsis* and rice (Debernardi *et al*., 2012 and Sunkar *et al*., 2005). *OsmiR396c* is one of multiple *OsmiR396* loci in rice, and 11 of the 12 *OsGRFs* in the rice genome have a *miR396* target site (Choi *et al*., 2004). It has been shown that overexpression of *OsmiR396d* caused a similar effect to the knockdown of *OsGRF6* and *OsGRF10*, and downregulation of the expression of most GRFs (Liu *et al*., 2014). Thus, it is likely that *miR396* negatively regulates *GRF* expression during leaf development. The expression level of *OsmiR396c* was highest in P4-7, not in the basalmost part of the P4 (P4-7), in the early and middle stages in wild-type controls (Figure 3-3F). Based on the *OsCDKB2* expression pattern, P4-7 was predicted to be a transition region where active cell division is inactive. Thus, the expression pattern of *OsmiR396c* suggested that *OsmiR396* acts to maintain the transition region by suppressing *OsGRFs*, although the accumulation pattern of mature *miR396* along the P4 leaf axis should be determined in future studies.

CHAPTER 4

Effects of altered external and genetic factors on rice leaf development

4.1 Introduction

Plant growth and development are influenced by various internal and external factors, such as genetic, hormonal and environmental ones. As an environmental factor, light is the most well studied factor for plant growth. It is known that quality and duration of light exposure are essential to seed germination and flowering in some plants. Moreover, light determines morphogenesis of seedlings. For instance, dark-grown seedlings showed etiolated phenotypes, e.g., distinct apical hook, elongated hypocotyls, rolled cotyledons and undeveloped chloroplast (Yang *et al.,* 2007). In contrast, light-grown seedlings showed suppressed hypocotyls, expanded leaves and normal chloroplast differentiation (Chory *et al.,* 1996). Analyses for genetic regulation of this phenomenon, photomorphogenesis, have been done extensively, which contribute to good understanding how plant can respond to external factors (Nomura *et al*., 2000, Ogawa *et al*., 2012 and Zhu *et al*., 1998).

Plant hormones (phytohormones) are also known to be internal factors affecting plant growth and development. Genetic and physiological studies have revealed functional roles of each plant hormone for plant growth and development. Plant hormones are required for various aspects of plant growth and development, and roles of several plant hormones on the leaf development have been suggested. For example, GA is known to control leaf growth. The maximum site of GA biosynthesis is located in the division zone of leaf primordia where cell proliferation is active. In contrast, GA catabolism is activated at the onset of leaf elongation (Nelissen *et al.,* 2012). Brassinosteroid (BR) and auxin are also necessary for normal leaf growth. It was reported that loss-of-function of BR and auxin biosynthesis genes affect leaf shape and size in *Arabidopsis*, maize and rice (Zhiponova *et al.,* 2013, Nakaya *et al.,* 2002, Sakamoto *et al.,* 2013 and Zhang *et al.,* 2009, Yoshikawa *et al*., 2014).

On the other hand, it has been reported that many genetic factors affecting leaf development (Gonzalez *et al.,* 2012, Verkest *et al.,* 2005, Liu *et al.,* 2009, Mecchia *et al.,*

2013 and Rodriguez *et al.*, 2010). These include genes regulating various processes of leaf development, such as axis determination, tissue differentiation, cell division and cell elongation process. Mutants defective in these processes show characteristic phenotypes in final shape and size of the leaf.

In most cases, although the morphological change of the leaves for these factors were described, the molecular changes occurring during leaf development and leading to the final morphology have not been clarified. Therefore, to understand how internal and external factors affect leaf development in rice, effects of treatment of some plant hormones and darkness on rice leaf development were analyzed using molecular markers. In addition, the expression change of the marker genes in several leaf morphogenetic mutants was also examined.

4.2 Materials and Methods

4.2.1 Plant materials

Nipponbare was used for plant hormone treatments. As leaf morphogenetic mutants, *liguleless*, *plastochron1-4*, *drooping leaf-5*, *dwarf18-h*, *dwarf1-3*, *dwarf61-2* and *precocious,* which are maintained in our laboratory were used.

4.2.2 Phytohormone treatments and growth conditions

Nipponbare seeds were sterilized with 1% NaClO (Sodium hypochloride solution) for 60 min and washed with the distilled water 3 times. They were cultured on Murashige and Skoog (MS) medium contained various phytohormones at the different concentrations. As an auxin, 10^{-7} M 2,4-dichlorophenoxyacetic acid (2,4-D), as a gibberellic acid (GA) 10^{-6} M GA_3, as a cytokinin (CK), 10^{-6} M kinetin, as a brassinosteroid (BR), 10^{-6} M 24-epiBL were used. For dark and light conditions, sterilized seeds were sown on MS medium under continuous light and were grown in the culture boxes covered with and without aluminium foil. Seedlings in all treatments were grown in a growth chamber under continuous light at 28°C. For morphogenetic mutant, seeds were sterilized and sown on the soil.

4.2.3 Morphological analysis

After sowing, the number of emerged leaves of the seedlings in hormone treatments, except for in dark condition were determined. Leaf length of P4 was measured when the tip of P4 leaf blade was just emerged from 4^{th} leaf both in hormone treatments and mutants. At least ten seedlings were used for the measurements. To confirm the stage of P4 leaf, P1 to P3 leaf primordia and SAM were sampled and analyzed by using paraffin section as describe in Chapter 2.

4.2.4 Gene expression analysis

Dissected P4 leaf primordia used for morphological analysis, including plant hormone- and darkness-treated plants, and various morphogenetic mutants, were divided into eight segments and they were designated as P4-1 to P4-8 along the longitudinal axis. RNA

extraction of these parts and gene expression analysis were performed by the same method as described in Chapter 3.

4.3 Results

4.3.1 Phenotypic analysis of rice seedling under the treatment of several plant hormones and darkness

- Auxin (2,4-D)

Rice seedlings grown on the medium containing 2,4-D at 18 days after sowing (DAS) showed a short stature and a short root phenotype (Figure 4-1B and 4-1C). Generally, leaf emergence of 2,4-D-treated plants was similar to that of wild-type. It was comparable to that of wild-type at the early growth stage (2-6 DAS), and slightly lower at the middle and late growth stages (6-18 DAS) (Figure 4-1D). Next, the leaf length of wild-type and 2,4-D-treated seedlings were measured. Both of leaf blade and sheath of 2,4-D-treated seedlings were significantly shortened (Figure 4-1E). Thus, 2,4-D treatment does not affect the leaf emergence, but negatively affect the entire growth of the leaf.

- Brassinosteroid (BR)

The seedlings grown on MS medium contained with BR showed a short stature and excess bending of lamina joint of the leaves (Figure 4-2B and 4-2C). The number of emerged leaves was lower than that of wild-type throughout their growth stages, except at 6 DAS (Figure 4-2D). Length of BR-treated leaf blade and sheath are significantly shortened (Figure 4-2E). Accordingly, BR influences both the leaf emergence and the leaf growth in addition to the lamina joint bending.

- Cytokinin (CK)

CK-treated seedlings exhibited shorter leaves and over-production of longer roots (Figure 4-3B and 4-3C). The leaf emergence was lower than that of wild-type throughout their growth stages (Figure 4-3D). The length of leaf blade and sheath was significantly shorter than that of wild type (Figure 4-3E). Thus, CK affects both the leaf emergence and the leaf growth, which is similar to that BR. However, the effect on the growth of leaf sheath was more significant than that of BR.

- Gibberellins (GA)

GA treatment was different from other plant hormones in which GA-treated seedlings produced longer leaves and showed higher stature than that of wild-type control (Figure 4-4A to 4-4D). Although the number of emerged leaves was similar to that of wild-type control in the early growth stage (2– 4 DAS) (Figure 4-4E), it became gradually lower than that of wild type in the later developmental stage (6–16 DAS). Leaf length of all GA-treated leaves was significantly longer than that of wild type (Figure 4-4F). The results indicate that GA has a positive effect on leaf growth but negative on leaf emergence.

- Darkness

Dark-grown seedlings showed a typical etiolated phenotype, i.e., high stature with yellowish leaves (Figure 4-5B and 4-5D). The 4th leaf was emerged at 10 DAS in light condition, while the 4th leaf was at 14 DAS in dark condition. Thus, it was expected that leaf emergence of dark-grown seedling was lower than that of light-grown seedling. Then, the size of those leaves was measured. Although the length of coleoptile and leaf sheath was elongated, the length of 2nd and 3rd leaf blade was not significantly changed (Figure 4-5E). The results indicate that dark condition mainly enhances the expansion of coleoptile and leaf sheath.

These results indicate that four plant hormones and dark condition differently influence on the leaf development. Thus, each factor is expected to affect gene expression profile during leaf development in a different way.

4.3.3. Gene expression analysis in hormone-treated plants

After measuring leaf length, the dissected P4 leaf primordium of the 5th leaf of various hormone-treated seedlings, was applied to the expression analysis using marker genes. Exceptionally, P4 leaf primordium of the 4th leaf of the GA-treated plant was used due to the slow leaf emergence. The P4 leaf primordium was further dissected into eight parts and expression profile of five marker genes, *OsCDKB2*, *OsTCP1*, *OsTCP12*, *OsGRF10*, *pri-miR396c,* in these eight parts were analyzed by real-time PCR. In addition, to confirm the stage of P4 leaves, shoot apices of each condition was examined by paraffin sections

(Figure 4-7A to 4-7D). For comparison of gene expression pattern between wild-type and each condition, the expression pattern of wild-type P4 leaf in the three growth stages was reconstructed from the data in Chapter 3 (Figure 4-6)

- Auxin (2,4-D)

The shoot apex of 2,4-D-treated seedling showed that P1 leaf primordium had just emerged from the flank of SAM (Figure 4-7A), indicating that P4 leaf primordium sampled was in early P4 stage. However, expression patterns of five genes along the apical-basal axis of 2,4-D-treated P4 leaves were similar to that of wild-type in the middle stage (Figure 4-6B and 4-7E). This suggests that auxin may affect progression of leaf stage. Although expression trend of each gene was generally similar to that of wild-type, expression pattern of *OsTCP12* in 2,4-D-treated P4 leaf was different from that of wild-type. In wild-type, two peaks of *OsTCP12* expression were observed at the basal and middle parts of the P4 leaf, but only one peak at the leaf base (P4-8) was detected in 2,4-D-treated P4 leaves. Thus, the results indicated that 2,4-D treatment does not affect the expression pattern of most of the marker genes other than that of *OsTCP12*.

- Brassinosteroid (BR)

P1 leaf primordium of BR-grown seedlings was similar to that of wild-type in the middle stage (Figure 4-7B). Compared with the gene expression patterns of the wild-type in the middle stage (Figure 4-6B), expression pattern of *OsTCP1* and *OsGRF10* was not significantly altered. Interestingly, expression level of *OsCDKB2* was elevated throughout P4 leaf along the longitudinal axis (Figure 4-7F). In addition, the expression pattern of *pri-miR396c* was altered, that is, the expression peak at the P4-7 was lost (Figure 4-7F). Expression change of *OsTCP12* was also observed in BR-treated leaf. Similar to the expression change in the auxin-treated plants, the one peak of the *OsTCP12* was not observed at the middle part of P4 leaf. Accordingly, BR affects expression level of *OsCDKB2* in the entire of the P4 leaf and the pattern of *pri-miR396c* and *OsTCP12* by diminishing the expression peak.

- Cytokinin (CK)

Shoot apex of CK treatment plants indicated that the stage of P4 was predicted to be the early or middle stage (Figure 4-7C). Expression pattern of five marker genes in CK treatment was similar to that of 2,4-D treatment (Figure 4-7E and 4-7G), that is, only one peak of *OsTCP12* expression was observed at the base of the P4 leaf.

- Gibberellins (GA)

Based on the stage of P1 in the shoot apex of the GA-treated plants, the stage of P4 sampled here was predicted to be the middle stage (Figure 4-7D). Expression patterns of five marker genes, *OsCDKB2, OsGRF10, OsTCP1, OsTCP12* and *pri-miR396c*, in the GA-treated plants were also similar to those in wild-type controls at the middle stage (Figure 4-6B and 4-7H). The level of the *pri-miR396c* expression was decreased in the basal parts and the expression was almost lost in the apical and middle part of the leaf. The expression peak of *OsTCP12* was lost in the middle part of the leaf, which is similar to other conditions (Figure 4-7H). Thus, GA affects expression level of *pri-miR396c* in the entire of the P4 leaf and the pattern of *OsTCP12.*

4.3.3.3 Gene expression analysis in various morphogenetic mutants

Many mutations affecting leaf morphogenesis have been identified in rice. To understand the relationship between mutant phenotype and the process of leaf development, I performed expression analysis of five genes—*OsCDKB2, OsGRF10, OsTCP1, OsTCP12*, and *pri-miR396c*—in the P4 leaf primordium of seven known mutants showing defects in leaf morphogenesis.

- ***liguleless (lg)***

The *lg* mutant completely lacks ligules and lamina joints (Figure 4-8A) (Lee *et al*., 2007). The causal gene, *OsLG1*, encodes an SBP (SQUAMOSA promoter Binding Protein) domain-containing protein and is specifically expressed in the ligule, lamina joint, and the base of the leaf sheath of the leaf (Lee *et al*., 2007). Based on the stage of P1 in the shoot apex of the *lg* mutant, the stage of P4 sampled here was predicted to be the middle stage (Figure 4-8H). The expression patterns of the five marker genes in the *lg* mutant (Figure 4-

9A) were almost identical to those of wild-type controls in the middle stage (Figure 4-6B). These observations indicated that the *OsLG1* gene is not involved in the process of leaf development other than in ligule and lamina joint differentiation along the apical–basal direction.

- ***drooping leaf* (*dl*)**

The midrib is a structure that is formed along the midvein of the leaf blade to maintain an upright angle of the leaf. The *dl* mutants show a defect of midrib formation that causes a drooping leaf phenotype (Figure 4-8B) (Yamaguchi *et al*., 2004). *DL* encodes a member of the YABBY family of transcriptional regulators, which functions in cell proliferation in the central domain of the leaf (Yamaguchi *et al*., 2004 and Ohmori *et al*., 2011). Based on the stage of P1 in the shoot apex of the *dl* mutant, the stage of P4 sampled here was predicted as the middle stage (Figure 4-8I). The expression patterns of *OsCDKB2*, *OsGRF10*, *OsTCP1*, and *pri-miR396c* in *dl* mutants were similar to those of the wild-type controls in the middle stage (Figure 4-6B and 4-9B). However, the expression level of *OsTCP12* was elevated in the middle part of the leaf. The position of the expression peak of *OsTCP12* relative to the leaf axis was unaffected.

- ***dwarf61* (*d61*)**

The *d61* mutant showed a dwarf phenotype caused by inhibited elongation of the culm, and also showed reduced leaf bending at the lamina joint and shorter leaf sheath (Figure 4-8C) (Yamamuro *et al*., 2000). The *d61* mutant has a mutation in the *OsBRI1* gene, which encodes a brassinosteroid (BR) receptor kinase (Yamamuro *et al*., 2000 and Sakamoto *et al*., 2013). Based on the stage of P1 in the shoot apex of the *d61* mutant, the stage of P4 sampled here was predicted to be the middle stage (Figure 4-8J). The expression patterns of *OsCDKB2*, *OsGRF10*, *OsTCP1*, and *pri-miR396c* in the *d61* mutant were similar to those in wild-type controls in the middle stage, although the level of the *OsTCP12* expression was elevated in the apical and middle parts of the leaf (Figure 4-6B and 4-9C).

- ***dwarf1* (*d1*)**

The *d1* mutant has a mutation in the gene encoding the α-subunit of the heterotrimeric G protein, which affects plant height and seed size (Ueguchi-Tanaka *et al*., 2000). The leaf length of the *d1* mutant is shortened compared with the wild-type (Figure 4-8D, Table4-1). Based on the stage of P1 in the shoot apex, the stage of P4 in *d1* sampled here was predicted to be the early stage (Figure 4-8K). Despite this early stage, the expression patterns of *OsCDKB2*, *OsGRF10*, and *OsTCP1* were similar to those of wild-type controls in the middle stage (Figure 4-6B and 4-9D). In addition, the expression patterns of *pri-miR396c* and *OsTCP12* were very different from those of the wild-type. The expression peak of *OsTCP12* was detected at P4-4 (Figure 4-9D), in contrast to the peak seen at the early stage in wild-type (Figure 4-6A), although expression levels in the basal part were higher than those in the wild-type controls. The expression pattern of *pri-miR396c* was similar to that in the late stage of wild-type controls (Figure 4-6C and 4-9D). Thus, the expression patterns of multiple genes in the P4 leaves of *d1* were markedly disturbed.

- ***dwarf18* (*d18*)**

The *d18* mutant shows a dwarf phenotype that is caused by a defect in the gibberellin (GA) biosynthetic gene *OsGA3ox2* (Sakamoto *et al*., 2004) (Figure 4-8E). As leaf elongation of *d18* is severely affected (Table 4-1), I sampled four rather than eight parts of the *d18* P4 leaf. Based on the stage of P1 in the shoot apex, the stage of P4 in *d18* was predicted to be the early stage (Figure 4-8L). Although, it is difficult to compare gene expression patterns between four parts of *d18* and eight parts of wild-type controls, the changes in expression of *OsCDKB2*, *OsGRF10*, *OsTCP1*, and *pri-miR396c* along the leaf axis were similar (Figure 4-9E). This pattern suggested that the P4 leaf of *d18* showed a similar expression profile to the wild-type, despite the markedly reduced length of P4 in the mutant (Table 4-1).

- ***plastochron1* (*pla1*)**

The characteristic phenotype of the *pla1* mutant is rapid production of short leaves (Figure 4-8F) (Itoh *et al*., 1998). *PLA1* encodes a member of the cytochrome P450 family,

CYP78A11, the substrate of which is unknown (Miyoshi *et al*., 2004). It was suggested previously that the shortened *pla1* leaf is due to precocious maturation of leaf primordia (Kawakatsu *et al*., 2006). Based on the stage of P1 in the shoot apex, the stage of P4 leaf primordium of *pla1* was predicted to be the middle stage (Figure 4-8M). However, expression patterns of *OsCDKB2*, *OsGRF10*, and *OsTCP1* were similar to the late stage of the wild-type control (Figure 4-6C and 4-9F). The expression of *pri-miR396c* showed an intermediate pattern between middle and late stages (Figure 4-6B, 4-6C and 4-9F), whereas the expression peak of *OsTCP12* was the same as that of wild-type controls in the middle stage (Figure 4-6B and 4-9F). Thus, *pla1* affects the relative positions of the marker gene expression peaks.

- ***precocious* (*pre*)**

PRE gene encodes the allene oxide synthase (*AOS*) that is involved with jasmonic acid (JA) biosynthesis. Although it is well known that JA is involved with the response to a range of stresses in plants (Avanci *et al.*, 2010), *pre* mutant displays a production of longer leaf and precocious transition of juvenile phase (Isono *et al*., unpublished results) (Figure 4-8G and Table 4-1). Based on the stage of P1 in the shoot apex, the stage of P4 leaf primordium of *pre* was predicted to be the late stage (Figure 4-8N). Expression patterns of *OsCDKB2* and *OsGRF10* was similar to those of wild-type in the late stage (Figure 4-6C and 4-9G), while *OsTCP1*, *pri-mR396c* were similar to those of wild-type in the middle stage (Figure 4-6B and 4-9G). In addition, expression level of *OsTCP12* was higher than that of wild-type. Thus, *pre* mutation affects the relative positions of the expression peaks among the marker genes and expression level of *pri-mR396c* and *OsTCP12*.

These results indicated that marker gene expression pattern was affected in *dl*, *d61*, *d1*, *pla1* and *pre* mutants, but not in the *lg* mutant. Although I could not determine conclusively whether expression pattern of the marker genes was altered in *d18*, the trend of the expression profile was globally conserved compared to that of the wild-type controls. The results indicated that alteration of marker gene expression patterns is differed among the mutants, and the sensitivity of *pri-miR396c* and *OsTCP12* expression changes was high, while that of *OsCDKB2*, *OsGRF10*, and *OsTCP1* was low.

4.3.3.2 Expression analysis of *OsRBCS2* in dark-grown wild-type plants and in various morphogenetic mutants

In Chapter 3, the expression change of *OsRBCS2* along the longitudinal axis of the P4 leaf was not so obvious, except for that in the early stage, and the expression level was too different from that of the other five marker genes (Figure 3-3G). To confirm whether expression change and level of *OsRBCS2* reflect photosynthetic activity in P4 leaf, *OsRBCS2* expression pattern in dark-grown P4 leaf was observed.

Based on the stage of P1 in the shoot apex of the light- and dark-grown seedlings, the stage of P4 sampled here was predicted to be the middle stage (Figure 4-10A and 4-10B). The expression level of *OsRBCS2* in the light-grown seedling was highest at the middle part of P4, while the peak was not obvious in the dark-grown seedling (Figure 4-10C). Thus, the expression peak and level of *OsRBCS2* depends on light exposure. However, this pattern of the expression is not parallel to that of chloroplast differentiation along the longitudinal axis of P4 leaf. That is, chloroplast differentiation was more prominent at the tip of P4 leaf than that in the middle of the P4 as described in Chapter2. This indicates that *OsRBCS2* expression does not simply reflect the maturation and differentiation of chloroplasts, and may not reflect photosynthetic activity.

I also examined expression pattern of *OsRBCS2* in various leaf morphogenetic mutants. Expression level of *OsRBCS2* was varied among mutants (Figure 4-10D). Expression level in *lg* mutant is highest and that in *d18h* is lowest. The expression peak was generally observed at sub-apical part of the P4 leaves rather than tip of P4, although some mutants have a shifted peak to the corresponding stage of the wild-type.

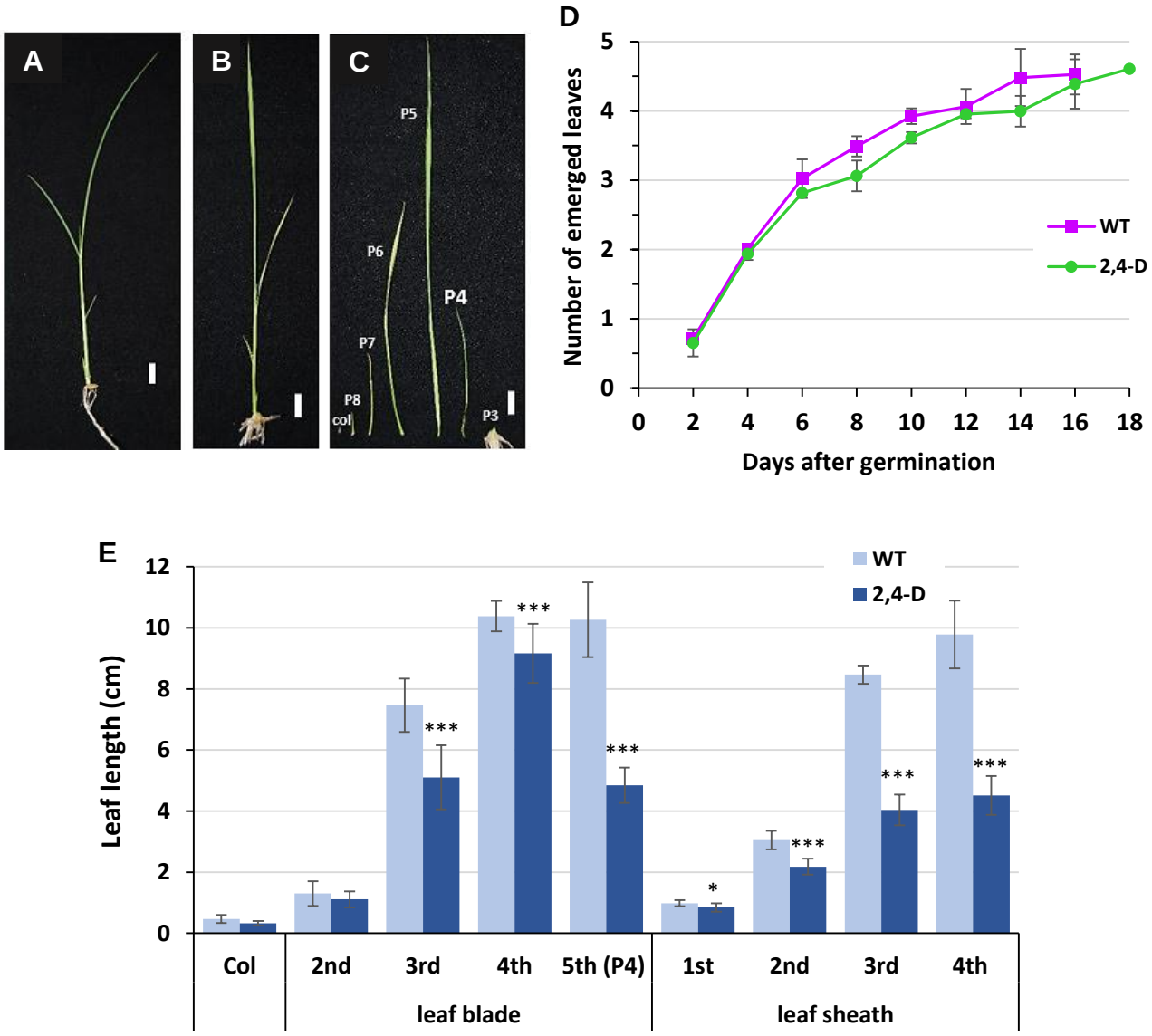

Figure 4-1. Phenotypic analysis of auxin (2,4-D) treated plants.

A, Control seedling (non-treatment). **B,** 2,4-D-treated seedling**. C,** Dissected leaves of 2,4-D-treated seedling. **D,** Number of emerged leaves of control and 2,4-D-treated seedlings. **E,** Length of leaves when the P4 leaf was sampled. Single (*) and triple (***) asterisks indicate the significant difference between control and 2,4-D-treated seedlings at $P<0.05$ and $P<0.001$ by Student's *t-test* analysis, respectively. Error bars in **D** and **E** represent ±SD, $n \geq 10$ for three replications**.** Scale bars in **A-C** = 1 cm.

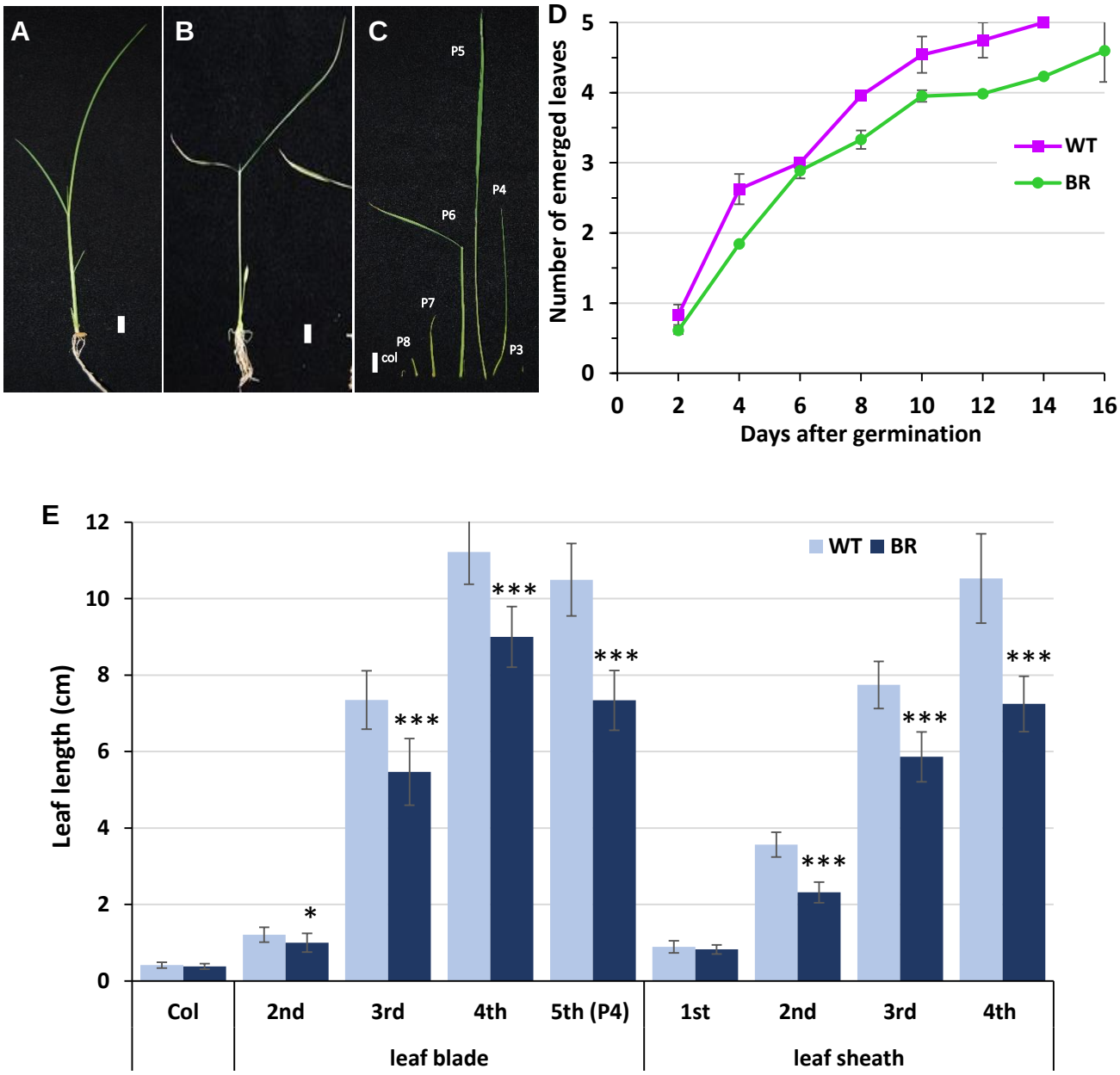

Figure 4-2. Phenotypic analysis of brassinosteroid (BR)-treated plants.

A, Control seedling (non-treatment). It is the same picture as shown in Figure 4-2A. **B,** BR-treated seedling. **C,** Dissected leaves of BR-treated seedling. **D,** Number of emerged leaves of control and BR-treated seedlings. **E,** Length of leaves when the P4 leaf was sampled. Single (*) and triple (***) asterisks indicate the significant difference between control and BR-treated seedlings at $P<0.05$ and $P<0.001$ by Student's *t-test* analysis, respectively. Error bars in **D** and **E** represents ±SD, $n \geq 10$ for three replications. Scale bars in **A-C** = 1 cm.

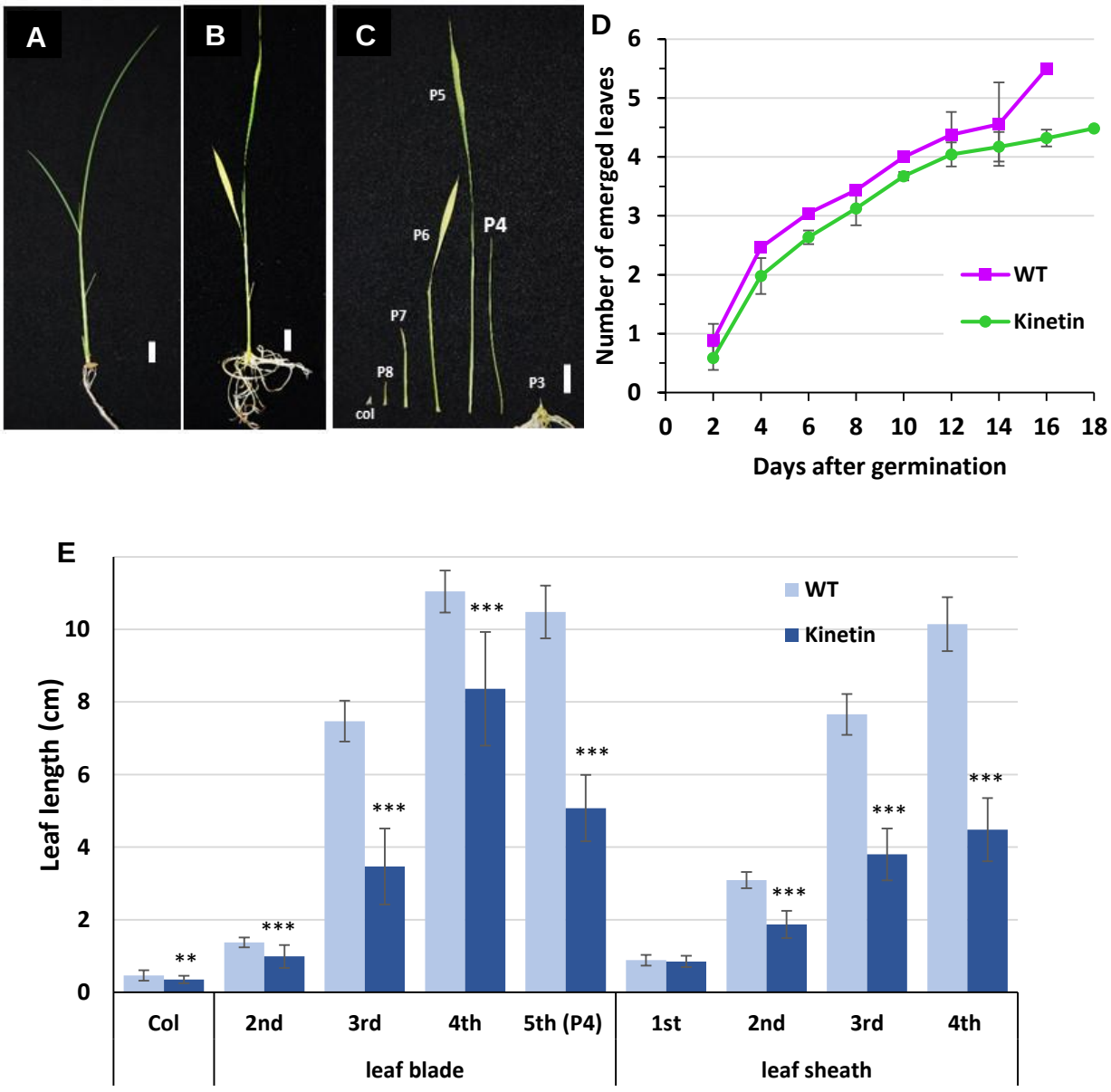

Figure 4-3. Phenotypic analysis of cytokinin (kinetin)-treated plants.

A, Control seedling (non-treatment). It is the same picture as shown in Figure 4-2A. **B,** Kinetin-treated seedling**. C,** Dissected leaves of kinetin-treated seedling. **D,** Number of emerged leaves of control and kinetin-treated seedlings. **E,** Length of leaves when the P4 leaf was sampled. Single (*) and triple (***) asterisks indicate the significant difference between control and kinetin-treated seedlings at $P<0.05$ and $P<0.001$ by Student's *t-test* analysis, respectively. Error bars in **D** and **E** represents ±SD, $n \geq 10$ for three replications. Scale bars in **A**-**C** = 1 cm.

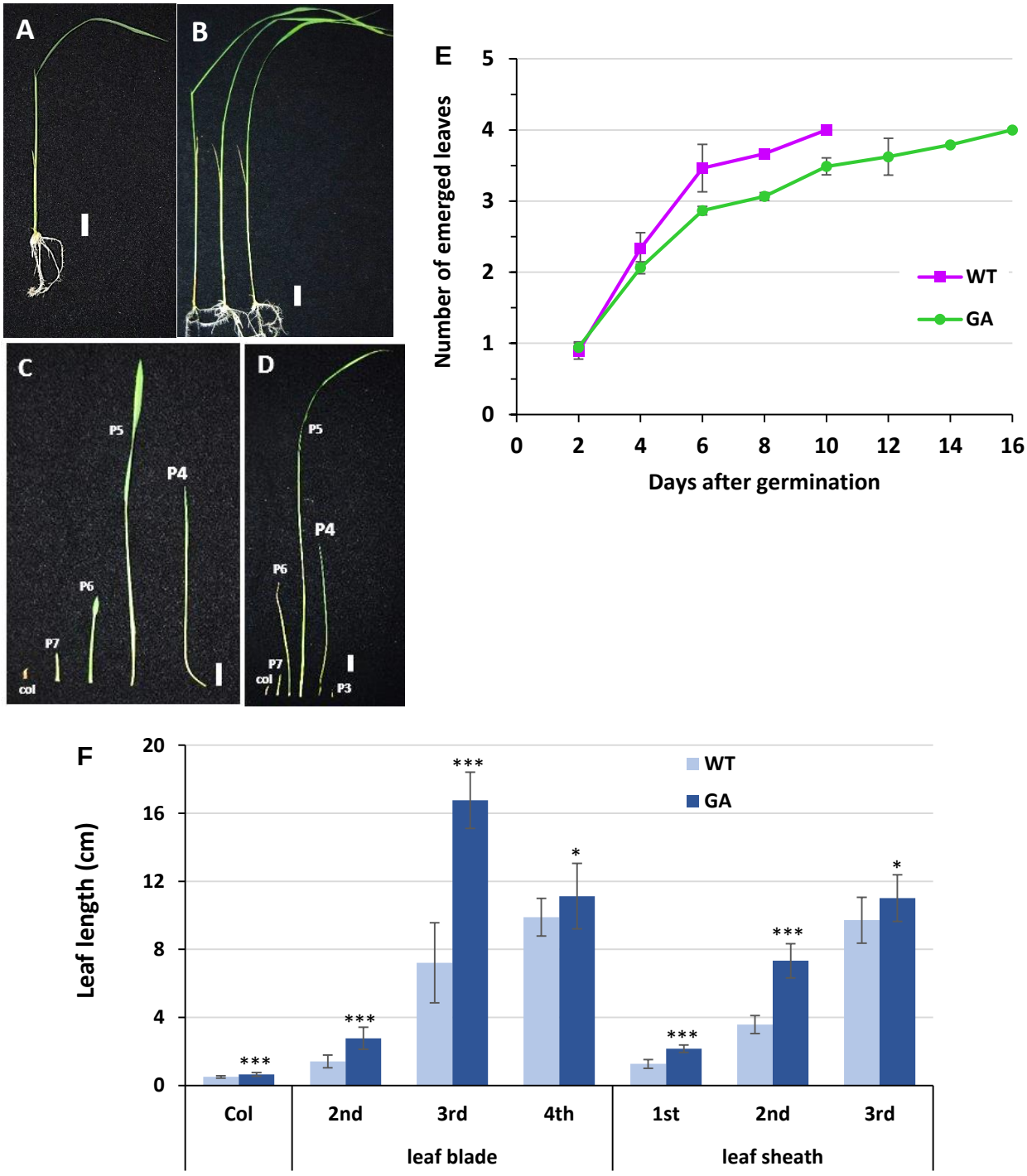

Figure 4-4. Phenotypic analysis of gibberellin (GA)-treated plants.

A, Control seedling (non-treatment). **B,** GA-treated seedlings. **C,** Dissected leaves of control seedling. **D**, Dissected leaves of GA-treated seedling. **E,** Number of emerged leaves of control and GA-treated seedlings. **F,** Length of leaves when the P4 leaf was sampled. Single (*) and triple (***) asterisks indicate the significant difference between control and GA-treated seedlings at $P<0.05$ and $P<0.001$ by Student's *t-test* analysis, respectively. Error bars in **D** and **E** represents ±SD, $n \geq 10$ for three replications**.** Scale bars in **A**-**D** = 1 cm.

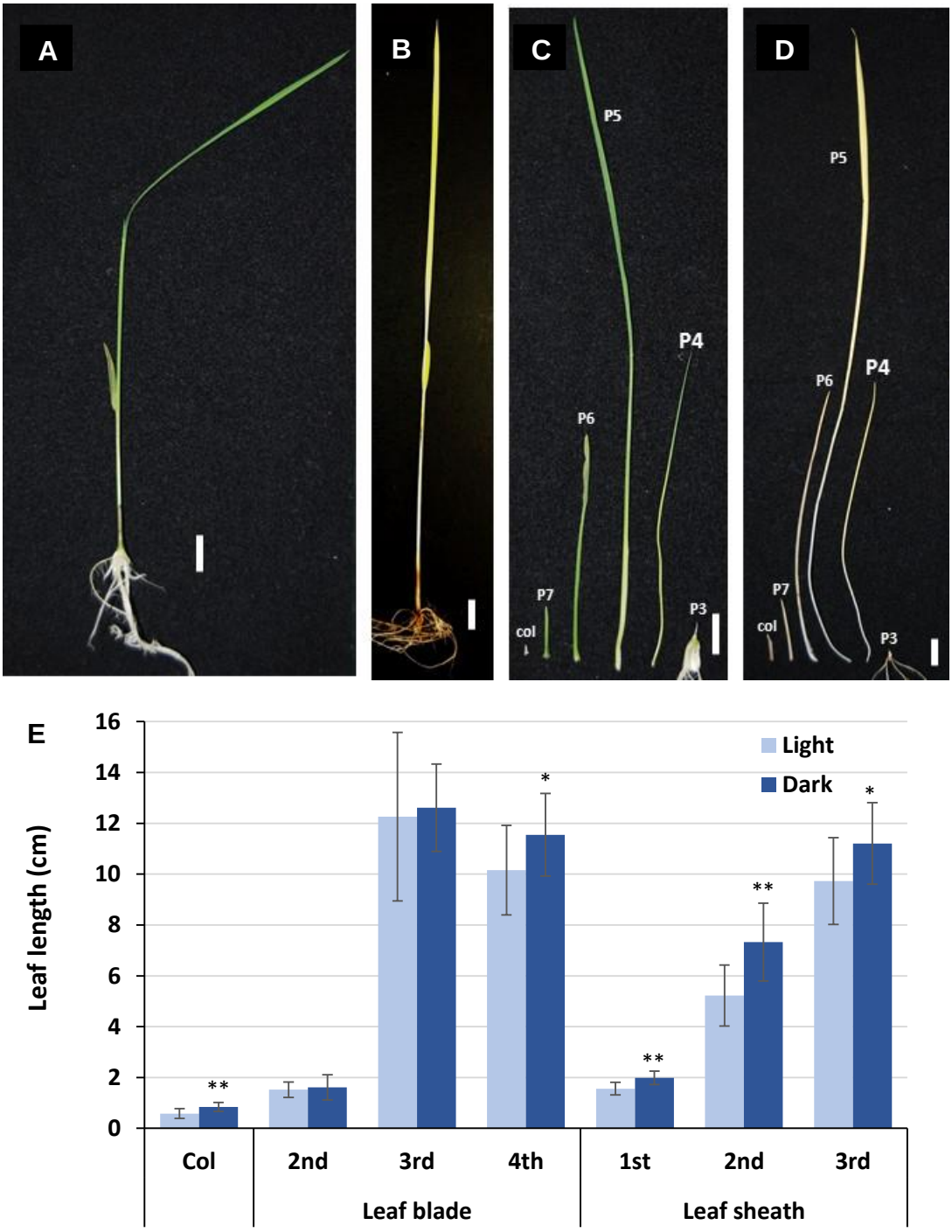

Figure 4-5. Phenotypic analysis of rice seedlings grown under light and dark conditions.

A, Seedling under light condition. **B,** Seedling under dark condition**. C,** Dissected leaves under light condition. **D**, Dissected leaves under dark condition. **E,** Length of leaves when the P4 leaf was sampled. Single (*) and double (**) asterisks indicate the significant difference between light and dark grown seedlings at $P<0.05$ and $P<0.01$ (Student's *t-test*), respectively. Error bars in **D** and **E** represents ±SD, $n \geq 10$ for three replications. Scale bars in **A**-**D** = 1 cm.

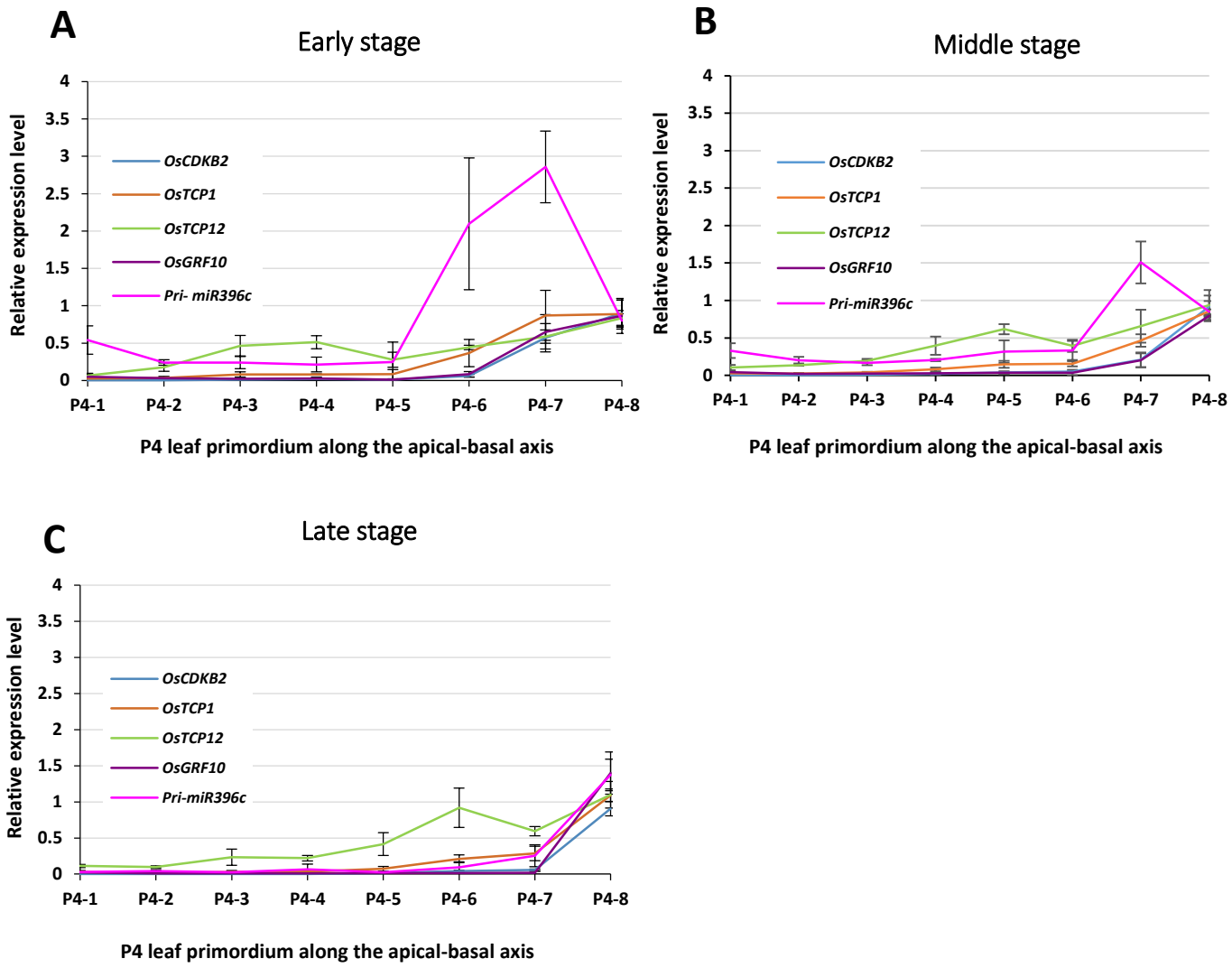

Figure 4-6. Expression pattern of five marker genes along the apical-basal axis of P4 leaf primordium at three developmental stages.

A-C, Real-time PCR result at three developmental stages was re-constructed from the data of Figure 3-3. **A,** Early stage. **B,** Middle stage. **C,** Late stage. P4-1 to P4-8 along the horizontal axis indicate the position of the P4 leaf along the longitudinal axis. Expression level was normalized relative to that of an internal control (*OsRAD6*).

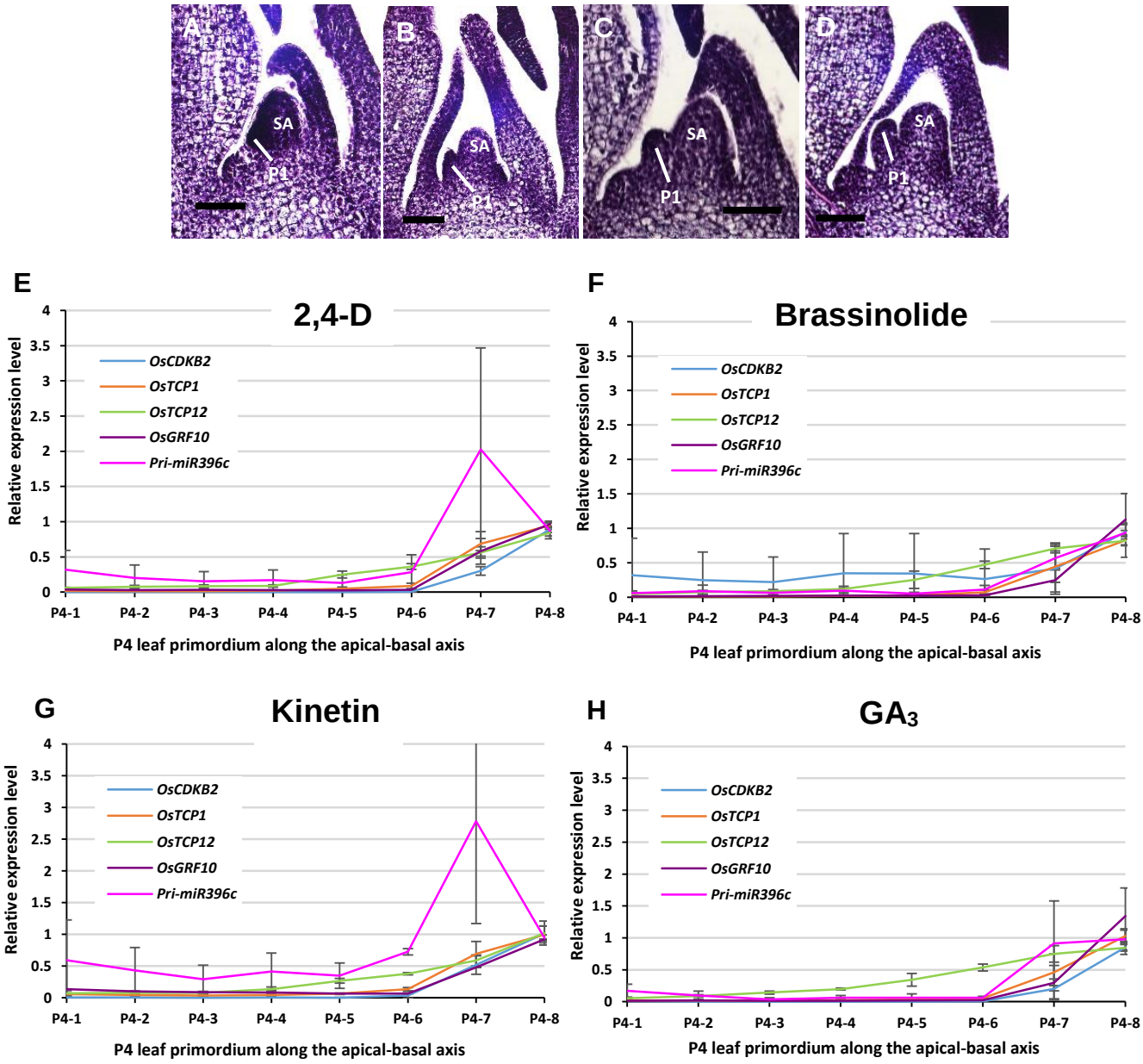

Figure 4-7. Gene expression analysis of phytohormone-treated plants.

A-D, Longitudinal section of shoot apex in phytohormone-treated plants. **E-G,** Expression patterns of five marker genes in phytohormone-treated plants. **A, E,** 2,4-D. **B, F,** Brassinolide. **C, G,** Kinetin. **D, H,** GA_3. Expression level was normalized relative to that of an internal control (*OsRAD6*). P4-1 to P4-8 along the horizontal axis indicate the position of the P4 leaf along the longitudinal axis. P1; P1 leaf primordium. P2; P2 leaf primordium. SA; shoot apex. Scale bars in **A-D** = 50 μm.

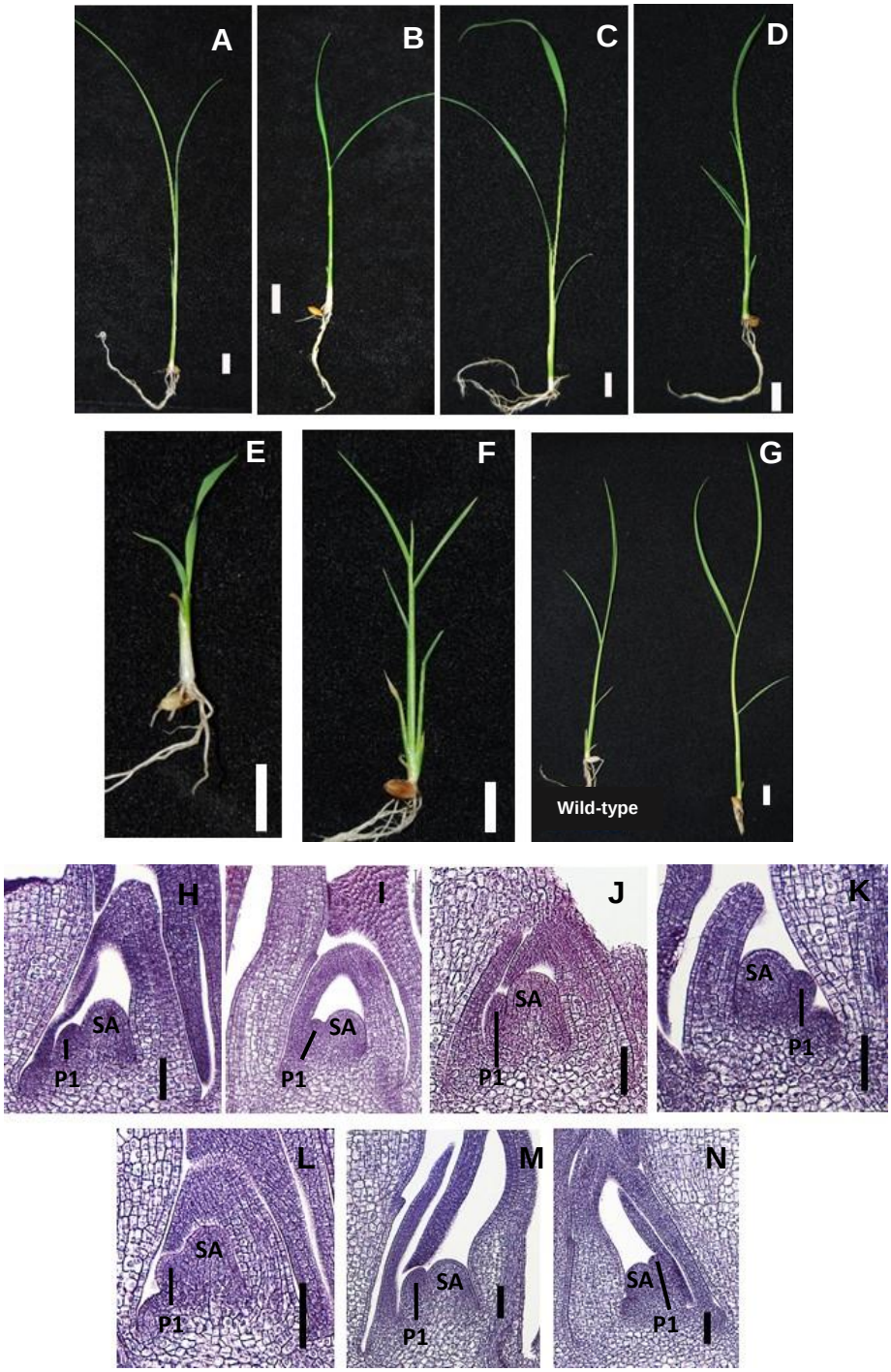

Figure 4-8. Phenotypes of leaf morphogenetic mutants.

A–G, Seedling phenotypes. **H–N,** Longitudinal section of shoot apex. **A, H,** *lg*. **B, I**, *dl*. **C, J**, *d61*. **D, K**, *d1*. **E, L**, *d18h*. **F, M**, *pla1-4*. **G, N**, *pre.* P1; P1 leaf primordia. SA; shoot apex. Scale bars in **A-G** = 1 cm, **H-N** = 50 µm.

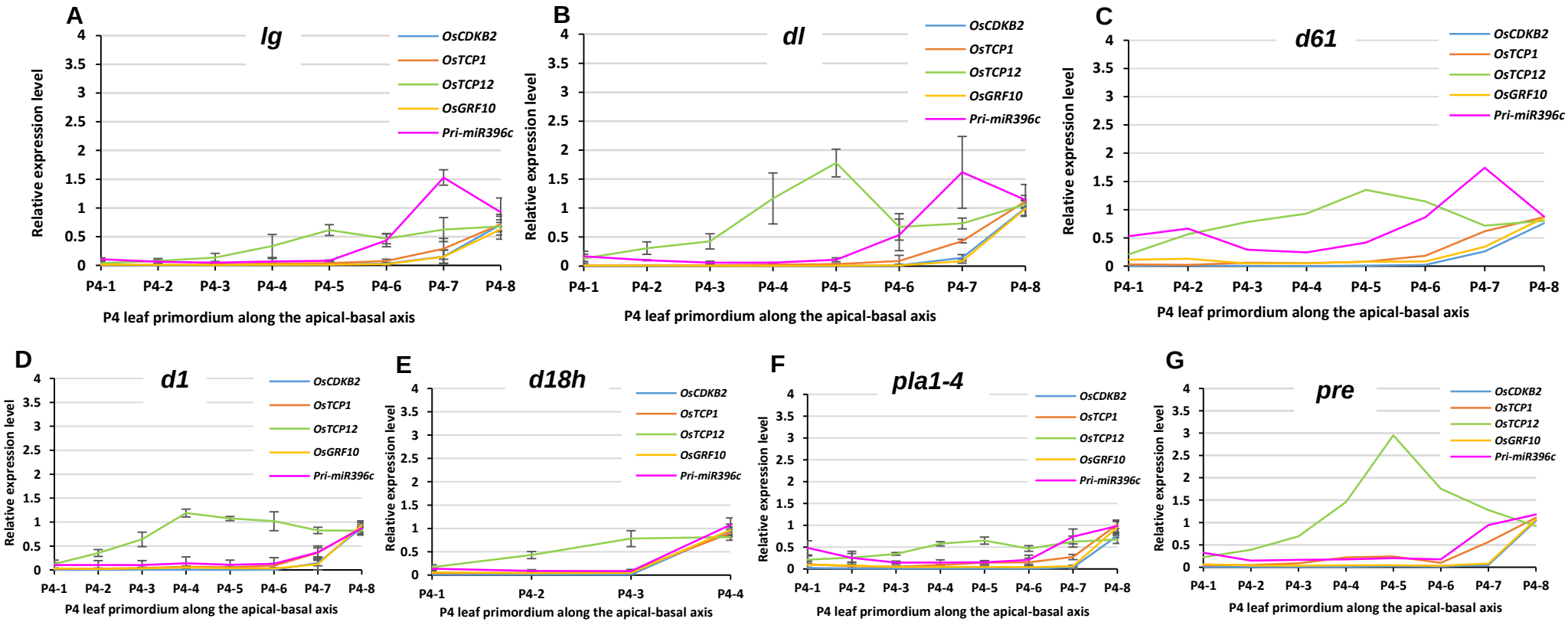

Figure 4-9. Expression analysis of five marker genes along the apical-basal axis of the P4 leaf primordium in leaf mutants.

A, *lg*. **B,** *dl*. **C,** *d61*. **D,** *d1*. **E,** *d18h*. **F,** *pla1-4*. **G,** *pre*. P4-1 to P4-8 along the horizontal axis indicate the position of the P4 leaf along the longitudinal axis. Expression level was normalized relative to that of an internal control (*OsRAD6*).

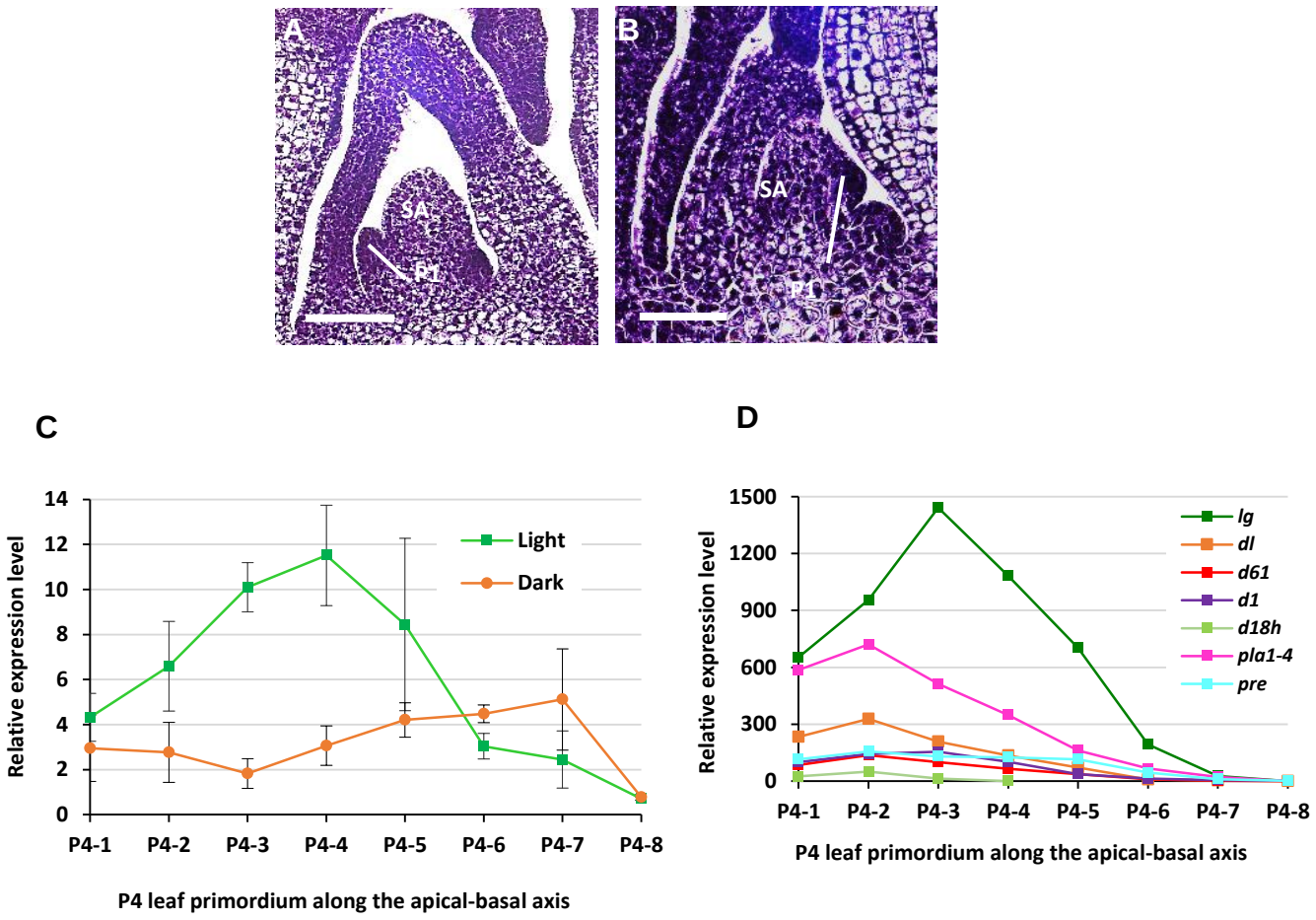

Figure 4-10. Expression pattern of *OsRBCS2* gene.

A, Longitudinal section of shoot apex in light condition. **B,** Longitudinal section of shoot apex in dark condition. **C,** Expression pattern of *OsRBCS2* in the light and dark conditions. **D,** *OsRBCS2* expression pattern in various morphogenetic mutants. P4-1 to P4-8 along the horizontal axis indicate the position of the P4 leaf along the longitudinal axis. Expression level was normalized relative to that of an internal control (*OsRAD6*). P1; P1 leaf primordium. SA; shoot apex. Scale bars in **A** and **B** = 50 µm.

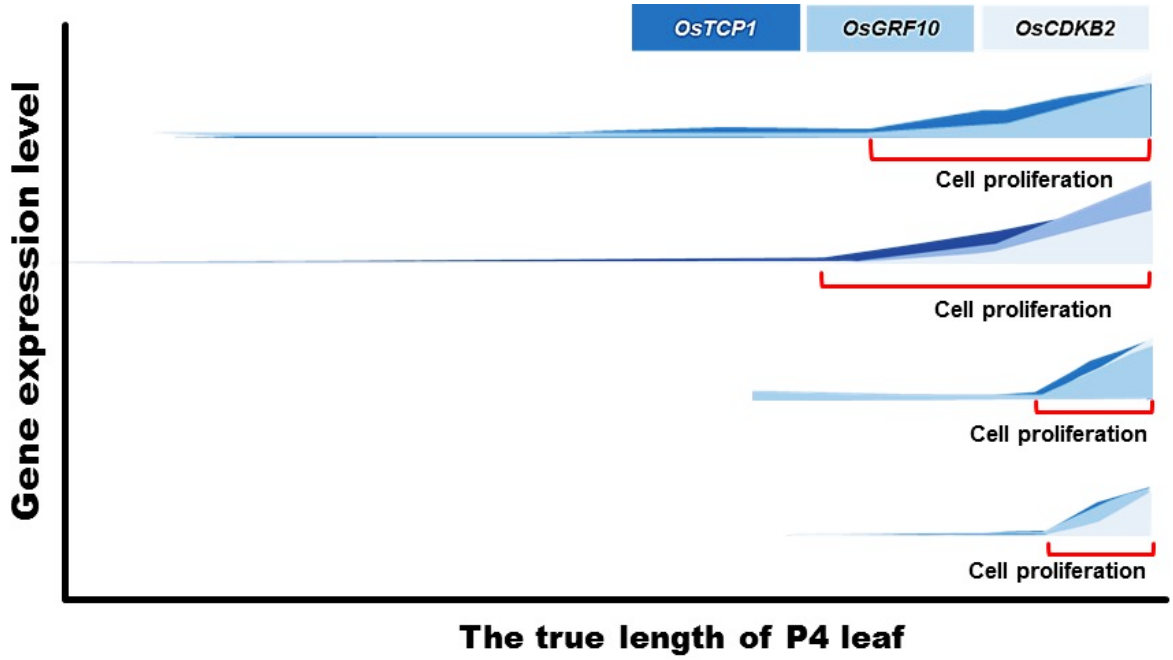

Figure 4-11. Schematic comparison of cell-proliferation domain between wild-type and hormone-treated P4 leaves.

Horizontal axis represents the absolute length of P4 leaf along the longitudinal axis. Bracket indicates the domain where cell proliferation activity is high.

Table 4-1. The length of P4 leaf primordium of wild-type in different developmental stages and of various morphogenetic mutants.

Plant samples	**Average length of P4 leaf (cm)**
wild-type at the early stage of P4 leaf primordium	6.7
wild-type at the middle stage of P4 leaf primordium	10.3
wild-type at the late stage of P4 leaf primordium	13.7
lg	5.26
dl	6.23
d18h	2.10
pla1-4	8.39
d1	5.88
d61	8.50
pre	9.00

4.4 Discussion

4.4.1 Effect of phytohormone application on morphological and gene expression changes in leaf

It is known that plant hormones have roles in various aspects in plant growth and development (Clouse and Sasse, 1998, Sakamoto *et al.*, 2004, Hardtke *et al.*, 2007, Zhang *et al.*, 2009, Scarpella *et al.*, 2010, Nelissen *et al.*, 2012 and Sakamoto *et al.*, 2013). However, how each hormone affects leaf development and gene expression pattern is poorly understood. Thus, I examined the response of leaf development and change of gene expression pattern for four major plant hormones. Generally, auxin, kinetin and brassinolide applications showed negative effect to the leaf growth and the emergence of leaves, although the number of leaves was not affected in auxin treated leaf. In contrast to these three hormones, GA treatment induced leaf elongation. The responses of leaf growth to these plant hormones have been demonstrated in the other studies (Mimura *et al.*, 2012 and Zhiponova *et al.*, 2013), which are basically consistent with my results.

Gene expression analysis indicates that hormone treatments affect expression of at least one marker gene of the P4 leaf. Auxin treatment affected expression pattern of *OsTCP12*, BR treatment did that of *OsCDKB2, OsTCP12* and *pri-miR396c*, CK treatment did that of *OsTCP12*, and GA treatment did that of *OsTCP12* and *pri-miR396c*. Interestingly, expression pattern of *OsCDKB2, OsTCP1*, *OsGRF10* did not change significantly in all conditions except for BR treatment.

Regarding of expression pattern of BR-treated P4 leaf, constant low expression of *OsCDKB2* throughout P4 leaf along the longitudinal axis was observed. Since the expression of *OsCDKB2* represents cell division activity, it is suggested that cell division was activated throughout the BR-treated P4 leaf. Although BR is more effective to young tissues than mature ones (Clouse and Sasse, 1998), the most prominent effect of BR to rice leaves is lamina joint bending. This response was also observed in this experiment (Figure 4-2A). BR is well-known to stimulate cell elongation, but several reports indicated that BRs are involved in cell division by enhancing expression of cell-cycle related genes, such as *CYCD3*, *CYCB1;1*, *H4*, in *Arabidopsis*. In addition, they are required for differentiation of the cell in leaf margins (Ramirez-Parra *et al*., 2005, Hardtke

et al., 2007 and Zhiponova *et al*., 2013). Thus, it was possible that BR treatment could activate cell division even in the mature tissue such as lamina joint and apical parts of the P4.

On the other hand, the constant pattern of the *OsCDKB2* expression in auxin, CK and GA treated plants would not be consistent with the change of their leaf length. However, if considering the leaf length of P4 that was sampled in these conditions, change of the expression domain of *OsCDKB2*, *OsTCP1*, *OsGRF10* was clearly correlated with that of the length of the P4 (Figure 4-11). That is, in auxin- and CK-treated leaves whose length was shortened, the range of expression domain of *OsCDKB2, OsTCP1*, *OsGRF10* was reduced. In GA-treated leaves whose length was elongated, the range of expression domain of *OsCDKB2, OsTCP1*, *OsGRF10* was increased. This indicates that the treatment of these hormones would affect the range of cell proliferation domain in the base of the P4 leaf, which resulted in suppressed and enhanced leaf growth. Moreover, the constant proportion of "active" cell proliferation domain (P4-7, 8) and "inactive" domain (P4-1 to 6) along the longitudinal axis of the P4 leaf among the conditions would suggest that an unknown mechanism to keep the relative position of the cell proliferation to cell maturation along the longitudinal axis of the leaf.

4.4.3 Effect of mutations affecting leaf morphology on the gene expression patterns of six maker genes

I performed expression analysis using marker genes to examine leaf development of several known mutants. My results showed that expression of at least one of these marker genes was affected in most of the mutants, indicating that the set of marker genes used in this study can detect genetic and developmental alterations in most of the mutants. Only the *lg* mutant did not show any changes in gene expression pattern (Figure 4-9A). To my knowledge, *lg* mutant shows no abnormalities other than in ligule, auricle, and lamina joint formation during leaf development, although *OsLG1* expression in the leaf sheath was reported (Lee *et al.*, 2007). Therefore, my results were consistent with the previous knowledge about *lg* and suggested that *OsLG1* does not affect leaf growth pattern during development (Lee *et al.*, 2007).

The expression peaks of all of the marker genes examined were unaffected in the *dl* mutant (Figure 4-9B). This suggests that *dl* mutation does not influence leaf development along the apical–basal axis. However, the expression level of *OsTCP12* was elevated at the middle part of P4. The expression of *DL* in the P4 leaf were specifically detected in the central region abaxial to the central vascular bundle, and *DL* is known to be responsible for thickening of the tissue by promoting cell proliferation during leaf development (Yamaguchi *et al*., 2004). This suggests that the elevated *OsTCP12* expression in *dl* is related to the altered cell proliferation pattern in the leaf primordia that was not represented by *OsCDKB2* expression. Thus, it is possible that *OsTCP12* modulates leaf shape by repressing cell proliferation in the middle part of P4 independent of the major cell proliferation process in the basalmost part of P4.

In the case of *d61*, the expression patterns of all marker genes were also similar to those in the wild-type, but expression level were increased in the apical and middle parts of P4 (Figure 4-9C). As *d61* is a loss-of-function mutant of the brassinosteroid receptor *OsBRI1* (Sakamoto *et al*, 2013), my results suggest that impaired brassinosteroid signaling does not disturb leaf development along the apical–basal axis. However, *OsTCP12* expression was elevated in the middle part of P4. Although BR is known to regulate mainly cell elongation rather than cell proliferation in rice leaves, some reports suggested that BR also regulates cell proliferation in *Arabidopsis* (Nakaya, *et al*., 2002). In addition, BR-deficient mutants showed a strong phenotype with severely malformed leaf blades (Sakamoto, *et al*., 2013). Thus, elevated *OsTCP12* expression could be related to changes in cell proliferation pattern in the *d61* leaf blade, although the degree of morphological alteration would be subtle in the *d61* allele used in this study.

In contrast to *d61*, the expression patterns of marker genes in *d1* were very different from those in the wild-type controls (Figure 4-9D). The expression patterns of *OsCDKB2* and *OsGRF10* in *d1* were similar to those in the middle stage of wild-type (Figure 4-6B and 4-9D), and that of *pri-miR396c* in *d1* was similar to the pattern seen in the late stage in wild-type controls (Figure 4-6C and 4-9D). In addition, the second expression peak of *OsTCP12* was seen in P4-4 in the *d1* mutant, but in the early stage in wild-type controls (Figure 4-6A and 4-9D). This suggests that the relative positions of expression peaks

among the marker genes were shifted in *d1* leaf primordia. Although it is difficult to predict the types of changes occurring in the *d1* leaf primordia, my expression analysis indicated that the coordinated cell proliferation pattern would be impaired. In fact, *D1* was shown to regulate cell proliferation by affecting multiple signaling pathways, such as GA and BR (Nakaya, *et al*., 2002 and Oki, *et al*., 2009). Thus, the alteration of expression pattern observed in *d1* would be a result of integrated defects in multiple pathways.

Although the resolution of expression change along the apical–basal axis was low, the expression patterns of marker genes in *d18h* were considered to be similar to those in the wild-type (Figure 4-9E). The *d18h* mutant used in this study has a null allele of the GA biosynthetic gene, *OsGA3ox2*, and is predicted to contain a reduced level of bioactive GA (Sakamoto *et al.*, 2004). As GA promotes cell elongation and cell proliferation, the similar expression profile may contradict the effect of GA on leaf development. However, P4 in *d18h* was about five- to six-fold shorter than that in wild-type controls (Table 4-1). Similar to hormone-treated leaves, if considering the change in *d18h* expression based on the absolute scale of leaf length, the region in which active cell division occurs is more restricted in the basal region compared to the wild-type P4. Accordingly, GA may regulate the range of the region of cell proliferation in the developing leaf.

The expression patterns of marker genes in the *pla1*-P4 leaf at the middle stage were similar to those in wild-type controls at the late stage (Figure 4-9F and 4-6C, respectively). This indicated that the leaf stage based on the expression profile of marker genes was advanced compared to the actual developmental stage in *pla1*. This result was consistent with previous reports that *pla1* showed precocious leaf maturation. However, the expression peak of *OsTCP12* in *pla1* was still similar to that in the middle stage of wild-type controls (Figure 4-9F and 4-6B, respectively). Accordingly, *pla1* mutation affected the relative timing of expression peaks of some genes rather than affecting the entire process of leaf maturation.

The expression patterns of *OsCDKB2* and *OsGRF10* in *pre* were similar to those in the late stage of wild-type (Figure 4-6C and 4-9G), and that of *OsTCP1* and *pri-mR396c* in *pre* was similar to the pattern seen in the middle stage in wild-type controls (Figure 4-6B

and 4-9G). In addition, the expression level of *OsTCP12* was elevated in P4-5 in the *pre* mutant (Figure 4-9G). Thus, multiple abnormalities of expression pattern and level of marker genes were detected in the pre mutant. Although some studies indicated that JA regulates not only stress response but also developmental pathways (Avanci *et al.*, 2010), it is not well understood how JA affects the plant growth and gene expression. In the case of *pre*, although the length of the leaves was elongated, detailed phenotype was not revealed. My results would suggest that JA pathway control the leaf size and/or shape through complex mechanisms of gene regulation.

4.4.2 Expression profile of *OsRBCS2* gene

OsRBCS2 encodes one of the RubisCO small subunits in rice. *OsRBCS2* are highly expressed in the rice leaf blade and there is a positive correlation between the expression level of *RBCS* and maximal RubisCO contents (Morita *et al*., 2014 and Ogawa *et al*., 2012), suggesting that the expression level was strongly associated with photosynthetic-related activity. However, the expression analysis of *OsRBCS2* indicated that the expression level did not simply reflect photosynthetic activity in my experimental conditions. First, the expression level did not gradually elevated as the developmental stage progress (Figure 3-3G). Second, the expression peak of the *OsRBCS2* was not detected in the apical part of the P4 leaf where mature chloroplasts was seen (Figure 4-10C), although the expression peak was not observed in the dark-treated plants. It was suggested that transcripts of *RBCL* and *RBCS* mRNAs is detectable in very young leaf primordia, and the there was no correlation in the accumulation pattern of their mRNAs and the proteins (Patel and Berry, 2008). Therefore, it might be possible that higher expression of *OsRBCS2* in the sub-apical part of P4 leaf is related to the initiation of photosynthesis rather than activation of photosynthesis or chloroplast differentiation.

On the other hand, expression level of *OsRBCS2* was highly variable among morphogenetic mutants, although the expression pattern along the longitudinal axis was generally conserved. It was not clear why the expression level was so different among the mutants. One possibility is that the causal genes regulate not only developmental traits but also photosynthesis-related processes. Alternatively, *OsRBCS2* expression level is

very sensitive to environmental cues, such as a seedling density and the time of sampling that I could not predict.

CHAPTER 5

Mutant affecting morphology and gene expression pattern of rice leaf

5.1 Introduction

It is expected that leaf development is controlled by numerous number of genes. To identify key genes regulating leaf development, morphogenetic mutants and the function of their causal genes has been analyzed (Berná *et al*., 1999 and Pérez-Pérez *et al*., 2009). Although most of the analyses were performed in dicotyledonous plants, considerable number of genes has been identified in grass species, such as rice and maize (Li *et al*., 2013, Smith *et al*., 1996 and Wu *et al*., 2010). In particular, mutations affecting grass-specific morphogenetic traits are important for understanding characteristic nature of leaf in grasses.

As mentioned in Chapter 2, rice leaf consists of three parts along the longitudinal axis, leaf blade, leaf sheath and blade-sheath boundary. At the blade-sheath boundary, three different grass-specific tissues were differentiated. The ligule is a membranous structure that adaxially formed at the top of the leaf sheath. The auricle is a pair of fringe-like tissues enclosing leaf axis at the margin of the blade-sheath boundary. The lamina joint is a tissue that controls angle of leaf blade by its expansion. On the other hand, rice leaves differentiate grass-specific tissue along the central marginal axis of the leaf. The midrib is a structure that is formed along the midvein of the leaf blade to maintain an upright angle of the leaf.

Several mutations affecting the formation of these grass-specific tissues have been reported. *Liguleless* genes in rice and maize are involved with ligule formation and the establishment of blade-sheath boundary (Lee *et al.*, 2007, Moon *et. al.,* 2013 and Walsh *et. al.,* 1998). Loss-of-function of *DL* gene resulted in the defective midrib formation and led to drooping leaf phenotype (Yamaguchi, 2004 and Ohmori *et al.,* 2011).

Since these homologous genes in *Arabidopsis* did not show comparable phenotypes, they regulate leaf development in grass-specific manner. However, a number of mutants

affecting leaf morphology and grass-specific morphological traits in rice is still insufficient. Therefore, to find a new genetic factor controlling leaf development in rice, I identified a novel mutant that affects leaf morphology and its phenotype was characterized. In addition, expression changes of marker genes in developing leaf primordia were also analyzed.

5.2 Materials and Methods

5.2.1 Plant materials

12T-S-221 was originally identified from M_2 population of cv. Taichung 65 mutagenized using N-methyl- N-nitrosourea. Mutant and wild-type seeds were sterilized with 1% NaClO (Sodium hypochloride solution) for 60 min and washed with the distilled water. They were cultured on the soil and grown in a growth chamber under continuous light at 28°C. Mutant seedlings about 16-18 days after sowing were used for observation of phenotypes in the early stage. To investigate the morphological phenotypes at the mature stage, mutant seedlings were transplanted into buckets and grown in a greenhouse under natural condition (30°C in daylight and 20°C at night).

5.2.2 Morphological analysis

Leaf length of leaves was measured when the tip of leaf blade of P4 leaf primordium was just emerged from 4th leaf (Figure 5-1A). To confirm the growth stage of P4 leaves, P1 to P3 leaf primordia and shoot apex were sampled and analyzed by paraffin sections. Leaf anatomy was also observed as described in Chapter 2.

5.2.3 Estimation of leaf emergence

To estimate leaf initiation, leaf age of wild-type and 12T-S-221 seedlings showing mutant phenotypes was recorded in every two days.

5.2.4. Gene expression analysis

P4 leaves of mutant seedlings at 16-18 DAS were sampled and divided into eight segments as defined in Chapter 3 and 4. Preparation of total RNAs and their cDNA was followed by the same methods as described in Chapter 3. Five marker genes, namely, *OsCDKB2*, *OsTCP1*, *OsGRF10*, *OsTCP12* and *pri-mR396c* were applied to gene expression analysis by real-time PCR. The average of expression level of each gene was normalized to an internal control, *OsRAD6*.

5.2.5. Genetic analysis

For mapping, heterozygous 12T-S-221 plants (spp. japonica) were crossed with cv. Kasalath (spp. indica), and mutant plants showing the abnormal phenotype in the F_2 population were used. They were sown on the soil and grown in a greenhouse under natural condition. About 20 days after sowing, 285 plants of F_2 population were screened to isolate 56 homozygous plants showing mutant phenotypes. For rough mapping, STS and CAPS markers obtained from the rice genome database were used. List of DNA markers around the candidate region were shown in Table 5-1.

- *DNA isolation*

To isolate genomic DNA, plant samples were grinded by Shaker Master (BMS, model BMS-M10N21) with TPS buffer (0.1M Tris, 1M KCL, 0.01M EDTA). Then, samples were incubated at 70°C for 30 min and were centrifuged at 4°C, 15000 rpm for 15 min. The supernatant were transferred and equal volume of Isopropanol was added. The solutions were centrifuged at 4°C, 15000 rpm for 10 min. Then, DNA pellets were washed with 70% EtOH and dissolved with TE buffer.

5.3 Results

5.3.1. Phenotypes of 12T-S-221 mutant

12T-S-221 was originally identified as a recessive mutant showing abnormal leaf blade and sheath boundary. Thus, it was considered that the mutant has a defect in a process of leaf development along the apical-basal axis.

First, phenotypes of young and mature plants of the mutant were observed. At the early growth stage, the mutant plants showed identical phenotypes to those of the wild-type sibling by 10 DAS. However, a few seedlings produced leaf blade of 1st leaf that was not normally observed in the wild type (Figure 5-1A). About 15 DAS, homozygous seedlings showed abnormal phenotypes, e.g., erect leaves, dwarfism, short statures compared with the wild-type siblings (Figure 5-1B). Although mutant phenotypes were variable but the most characteristics were abnormal blade-sheath boundary with or without rudimentary ligule and auricles in 3rd leaf and 4th leaf in some seedlings (Figure 5-1C). Careful observation of the mutant leaves indicated that abnormality of the leaf blade-sheath boundary was also variable, e.g., disrupted boundary along the longitudinal axis (Figure 5-1E to 5-1G), complete lack of the ligule (Figure 5-1F and 5-1G), and abnormal shape of auricles (Figure 5-1G).

At mature stage, some leaves of the mutant plants also showed incomplete lamina joint, but the phenotype was not observed in all leaves (Figure 5-1H). At the reproductive stage, mutant plant produced sterile panicles (Figure 5-1I) whose spikelets were irregular-shaped (Figure 5-1J and 5-1K). Abnormality of the spikelets was mainly detected in palea, that is, degenerated and reduced size of the palea. As the mutant was completely sterile, pollen grains were stained with iodine-potassium-iodide (IKI) solution. Pollen grains derived from irregular spikelets were completely unstained with IKI (Figure 5-1L). However, pollen grains derived from normal spikelets were partially stained (Figure 5-1M). Consequently, one of the reasons for the sterility of the mutant may be dysfunctional pollens.

➢ *Surface and inner structure of 12T-S-221 mutant leaves*

To analyze 12T-S-221 mutant phenotypes in more detail, surface structure of leaf primordia was observed by scanning electron microscope (SEM). First, I observed the immature stage (SA, P1 and P3) and mature stage (P5) of leaf primordium. The results showed that epidermal structure of SA, P1 and P3 leaf primordia (Figure 5-2A and 5-2B) were identical to those of wild-type observed in Chapter 2 (Figure 2-2A and 2-2B). The epidermal surface of leaf blade and sheath of P5 leaf was also identical to that of wild-type (Figure 2-2J, 2-2M and 5-2C, 5-2D). However, the lamina joint of P5 leaf primordium was significantly restricted in the small part of the leaf blade-sheath boundary (Figure 5-2F). In addition, the ligule was rudimentary and the auricles were completely absent (Figure 5-2F). I also observed inner structure of the leaf blade-sheath boundary. In the base of the leaf blade, one margin of the leaf has a similar feature to that of wild-type leaf blade, whereas the other side had a lamina joint-like structure with two vascular bundles (Figure 5-2H). However, the structure of the leaf sheath was identical to that of wild-type (Figure 2-3G and 5-2G). These observations indicate morphological and histological features of immature and mature leaves of the mutant were similar to those of wild-type, except for the structure of the leaf blade-sheath boundary.

Next, to clarify the morphogenetic change of the mutant leaf in the transition stage, I observed epidermal surface of P4 leaf primordium along the longitudinal axis. Epidermal features such as trichome, papillae and stomata were present on its surface from the tip (P4-1) to sub-basal part (P4-7) of P4 leaf (Figure 5-3A to 5-3G), while those characteristics was not observed on the basal leaf blade and sheath of P4 (Figure 5-3H, 5-3K and 5-3L). The boundary of leaf blade and sheath of P4 leaf was also identical to that of wild-type (Figure 2-2H and 5-3J). Paraffin sections of P4 mutant leaf along the longitudinal axis revealed that pattern of the histological changes of P4 leaf was similar to those of the wild-type (Figure 5-3M to 5-3U).

These observations indicate that abnormality of 12T-S-221 in the leaf was mostly observed at the boundary of the leaf blade and sheath in the mature stage. Thus, it is considered that one of the possible functions of the causal genes of 12T-S-221 is to regulate proper growth of the boundary of the leaf blade and sheath. In addition, the causal

genes of 12T-S-221 not only affect the boundary of leaf blade and sheath formation but also influence on the spikelet development and the fertility.

- *Leaf emergence and leaf growth of 12T-S-221 mutant*

Next I examined leaf emergence rate and leaf growth of the mutant. The results indicated that leaf emergence rate of the mutant was not altered, but leaf number was fewer than that in wild-type sibling (Figure 5-4C). At 18 days after germination (DAG), five leaves were emerged in the mutant seedlings, while seven leaves were done in wild-type sibling (Figure 5-4A and 5-4B). Leaf length of the mutant seedlings was compared with wild-type sibling when P4 leaf primordium (5^{th} leaf) had just emerged from P5 leaf sheath. P6 leaf primordium (3^{rd} leaf) of the mutant was significantly shorter than that of wild-type sibling (Figure 5-4D). In addition, the length of the 1^{st} leaf (P8 leaf primordium) was significantly longer than that of wild-type sibling, however the length of most of leaves was shorter than those of wild-type sibling (Figure 5-4D).

5.3.4. Expression pattern of marker genes along apical-basal axis of P4 leaf primordium in 12T-S-221 mutant

Expression pattern of five marker genes— *OsCDKB2*, *OsTCP1*, *OsTCP12*, *OsGRF10* and *pri-miR396c*—in the eight parts of P4 leaf primordium were analyzed by real-time PCR. To confirm the stage of P4 leaf sampled mutant for this analysis, SAM and P1 to P3 leaf primordia were observed. Based on the stage of P1 leaf primordium, the stage of P4 sampled here was predicted to be the late stage of wild-type in Chapter 3 and 4 (Figure 3-2F and 5-5B). Expression analysis revealed that the expression pattern of some genes were different from those of wild-type in the late stage (Figure 4-6C and 5-5C). Although the expression patterns of *OsCDKB2*, *OsTCP1* and *OsGRF10* was similar to that of the wild type, up-regulation of *OsTCP12* was observed in the middle part of P4 (Figure 5-5C). In addition, expression of *pri-miR396c* has two peaks, that is, one peak appeared in the basal part of P4 leaf and the other one was in the middle part (P4-5) of P4 (Figure 5-5C).

5.3.5. Mapping of the causal genes of 12T-S-221 mutant

To identify the causal gene that is associated with the mutant phenotypes of 12T-S-221, F_2 population of 12T-S-221 crossed with cv. Kasalath was generated. Total 56 mutant plants showing dwarfism, short stature and erect leaves were used for mapping. Rough mapping and fine mapping refined the candidate region to 100 to 115 cM on chromosome 3 (Figure 5-6). Based on the genotypic result, the causal gene of 12T-S-221 is possibly located around 103 cM on chromosome 3 nearer to the marker, OSJNBb0065L20-K-3 (Figure 5-6).

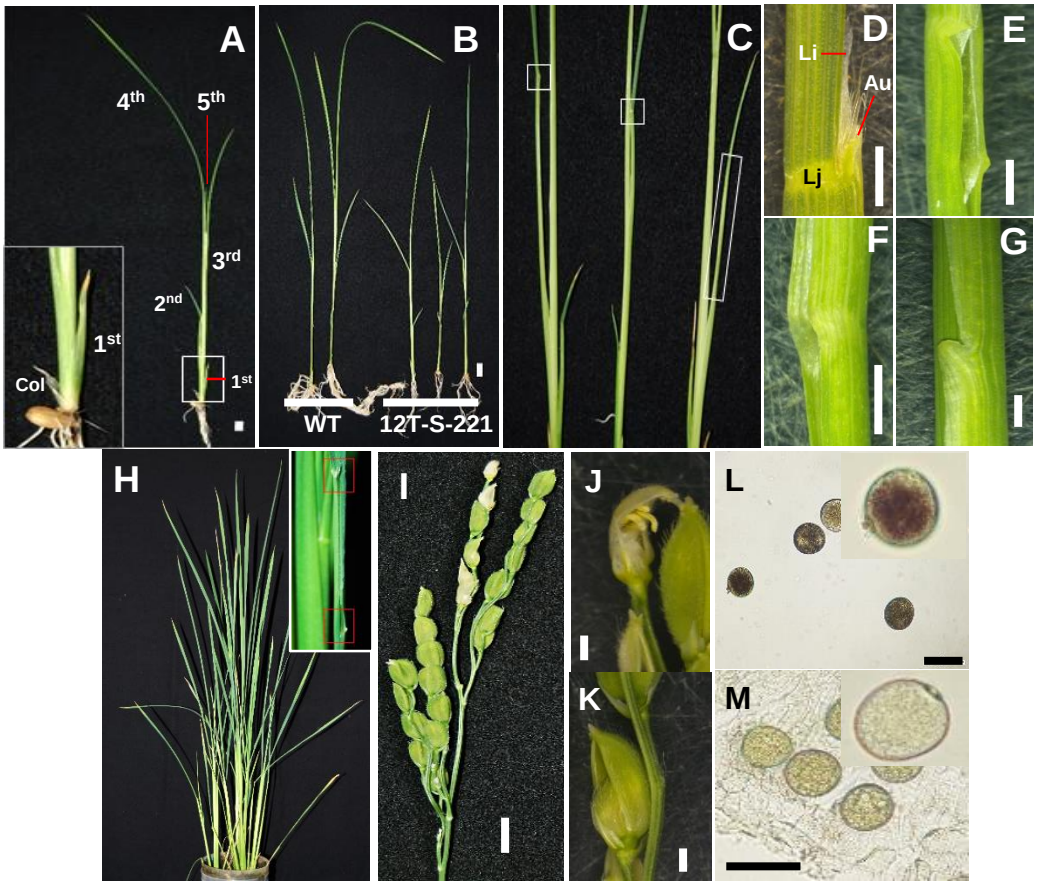

Figure 5-1 Phenotypes of 12T-S-221 mutant.

A, Phenotype of the mutant seedling. Leaf number is labeled. Inset shows the first leaf with leaf blade. **B,** Wild-type siblings (left) and mutant (right) seedlings at 15 DAS. **C,** Abnormal leaf blade-sheath boundary of the 3rd leaf mutant. Boxes indicates the position of the leaf blade-sheath boundary. **D-G,** Variation of abnormal boundary. **D**, WT sibling. **E,** 12T-S-221 mutant leaf with a disrupted blade-sheath boundary. **F,** Mutant leaf without a ligule and auricles. **G,** Mutant leaf with abnormal auricles. **H,** Mature plant of 12T-S-221 at 52 DAS. Inset indicates abnormal l leaf blade-sheath boundary. **I,** Phenotype of mutant panicle. **J,** Flattened anthers of mutant spikelet. **K,** Mutant spikelet with a reduced palea. **L-M,** Pollen grains of the mutant. Pollens were stained with IKI solution. **L,** Pollen grains from abnormal spikelets. **M,** Pollen grains from normal spikelets. Au; auricles, Lj; laminar joint and Li; ligule. Scale bars in **A-B and I** = 1 cm, **D-G** and **J-K** = 0.1 cm and **L-M** = 100 µm.

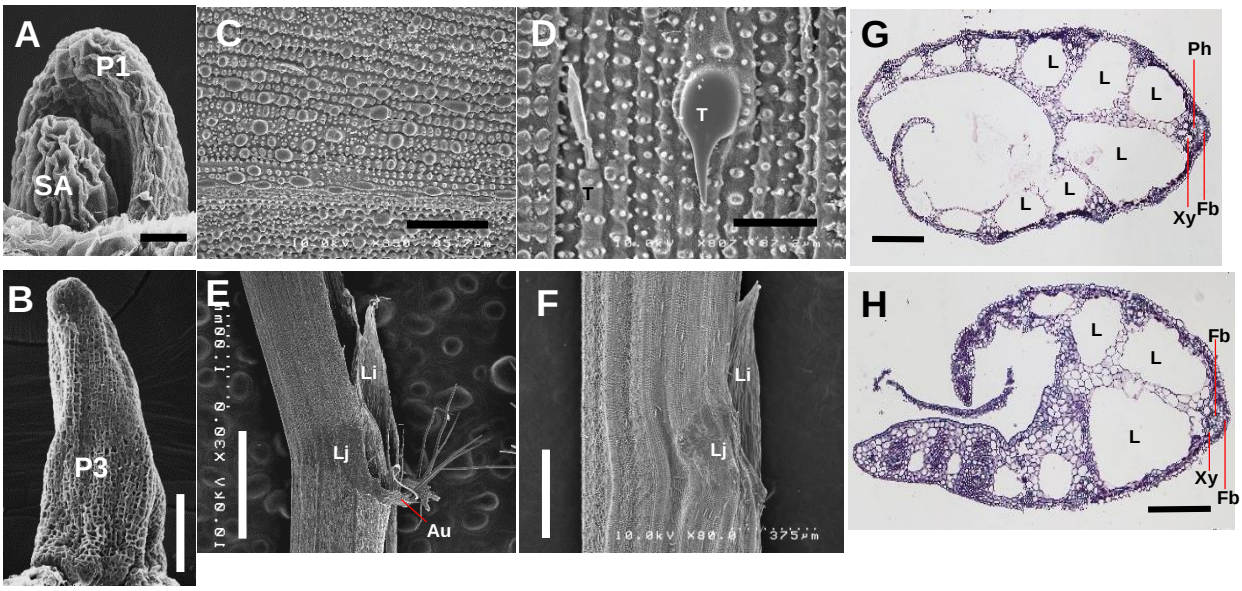

Figure 5-2 Structure of immature and mature leaves in 12T-S-221 mutant.

A, SEM image of shoot apex and P1 leaf primordium. **B,** P3 leaf primordium. **C,** Abaxial epidermis of P5 leaf primordium. **D,** High magnification image of **C**. **E,** Leaf blade-sheath boundary of WT P5 leaf. **F,** Leaf blade-sheath boundary of mutant P5 leaf. **G**, Cross section of mutant P5 leaf sheath. **H,** Cross section of mutant P5 leaf blade-sheath boundary. Au; auricles, Fb; fibre cells, L; lacuna, Li; ligule, Lj; laminar joint, Ph; phloem, SA; shoot apex, Xy; xylem. Scale bars in **A** = 16.7 µm, **B** = 60 µm, **C** = 85.7 µm, **D** = 37.2 µm, **E** = 1 mm, **F** = 375 µm, **G** and **H** = 200 µm.

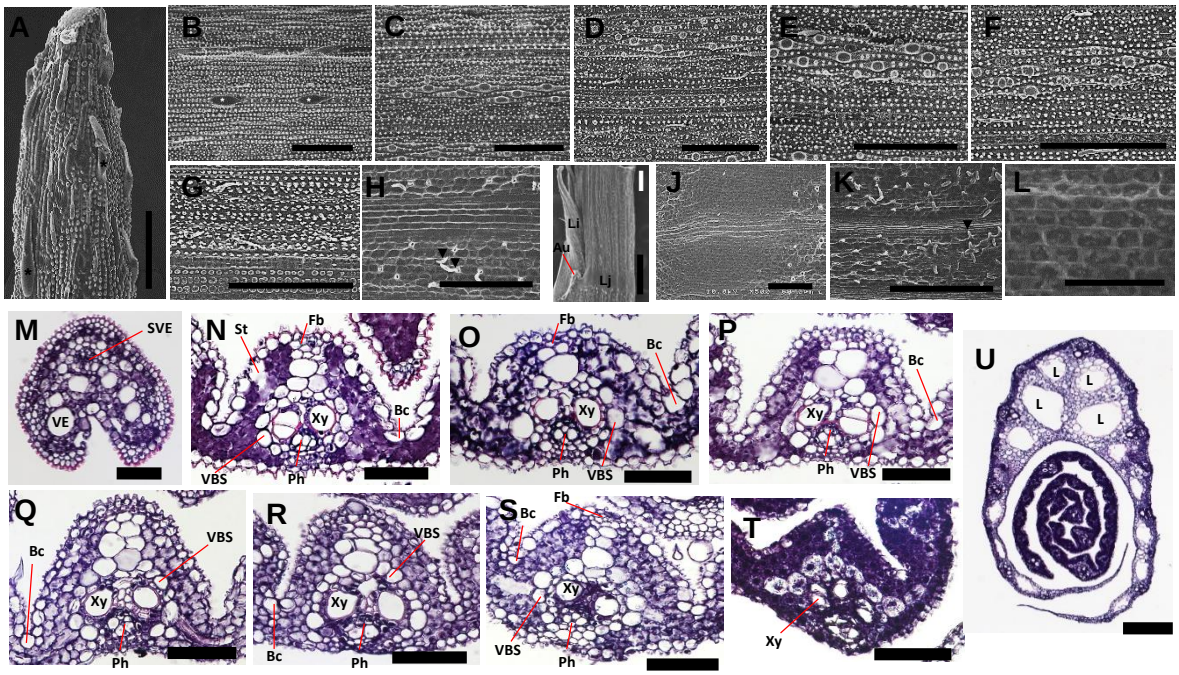

Figure 5-3 Surface and internal structure of P4 leaf primordium of 12T-S-221 mutant.

A-L, SEM images of eight segments (tip to base) along the longitudinal axis of mutant P4 leaf. **A-H,** P4-1 to P4-8, respectively. **I,** Leaf blade-sheath boundary of P4 leaf primordium. **J,** High magnification image of **I**. **K,** Abaxial epidermis of P4 leaf sheath. **L,** Adaxial epidermis of P4 leaf sheath. **M-U,** Cross sections of mutant P4 leaf along the apical-basal axis. **M-T,** P4-1 to P4-8, respectively. **U,** Leaf sheath. Asterisks indicate trichomes. Arrowhead indicated differentiated epidermal cells with hair-like structure. Au; auricles, BC; bulliform cells, Fb; fibre cells, L; lacuna, Li; ligule, Lj; laminar joint, Ph; phloem, St; stomata, SVE; small vessel element, VBS; vascular bundle sheath, VE; vessel element of large size, Xy; xylem. Scale bars in **A** and **J** = 60 µm, **B-H** and **K**= 100 µm, **I** = 500 µm, **L** = 30 µm, **M-T** = 50 µm and **U** = 200 µm.

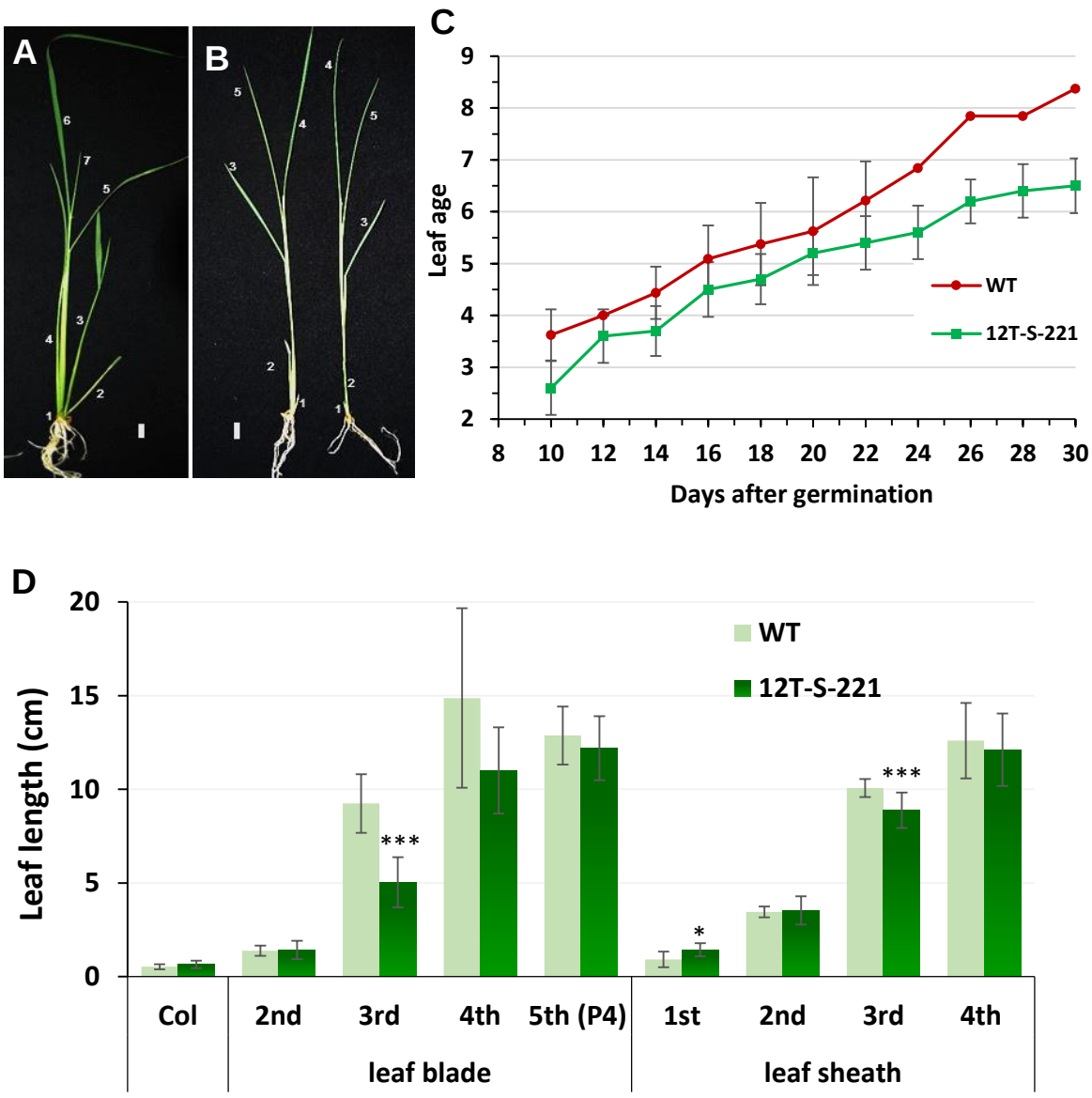

Figure 5-4 Phenotypic analysis of 12T-S-221 mutant.

A, wild-type seedling at 18 DAS. **B,** 12T-S-221 mutant seedlings at 18 DAS. **C,** Change of leaf ages in wild-type sibling and 12T-S-221 mutant. **D,** Leaf length of wild-type and the mutant. Error bars represent ±SD**.** Single (*) and triple asterisks (***) indicate the significant difference between WT and 12T-S-221 mutant at $P<0.05$ and $P<0.001$, respectively. Scale bars in **A** and **B** = 1 cm.

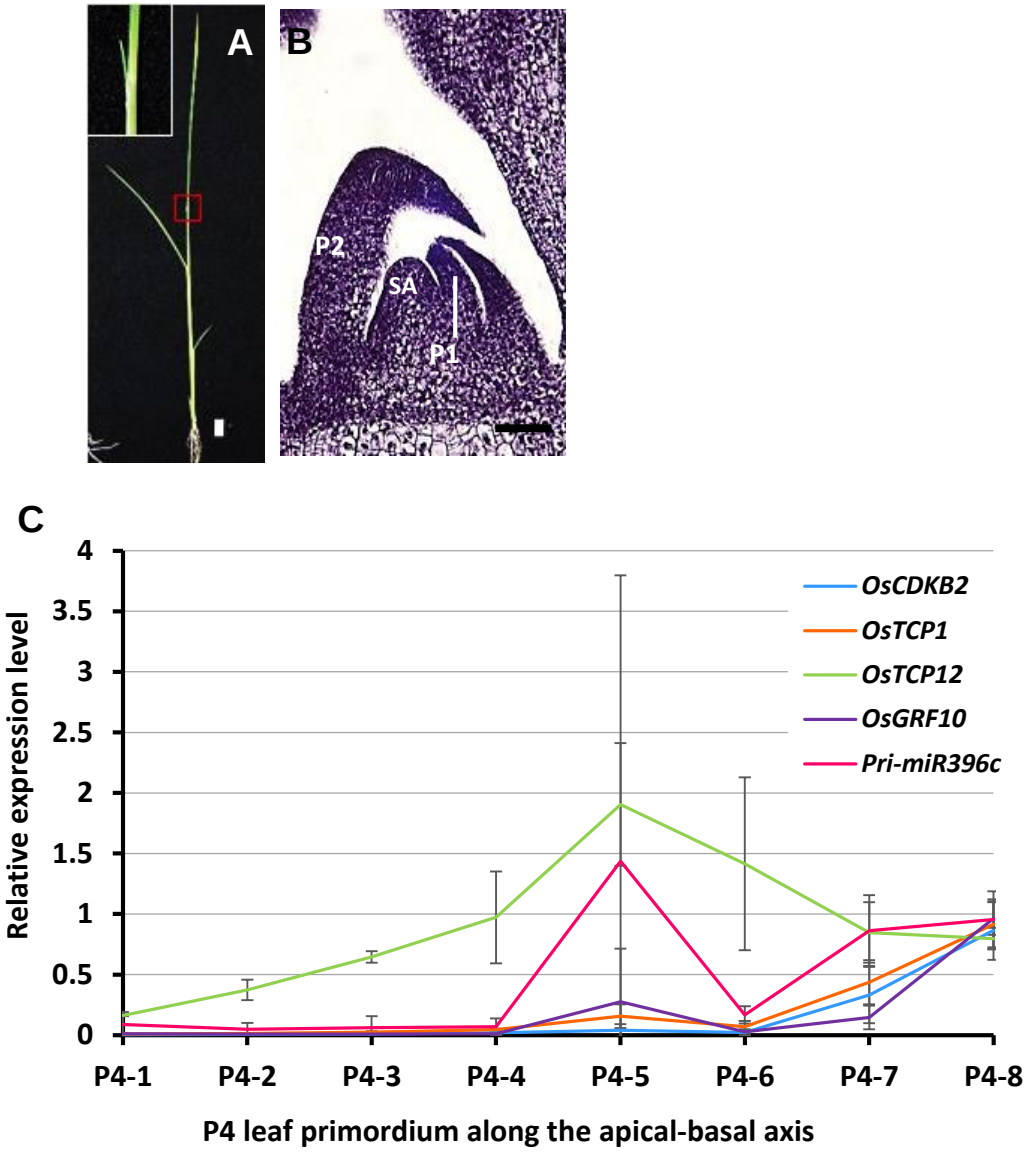

Figure 5-5 Expression analysis of five marker genes along the apical-basal axis of P4 leaf primordium of 12T-S-221 mutant.

A, Seedling of 12T-S-221 mutant when P4 leaf was sampled. Inset showed the tip blade of P4 leaf just emerged from P5 leaf sheath. **B,** Longitudinal section of shoot apex (SA), P1 and P2 leaf primordia. **C,** Expression pattern of five genes along the apical-basal axis. P4-1 to P4-8 along the horizontal axis indicates the position of the P4 leaf along the longitudinal axis. Expression level was normalized relative to that of an internal control (*OsRad6*). Scale bars in A = 1 cm and B = 50 μm.

Figure 5-6 Location of DNA markers around the candidate region of the causal gene.

Number of recombinant chromosomes was indicated under each marker.

Table 5-1. Primer sequences and the positions of DNA markers were used for mapping.

Marker	Marker position (cM)	Primer sequences		Recombination (%)
		5' primer	3' primer	
C65L20-S	100	TTCGCTCCCTCTGTATCTGT	CACTAACTACGACACCAAAT	3.49
OSJNBb0065L20-K-3	101	TTCGCTCCCTCTGTATCTGT	CACTAACTACGACACCAAAT	0.93
OSJNBa0092M19-T-1	115	AAGATCGACATACGCGGAGA	GCCGCCTGCAGATCAGAAGT	10.19

5.4 Discussion

5.4.1 12T-S-221 mutant is defective in leaf blade-sheath boundary

Phenotypes of 12T-S-221 mutant exhibited erect leaves, incomplete lamina joint, abnormal ligule and auricles, and dwarfism (Figure 5-1). At the reproductive phase, the mutant produced morphologically abnormal spikelets and showed sterility (Figure 5-1I to 5-1M). Thus, the 12T-S-221 mutant shows pleiotropic phenotypes in above-ground organs. However, internal and surface structures of the mutant leaves were not affected, indicating that the causal genes function is not involved with cell differentiation and specification process. Regarding of leaf development, the most characteristic phenotype of the mutant was abnormal formation of leaf-sheath boundary, that is, the boundary was sometime disrupted and oblique to the leaf axis. This indicates that possible function of the gene is to regulate normal growth of leaf blade and sheath boundary. Since variable phenotypes of the ligule, auricle and lamina joint was observed, these phenotypes would be secondary effects of abnormal establishment of leaf blade and sheath boundary. Mutants showing similar phenotypes to the mutant have been reported in maize and rice. Loss-of-function mutants of *LG1* (*LIGULELESS1*) and *LG2* genes in maize (Lee *et al.,* 2007, Moon *et. al.,* 2013 and Walsh *et. al.,* 1998), *lg* mutant (*OsLG1*) in rice showed lack of ligule, auricle and lamina joint. Although 12T-S-221 mutant showed defects in ligule and lamina joint formation similar to these mutants, pleiotropic phenotypes of 12T-S-221 indicate close genetic relationship between these mutants and 12T-S-221 is not likely. Other mutants affecting blade-sheath boundary is *auricleless* (*aur*) and *collarless* (*col*) in rice, *aur* mutant lacks the auricles and shows rudimentary ligules and *col* mutant lacks lamina joint establishment (Sanchez and Khush, 1998). Although these mutants might show more similar phenotype to 12T-S-221, detailed phenotypes of these mutants have not been described. *Liguleless narrow-Reference* (*Lgn-R*) in maize also showed similar phenotypes to 12T-S-221, that is, the failure of formation of leaf blade-sheath boundary was observed (Moon *et. al.,* 2013). However, *Lgn-R* is a dominant mutant that affects the mRNA level of *lg1* and *lg2* genes. Accordingly, 12T-S-221 mutants could be a novel recessive mutant affecting leaf blade-sheath boundary in rice.

5.4.2 Expression pattern of marker genes along the apical-basal axis of P4 leaf primordium of 12T-S-221

The results of expression analysis of marker genes indicated that mutation in 12T-S-221 mutant affect expression pattern of some marker genes (Figure 5-5C). The most conspicuous change is up-regulation of *OsTCP12* and two expression peaks of *pri-miR396c.* As discussed in Chapter 3 and 4, *OsTCP12* possibly modulates leaf shape by repressing cell proliferation, and *pri-miR396c* may acts to maintain the cell proliferation by suppressing *OsGRF*. Up-regulation both of genes in the middle part of P4 leaf (P4-5) might suggest that activity of minor cell proliferation events in the middle part of the 12T-S-221 mutants was suppressed, although no prominent morphological change in this leaf part was observed. Based on the results of the expression pattern of the various leaf morphogenetic mutants, it is interesting that the expression pattern of *OsTCP12* of 12T-S-221 was similar to that in *dl* mutant. Although 12T-S-221 did not show drooping leaf phenotype, it is necessary to observe whether midrib formation is affected or not in the 12T-S-221. On the other hand, expression pattern of marker genes in *lg* mutants is not similar to that of 12T-S-221 mutant. This is consistent with the possible function of the mutant is not related to that of *OsLG1* gene.

In summary, I identified a novel mutant affecting leaf blade-sheath boundary. Phenotype and gene expression analysis indicate that the gene function is mainly required for normal growth of leaf blade-sheath boundary. The gene was mapped a region of 100 to 115 cM on chromosome 3. It is expected that identification of the causal genes would contribute to further understanding of genetic mechanism for the establishment of leaf blade-sheath boundary in rice.

CONCLUSIONS

Modification of leaf size and shape should be a major target of plant breeding. However, the genetic mechanism regulation the leaf size and shape is still an unsolved problem of developmental biology in plants. Since the size and shape of the leaf depends on the spatial and temporal transition of cell proliferation and differentiation during leaf development, understanding of the regulatory mechanism would contribute to future breeding program.

In this thesis, I characterized the developmental progression and transition of various rice leaves in morphological, physiological and molecular viewpoints. My main findings are as follows.

1. In wild type, most parts of the P1 to P3 leaf primordium had immature characters, while P5 and P6 leaves were mature. The dynamic transitions of various aspects of developmental and physiological traits occur at the basal part of the P4 leaf blade. The traits included the epidermal structure, internal structure and cellular components. The transition would be determined independently of leaf blade and leaf sheath differentiation.

2. Molecular markers showing a dynamic expression pattern along the apical–basal axis of the P4 leaf were developed. The expression pattern of some marker genes, such as OsCDKB2, *OsTCP1* and *OsGRF10,* accounted for the transition from cell proliferation to cell differentiation in P4 leaf. The expression peaks of marker genes shifted toward the basal part of the P4 leaf as developmental stage progress, indicating that these genes are influenced by developmental and/or physiological events that proceed in the basipetal direction.

3. The molecular markers were applied to various growth conditions and mutants. Application of four major plant hormones affected the leaf growth and the emergence of leaves. Considering expression pattern of marker genes, the hormone treatments would affect the range of cell proliferation domain in the base of the P4 leaf. Alteration of marker gene expressions differed among the mutants, and the sensitivity of *pri-miR396c* and *OsTCP12*

expression changes was high, while that of *OsCDKB2*, *OsGRF10*, and *OsTCP1* was low. *OsRBCS2* expression level depends on light exposure, but does not simply reflect the maturation or differentiation of chloroplasts.

4. I identified a novel recessive mutant showing abnormal leaf morphology. Phenotypic and gene expression analyses indicate that a possible function of the gene is to establish normal boundary of leaf blade and sheath via modulating leaf growth.

My results revealed a part of the transition process of rice leaf development. The strategy using the molecular markers would be useful for characterizing leaf development of various conditions and mutants. Although functions of the marker genes and the causal gene of the mutant that I identified should be elucidated in the future, my results would provide basic knowledge regarding the developmental transition and its change caused by several factors during leaf development in rice.

References

Andriankaja, M., Dhondt, S., Bodt, S.D., Vanhaeren, H., Coppens, F., Milde, L.D., Mühlenbock, P., Skirycz, A. Gonzalez, N., Beemster, G.T.S. and Inźe, D. (2012) Exit from Proliferation during Leaf Development in *Arabidopsis thaliana*; A Not-So-Gradual Process. *Developmental Cell*, 22:64-78.

Avanci, N. C., Luche, D. D., Goldman, G. H. and Goldman, M. H. S. (2010) Jasmonates are phytohormones with multiple functions, including plant defense and reproduction. *Genet Mol Res*, 9(1): 484–505.

Blein, T., Hasson, A. and Laufs, P. (2010) Leaf development: what it needs to be compleax. *Curr Opin Plant Biol.*, 13:75-82.

Berna´, G., Robles, P. and Micol, J.L. (1999) A Mutational Analysis of Leaf Morphogenesis in *Arabidopsis thaliana*. *Genetics*, 152: 729–742.

Cave, G., Tolley, L.C. and Strain, B.R. (1981) Effect of carbon dioxide enrichment on chlorophyll content, starch content and starch grain structure in *Trifolium subterraneum* leaves. *Physiol. Plant*, 51:171-174.

Chatterton, N.J. and Silvius, J.E. (1980) Photosynthate partitioning into leaf starch as affected by daily photosynthetic period duration in six species. *Physiol. Plant*, 49:141-144.

Choi, D., Kim, J. H. and Kende, H. (2004) Whole genome analysis of the OsGRF gene family encoding plant-specific putative transcription activators in rice (*Oryza sativa* L.). *Plant and Cell Physiology*, 45, 897–904.

Chory, J., Chatterjee, M., Cook, R.K., Elich, T., Fankhauser, C., Li, J., Nagpal, P., Neff, M., Pepper, A., Poole, D., Reed, J. and Vitart, V. (1996) From seed germination to flowering, light controls plant development via the pigment phytochrome. *Proc. Natl. Acad Sci USA*, 93(22): 12066–12071.

Clouse, S.D. and Sasse, J.M. (1998) BRASSINOSTEROIDS: Essential Regulators of Plant Growth and Development. *Annual Review of Plant Physiology and Plant Molecular Biology*, 49: 427-451.

Debernardi, J.M., Rodriguez, R.E., Mecchia, M.A. and Palatnik, J.F. (2012) Functional specialization of the plant miR396 regulatory network through distinct microRNA-target interactions. *PLoS Genetics*, 8, e1002419.

Doonan, J. 2000. Social controls on cell proliferation in plants. *Curr Opin Plant Biol.* 3(6): 482–487.

Endo, M., Nakayama, S., Umeda-Hara, C., Ohtsuki, N., Saika, H., Umeda, M. and Toki, S. (2012) CDKB2 is involved in mitosis and DNA damage response in rice. *Plant Journal,* 69, 967–977.

Gonzalez, N., Vanhaeren, H. and Inzé, D. (2012) Leaf size control: complex coordination of cell division and expansion. *Trends in Plant Science,* 17(6):332–340.

Hardtke, C.S, Dorcey, E., Osmont, K.S. and Sibout, R. (2007) Phytohormone collaboration: zooming in on auxin–brassinosteroid interactions. *TRENDS in Cell Biology*, 17(10): 485–492.

Ichihashi, Y., Kawade, K., Usami, T., Horiguchi, G., Takahashi, T., and Tsukaya, H. (2011) Key proliferative activity in the junction between the leaf blade and leaf petiole of *Arabidopsis*. *Plant Physiology*, 157:1151–1162.

Itoh, J.-I, Hasegawa, H., Kitano, H. and Nagato, Y. (1998) A recessive heterochronic mutation, plastochron1, shortens the plastochron and elongates the vegetative phase in rice. *Plant Cell*, 10(9): 1511-1521.

Itoh, J.-I., Nonomura, K.-I., Ikeda, K., Yamaki, S., Inukai, Y., Yamagishi, H., Kitano, H., Nagato, Y. (2005) Rice plant development: from zygote to spikelet. *Plant and Cell Physiology*, 46:23–47.

Itoh, J.-I., Sato, Y., Nagato, Y. and Matsuoka, M. (2006). Formation, maintenance and function of the shoot apical meristem in rice. *Plant Mol Biol*, 60(6):827-42.

Kaufman, P. B. (1959) Development of the shoot of *Oryza sativa* L. - I., II., and III. Phytomorphology 9: 228-242, 277-311, 382-404.

Kawakatsu, T., Itoh, J., Miyoshi, K., Kurata, N., Alvarez, N., Veit, B. and Nagato, Y. (2006) PLASTOCHRON2 regulates leaf initiation and maturation in rice, Plant Cell, 18, 612–625.

Kieffer, M., Master, V., Waites, R. and Davies, B. (2011) TCP14 and TCP15 affect internode length and leaf shape in *Arabidopsis*. *Plant Journal*, 68:147-158.

Kim, J.H., Choi, D. and Kende, H. (2003) The AtGRF family of putative transcription factors is involved in leaf and cotyledon growth in *Arabidopsis*. *Plant Journal*, 36:94–104.

Kusumi, K. Chono, Y., Shimada, H., Gotoh, E., Tsuyama, M. and Iba, K. (2010) Chloroplast biogenesis during the early stage of leaf development in rice. *Plant Biotechnology*, 27 (1):85-90.

Kusumi, K., Hirotsuka, S., Shimada, H., Chono, Y., Matsuda, O. and Iba, K. (2010) Contribution of chloroplast biogenesis to carbon-nitrogen balance during early leaf development in rice. *J Plant Res*, 123(4): 617–622.

Lee, J., Das, A., Yamaguchi, M., Hashimoto, J., Tsutsumi, N., Uchimiya, H. and Umeda, M. (2003) Cell cycle function of a rice B2-type cyclin interacting with a B-type cyclin-dependent kinase. *Plant Journal*, 34(4), 417–425.

Lee, J., Park, J.-J., Kim, S.L., Yim, J. and An, G. (2007) Mutations in the rice liguleless gene result in a complete loss of the auricle, ligule, and laminar joint. *Plant Molecular Biology*, 65, 487–499.

Li, C., Potuschak, T., Colón-Carmona, A., Gutiérrez, R.A. and Doerner, P. (2005) *Arabidopsis* TCP20 links regulation of growth and cell division control pathways. *Proceedings of the National Academy of Sciences, U.S.A.,* 102, 12978–12983.

Li, D., Wang, L., Wang, M., Xu, Y.-Y., Luo, W., Liu, Y.-J., Xu, Z.-H., Li, J., Chong, K. (2009) Engineering *OsBAK1* gene as a molecular tool to improve rice architecture for high yield. *Plant Biotechnol J,* 7(8): 791–806.

Li, P., Ponnala, L., Gandotra, N., Wang, L., Si, Y., Tausta, S L., Kebrom, T. H., Provart, N., Patel, R., Myers, C.R., Reidel, E. J., Turgeon, R., Liu, P., Sun, Q., Nelson, T. and Brutnell, T.P. (2010) The developmental dynamics of the maize leaf transcriptome. *Nature Genetics,* 42:1060–1067.

Li, W., Wu, C., Hu, G., Xing, L., Qian, W., Si, H., Sun, Z., Wang, X., Fu, Y. and Liu, W. (2013) Characterization and Fine Mapping of a Novel Rice Narrow Leaf Mutant *nal9*. *Journal of Integrative Plant Biology*, 55 (11): 1016–1025.

Liu, D., Song, Y., Chen, Z., and Yua, D. (2009). Ectopic expression of miR396 suppresses GRF target gene expression and alters leaf growth in *Arabidopsis*. *Physiol. Plant*, 136: 223–236.

Liu, H., Guo, S., Xu, Y., Li, C., Zhang, Z., Zhang, D., Xu, S., Zhang, C. and Chong, K. (2014) OsmiR396d-regulated OsGRFs function in floral organogenesis in rice through binding to their targets OsJMJ706 and OsCR4. *Plant Physiology*, 165:160-174.

Martín-Trillo, M. and Cubas, P. 2010. TCP genes: a family snapshot ten years later. Trends Plant Sci. 15(1): 31–39.

Mecchia, M.A., Debernardi, J.M., Rodriguez, R.E., Schommer, C. and Palatnik, J.F. (2013) MicroRNA miR396 and RDR6 synergistically regulate leaf development. *Mechanisms of Development*, 130:2-13.

Mimura, M., Nagato, Y., Itoh, J.-I. (2012) Rice PLASTOCHRON genes regulate leaf maturation downstream of the gibberellin signal transduction pathway. *Planta*, 235(5): 1081–1089.

Miyoshi, K., Ahn, B.-O., Kawakatsu, T., Ito, Y., Itoh, J.-I. and Nagato, Y. (2004) PLASTOCHRON 1, a Timekeeper of Leaf Initiation in Rice, Encodes Cytochrome P450. Proceedings of the National Academy of Science of the USA, 101 (3): 875-880.

Moon, J., Candela, H. and Hake, S. (2013) The Liguleless narrow mutation affects proximal-distal signaling and leaf growth. Development. 15; 140(2): 405–412.

Morita K, Hatanaka T, Misoo S and Fukayama H. (2014) Unusual small subunit that is not expressed in photosynthetic cells alters the catalytic properties of rubisco in rice. *Plant Physiology*, 164(1):69-79.

Nakaya, M., Tsukaya, H., Murakami, N. and Kato, M. (2002) Brassinosteroids control the proliferation of leaf cells of *Arabidopsis thaliana. Plant and Cell Physiology*, 43, 239-244.

Nelson, T. (2011). The grass leaf developmental gradient as a platform for a systems understanding of the anatomical specialization of C_4 leaves. *Journal of Experimental Botany*, 62:3039-3048.

Nelissen, H., Rymen, B., Jikumaru, Y., Demuynck, K., Lijsebettens, M.V., Kamiya, Y., Inzé, D., Beemster, G.T.S. (2012) A local maximum in gibberellin levels regulates maize leaf growth by spatial control of cell division. *Curr Biol*, 10; 22(13): 1183–1187.

Nomura, M., Katayama, K., Nishimura, A., Ishida, Y., Ohta, S., Komari, T., Miyao-Tokutomi, M., Tajima, S. and Matsuoka, M. (2000) The promoter of *rbcS* in a C3 plant (rice) directs organ-specific, light-dependent expression in a C4 plant (maize), but does not confer bundle sheath cell-specific expression. *Plant Mol Biol*, 44(1): 99–106.

Ogawa, S., Suzuki, Y., Yoshizawa, R., Kanno, K. and Makino A. (2012) Effect of individual suppression of RBCS multigene family on Rubisco contents in rice leaves. *Plant Cell Environ*, 35(3): 546–553.

Ohmori, Y., Toriba, T., Nakamura, H., Ichikawa, H. and Hirano, H.Y. (2011). Temporal and spatial regulation of DROOPING LEAF gene expression that promotes midrib formation in rice. *Plant* J, 65(1):77–86.

Patel, M. and Berry, J.O. (2008) Rubisco gene expression in C4 plants. *J. Exp. Bot*, 59 (7): 1625-1634.

Pérez-Pérez, J.M., Candela, H., Robles, P., Quesada, V., Ponce, M.R. and Micol, J.L. (2009) Lessons from a search for leaf mutants in *Arabidopsis thaliana*. *Int. J. Dev. Biol*. 53: 1623-1634.

Ramirez-Parra, E., Desvoyes, B. and Gutierrez, C. (2005) Balance between cell division and differentiation during plant development. *Int J Dev Biol*, 49(5-6): 467–477.

Rodriguez, R.E., Mecchia, M.A., Debernardi, J.M., Schommer, C., Weigel, D. and Palatnik, J.F. (2010) Control of cell proliferation in *Arabidopsis thaliana* by microRNA miR396. *Development*, 137:103-112.

Sakamoto, T., Kitano, H. and Fujioka, S. (2013) Genetic Background Influences Brassinosteroid-Related Mutant Phenotypes in Rice. *American Journal of Plant Sciences*, 4 (2):212-221.

Sakamoto, T., Miura, K., Itoh, H., Tatsumi, T., Ueguchi-Tanaka, M., Ishiyama, K., Kobayashi, M., Agrawal, G.K., Takeda, S., Abe, K., Miyao, A., Hirochika, H., Kitano, H., Ashikari, M. and Matsuoka, M. (2004) An Overview of Gibberellin Metabolism Enzyme Genes and Their Related Mutants in Rice. *Plant Physiol*, 134:1642-1653.

Sanchez, A.C. and Knush, G.S. (1998) A gene for collarless phenotype in rice. *Rice Genet Newsletter*, 15:99-100.

Scarpella, E., Barkoulas, M. and Tsiantis, M. (2010) Control of Leaf and Vein Development by Auxin. *Cold Spring Harb Perspect Biol*, 2(1): a001511.

Sharma, R., Kapoor, M., Tyagi, A.K., and Kapoor, S. (2010) Comparative transcript profiling of TCP family genes provide insight into gene functions and diversification in rice and *Arabidopsis*. *Journal of Plant Molecular Biology and Biotechnology*, 1:24-38.

Smith, A.M. (2007) Starch Biosynthesis and Degradation in Plants. *Encyclopedia of* Life *Science*, John Wiley & Sons, Ltd. www.els.net.

Smith, L.G., Hake, S. and Sylvester, A.W. (1996) The tangled-1 mutation alters cell division orientations throughout maize leaf development without altering leaf shape. *Development*, 122:481-489.

Smith, R.A., Schuetz, M., Roach, M., Mansfield, S.D., Ellis, B. and Samuels, L. (2013) Neighboring parenchyma cells contribute to *Arabidopsis* xylem lignification, while lignification of interfascicular fibers is cell autonomous. *Plant Cell*, 25, 3988-3999.

Sunkar, R., Girke, T., Jain, P.K. and Zhu, J.K. (2005) Cloning and Characterization of microRNAs from rice. *Plant Cell*, 17:1397–1411.

Suzuki, Y., Ohkubo, M., Hatakeyama, H., Ohashi, K., Yoshizawa, R., Kojima, S., Hayakawa, T., Yamaya, T., Mae, T. and Makino, A. (2007) Increased Rubisco content in transgenic rice transformed with the 'sense' rbcS gene. *Plant and Cell Physiology*, 48, 626–637.

Takai, T., Adachi, S., Taguchi-Shiobara, F., Sanoh-Arai, Y., Iwasawa, N., Yoshinaga, S., Hirose, S., Taniguchi, Y., Yamanouchi, U., Wu, J., Matsumoto, T., Sugimoto, K., Kondo, K., Ikka, T., Ando, T., Kono, I., Ito, S., Shomura, A., Ookawa, T., Hirasawa, T., Yano, M., Kondo, M. and Yamamoto T. (2013) A natural variant of NAL1, selected in high-yield rice breeding programs, pleiotropically increases photosynthesis rate. *Sci Rep*., 3: 2149.

Tsukaya, H. and Uchimiya, H. (1997) Genentic analyses of the serrated margin of leaf blades in *Arabidopsis* combination of a mutantional analusis of leaf morphogenesis with the characterization of a specific marker gene expressed in hydathodes and stipules. *Mol. Gen. Genet*, 256:231-238.

Tsukaya, H., Inaba-Higano, K. and Komeda, Y. (1995) Phenotypic and molecular mapping of an acaulis2 mutant of *Arabidopsis* thaliana with flower stalks of much reduced length. *Plant Cell Physiol*, 36:239-246.

Ueguchi-Tanaka, M., Fujisawa, Y., Kobayashi, M., Ashikari, M., Iwasaki, Y., Kitano, H. and Matsuoka, M. (2000) Rice dwarf mutant d1, which is defective in the α subunit of the heterotrimeric G protein, affects gibberellin signal transduction. *PNAS*, 97(21): 11638–11643.

Verkest, A., Manes, C.L., Vercruysse, S., Maes, S., Schueren, E.V.D., Beeckman, T., Genschik, P., Kuiper, M, Inzé, D. and Veyldera, L.D. (2005) The cyclin-dependent kinase inhibitor KRP2 controls the onset of the endoreduplication cycle during *Arabidopsis* leaf development through inhibition of mitotic CDKA;1 kinase complexes. *Plant Cell*, 17: 1723–1736.

Walsh, J., Waters, C.A. and Freeling, M. (1998) The maize gene *liguleless2* encodes a basic leucine zipper protein involved in the establishment of the leaf blade–sheath boundary. *Genes Dev,* 12(2): 208–218.

Wang Y, Chantreau M, Sibout R and Hawkins S (2013) Plant cell wall lignification and monolignol metabolism. Frontiers in Plant Science, 4, 220, 1-14.

Wang, L., Czedik-Eysenberg, A., Mertz, R. A., Si, Y., Tohge, T., Nunes-Nesi, A., Arrivault, S., Dedow, L. K., Bryant, D. W., Zhou, W., Xu, J., Weissmann, S., Studer, A., Li, P., Zhang, C., LaRue, T., Shao, Y., Ding, Z., Sun, Q., Patel, R.V., Turgeon, R., Zhu, X., Provart, N.J., Mockler, T.C., Fernie, A.R., Stitt, M., Liu, P. and Brutnell, T.P. (2014) Comparative analyses of C4 and C3 photosynthesis in developing leaves of maize and rice. *Nature Biotechnology*, 32: 1158–1165.

Watanabe, Y., Nakamura, Y. and Ishii, R. (1997). Relationship between Starch Accumulation and Activities of the Related Enzymes in the Leaf Sheath as a Temporary Sink Organ in Rice (*Oryza sativa*). *Australian Journal of Plant Physiology,* 24(5):563 – 569.

Yamaguchi, T., Nagasawa, N., Kawasaki, S., Matsuoka, M., Nagato, Y. and Hirano, H.-Y. (2004) The YABBY gene DROOPING LEAF regulates carpel specification and midrib development in Oryza sativa. *Plant Cell*, 16:500– 509.

Yamamuro, C., Ihara, Y., Wu, X., Noguchi, T., Fujioka, S., Takatsuto, S., Ashikari, M., Kitano, H. and Matsuoka, M. (2000) Loss of Function of a Rice brassinosteroid insensitive1 Homolog Prevents Internode Elongation and Bending of the Lamina Joint. Plant Cell. 12(9): 1591–1606.

Yang, P., Chen, H., Liang, Y. and Shen, S. (2007) Proteomic analysis of de-etiolated rice seedlings upon exposure to light. *Proteomics*, 7(14): 2459–2468.

Yao, X., Ma, H., Wang, J. and Zhiponova, D. (2007) Genome-wide comparative analysis and expression pattern of TCP gene families in *Arabidopsis thaliana* and *Oryza sativa*. *Journal of Integrative Plant* Biology, 49:885–897.

Yoshikawa, T., Ito, M., Sumikura, T., Nakayama, A., Nishimura, T., Kitano, H., Yamaguchi, I., Koshiba, T., Hibara, K.-I., Nagato, Y. and Itoh, J.-I. (2014) The rice FISH BONE gene encodes a tryptophan aminotransferase, which affects pleiotropic auxin-related processes. *Plant J*., 78(6): 927–936.

Zhang, L.-Y., Bai, M.-Y., Wu, J., Zhu, J.-Y., Wang, H., Zhang, Z., Wang, W., Sun, Y., Zhao, J. Sun, X., Yang, H., Xu, Y., Kim, S.-H., Fujioka, S., Lin, W.-H., Chong, K., Lu, T. and Wanga, Z.-Y. (2009) Antagonistic HLH/bHLH Transcription Factors Mediate Brassinosteroid Regulation of Cell Elongation and Plant Development in Rice and *Arabidopsis*. *The Plant Cell*, 21: 3767–3780.

Zhang, B., Ye W., Ren D., Tian P., Peng Y., Gao Y., Ruan B., Wang L., Zhang G., Guo L., Qian Q., Gao Z.(2015) Genetic analysis of flag leaf size and candidate genes determination of a major QTL for flag leaf width in rice. *Rice*, 8:2.

Zhiponova, M.K., Vanhoutte, I. Boudolf, V., Betti, C., Dhondt, S., Coppens, F. Mylle, E., Maes, S., Gonza´lez-Garcı´, M.-P., Can˜o-Delgado, A.I., Inze´, D., Beemster, G.T.H., Veylder, L.D. and Russinova, E. (2013) Brassinosteroid production and signaling differentially control cell division and expansion in the leaf. *New Phytologist* 197: 490–502.

Zhu, Y., Gu, X., Zhao, H. and Chen, Z. (1998) Extracellular Calmodulin stimulates RbcS-GUS expression of etiolated transgenic tobacco plants in full darkness. *Plant Growth Regulation*, 25: 23–28.

Acknowledgement

First of all, I would like to express my earnest gratitude towards Associate Professor Jun-ichi Itoh, my supervisor, who diligently teach, guide, suggest and assist me regarding my research, scholarship, together with acceptance for his advisee. Without his invaluable supervision and his incessant assistance, my dissertation would not have completed.

I also would like to extend my sincere appreciation to Professor Yasuo Nagato who provided me warm welcome and gave me an opportunity to be a member of laboratory of Plant Breeding and Genetics. Additionally, I profoundly feel grateful to Assistant professor Ken-ichiro Hibara for providing me many valuable suggestions and guidance in regard to my research.

My gratitude also goes to all officers of the University of Tokyo for their wholehearted help and excellence service providing. In addition, I would like to express my special thanks to the University of Tokyo for accepting me as a doctoral student.

Last but not least, I am profoundly indebted to Japanese Government (Monbukagakusho: MEXT) scholarship for financial supports.